TECHNISCHE UNIVERSITÄT MÜNCHEN
Lehrstuhl für Medizintechnik

Controlled release of an antiproliferative drug from coronary stents

Magdalena K. Renke-Głuszko

Vollständiger Abdruck der von Fakultät für Maschinenwesen der Technischen Universität München zu Erlangung des akademischen Grades eines

Doktor-Ingenieurs (Dr.-Ing.)

genehmigten Dissertation.

Vorsitzender: Univ.-Prof. Wolfgang Polifke, Ph. D. (CCNY)

Prüfer der Dissertation:

1. Univ.-Prof. Dr. med., Dr.-Ing. habil. Erich Wintermantel
2. Prof. Dr. rer. nat. Hans P. Merkle, em. Eidgenössische Technische Hochschule Zürich / Schweiz (schriftliche Beurteilung)
3. Univ.-Prof. Dr.-Ing. Horst Baier (mündliche Prüfung)

Die Dissertation wurde am 17.09.2008 bei der Technischen Universität München eingereicht und durch Fakultät für Maschinenwesen am 12.12.2008 angenommen.

Abstract

Stenting is one of the most common and successful minimally invasive surgical methods to threat atherosclerosis. The main limitation of this method which occurs to date in approximately 30% of all treated patients is in-stent restenosis. This is a healing process with excessive cell proliferation resulting in a re-narrowing of the stented coronary artery.

This work studied possibilities of reducing the in-stent restenosis by developing long term biocompatible and effective custom made stent coatings which allow the user to select among adequate drug concentrations to be released and its kinetic behaviour.

Two different release controlling methods have been developed: drug release controlling by stent surface modification and release controlling by additional biodegradable polymer matrix application. It could be worked out that both methods offer reliable ways to positively influence future formation of in-stent restenosis.

Überblick

Stenting ist eine gängige, minimal-invasive chirurgische Methode zur Behandlung der Arteriosklerose. Hauptlimitation dieser Methode ist In-Stent Restenose, welche durch Zellwucherungen als Reaktion auf die Gefäßverletzung während der Stentimplantation verursacht wird.

In der vorliegenden Arbeit wurden Verfahren entwickelt für Optimierung der Stent-Oberflächen, für Beschichtung dieser Oberflächen mit Rapamycin, einen antiproliferativen Medikament und für die Verlängerung der Medikamenten-Freisetzung durch Zusatz eines abbaubaren Polymers.

Beide durchgeführte experimentelle Verfahren sind nun geeignet, im Tierversuch und der späteren Humanapplikation getestet zu werden.

Acknowledgments

In particular I like to thank Prof. Dr. Dr. Erich Wintermantel for giving me an opportunity to work in excellent Institute and for very interesting and challenging subject of my Dissertation.

I would like to express my gratitude to my referee, Prof. H. Peter Merkle, whose experience and pharmacological knowledge considerably improved my graduate experience. But first of all I want to thank for his understanding and patience in waiting for the last version of my thesis.

Dr. habil. Miroslawa El Fray deserves my gratitude for giving me the opportunity to scientific development and for introducing into the world of medical engineering during my studies at the Szczecin Universtity of Technlogy

Dr. Julia Will deserves my gratitude for her essential support at the difficult beginnings of my thesis. Special thanks for Dr. Markus Eblenkamp for critical proofreading and constructive discussions. Thanks are also due to Dr. Hector Perea for his help in editing English language of the thesis.

For special thanks deserved whole Team of ISAR-Project: Dr. Michael Stöver and Dr. Tom Schratzenstaller for support, friendly atmosphere and sometimes stormy but very productive discussions. Thanks Dr. Boris Behnisch from Translumina Inc. for providing the countless amounts of stents and for the creative discussions during laboratory work.

Moreover I like to thank all other persons who contributed to the success of this work: Shadi Sabeti, Sebastian Schmidt, Michael Geisler, Christian Zeilinger and Tim Bartels.

All colleagues from Zentralinstitut für Medizintechnik and Lehrstuhl für Medizintechnik for familiar and very productive atmosphere. Especially Susanne Schnell-Witteczek for help in laboratory and scanning microscopy and Uschi Hopfner and Dr. Joachim Aigner for introduction into cell biology.

Last but not least for special acknowledgments deserved my whole family:

Szczególne podziękowania składam całej mojej Rodzinie, przede wszystkim Rodzicom za niestrudzona wiarę we mnie i nieustanne zagrzewanie do walki oraz mężowi Marcinowi za cierpliwość i wsparcie każdego dnia oraz za pomoc w formatowaniu dokumentu i w rysunkach.

Moim kochanym urwisom: Michałowi i Mateuszowi dziękuję za to, że po prostu jesteście.

1 Introduction

According to the World Health Organization [1] coronary artery disease (CAD) is a leading cause of death in developed countries and is considered a serious health threat worldwide. CAD is usually caused by atherosclerosis, a narrowing of the coronary arteries sufficient enough to prevent adequate blood supply to the heart muscle (Fig. 1.1). It can progress to the point where the heart muscle is damaged due to lack of blood supply (heart attack) [2].

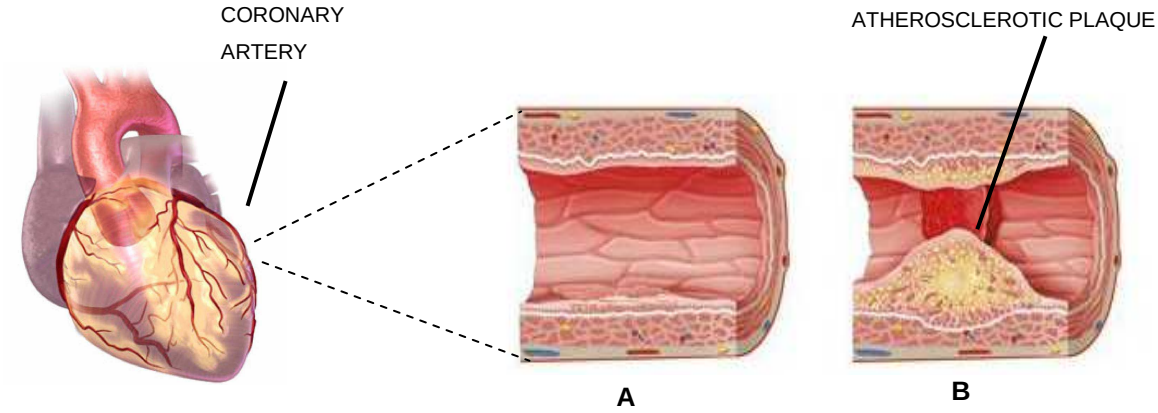

***Fig. 1.1**: Atherosclerosis; A: healthy coronary artery, B: coronary artery with plaque which cause reduced blood flow through artery. Modified according to medmovie.com, Lexington, USA.*

To present little details are known about the pathophysiology of atherosclerosis. The process of atherosclerosis formation involves a complex series of metabolic events, similar to a chronic inflammatory process, with the formation of atherosclerotic plaques as the end result.

Risk factors such as hypercholesterolemia, arterial hyperextension, diabetes mellitus or nicotine abuse are associated with an elevated basal activity and hyperaggregability of circulating blood platelets. Fatty streaks are the first grossly visible lesion in the development of atherosclerosis. It appears as an irregular off white to yellow-white discoloration near the luminal surface of the artery. Fatty streaks do not cause symptoms and are even already present in the aorta and coronary arteries of most individuals by the

age of 20 [6]. In regions exposed to increased shear forces, for example, vessel branching points, the contact between activated blood platelets and the endothelial surface can lead to the activation of endothelial cells, thus favoring the migration of monocytes through the release of thrombocytic inflammatory factors [3 - 5]. The injury of the endothelium, resulting in endothelial cell dysfunction, is the first step involved in the process of atherogenesis. Endothelial dysfunction triggers the accumulation of lipoproteins in the subendothelial space where chemical modification of low-density lipoprotein (LDL) occurs. Modified LDL recruits monocytes into the vessel wall where these cells are converted into macrophages that engulf the modified lipoproteins becoming foam cells. Activated endothelial cells also attack leukocytes and vascular smooth muscle cells (VSMC), which accumulate and proliferate in the arterial wall. These cellular components produce an excessive amount of connective tissue matrix leading to the formation of a mature fibrous plaque [4, 7]. Independently from the pathogenesis of atherosclerosis narrowing of coronary arteries can lead to heart muscle insufficiency and the result is often a heart attack.

One of the most common minimally invasive surgical and successful methods to treat ischemic disease is percutaneous transluminal coronary angioplasty (PTCA). Angioplasty is a medical procedure in which a balloon mounted onto a catheter is used to open narrowed or blocked coronary arteries. Once the catheter is positioned in the narrowed blood vessel, a balloon is repeatedly inflated and deflated to stretch or break open the blocked area. The major limitation of balloon angioplasty is the so called artery recoil. Elastic recoil or shrinking of the artery occurs within minutes and hours after angioplasty. It leads to a loss of up to 50% of the vessel diameter, especially in the part of the vessel that was not atherosclerotic before angioplasty. To improve the long-term stabilization and overcome artery recoil, coronary stents can be implanted [8].

A coronary stent is an artificial support device which is placed in the coronary artery to keep the vessel open after treatment of coronary artery disease. The stent is usually a stainless steel mesh tube that is available in various sizes to match the size of the artery and hold it open after the blockage has been treated (Fig 1.2). Randomized multicenter clinical trials comparing balloon angioplasty with intracoronary stenting have demonstrated a reduced incidence of restenosis after stenting due to the scaffolding properties of stents

inhibiting chronic constrictive vascular remodeling [9]. In-stent restenosis (ISR) is the most important long-term limitation of stent implantation for coronary disease, occurring in 20 – 30% of all patients [10, 11]. Restenosis following conventional stent implantation results from thrombus formation, smooth muscle cell proliferation and excessive production of cellular matrix [12-14]. Since Sigwart et al [15] reported the first implantation of a stainless steel stent in human coronary arteries, various intracoronary stents have been tested in an attempt to prevent occlusion and restenosis after angioplasty. Despite the high initial success rate, early and late complications such as thrombotic closure and restenosis have been reported with all currently available metallic stents[16].

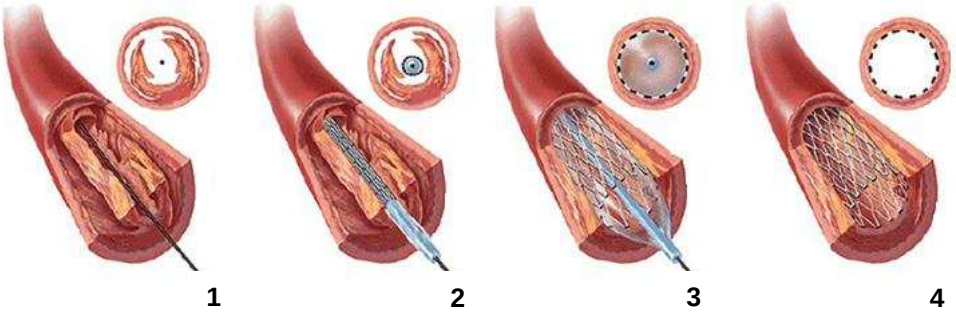

Fig.1.2: *Steps of stenting procedure. 1. Guide wire is introduced into the blocked coronary artery. 2. Stent mounted on balloon is positioned in narrowed area. 3. Stent is expanded due to balloon dilatation. 4. Balloon is deflated and removed, expanded stent remains in opened coronary artery. Modified according to medmovie.com Lexington, USA.*

Systemic administration of a wide variety of drugs has been tested in clinical trials for the prevention of restenosis showing little or inconclusive benefit so far [17]. These agents include:

- antithrombotic platelet aggregation inhibitors (aspirin) and anticoagulants (heparin)
- calcium channel blockers
- ACE inhibitors (Angiotensin Converting Enzyme)
- antioxidants

Due to similarity between underlying metabolic mechanisms of tumor growth and in-stent neointimal growth, antiproliferative agents are used to reduce in-stent restenosis (ISR). Initially, some drugs such as trapidil and tranilast failed probably due to limited effectiveness, insufficient doses or inappropriate release methods [18, 19].

One of the possibilities to solve the problem of restenosis is local drug delivery to the injured artery. There are several options for the route of drug delivery:

- direct contact of the drug with the arterial wall from the angioplasty device during the angioplasty procedure [20]
- drug-eluting coating on the stent itself [21].

The advantage of the second option is that drug delivery can be sustained much longer than that expected by direct release during the angioplasty procedure. Additionally, the drug is delivered right where restenosis would take place, that is, directly around the stent [22].

Since in-stent restenosis is mainly caused by cell proliferation, one of the ways to solve this problem is to inhibit the restenosis process by coating stents with antiproliferative and/or immunosuppressive drugs [23]. The introduction of coated stents (drug-eluting stents DES) has resulted in a reduction in the incidence of in-stent restenosis when compared with bare-metal stents [24, 25].

Despite these advantages, restenosis rates still remain substantially high in high-risk patients. Furthermore, the incidence of late stent thrombosis and restenosis [26, 27] has raised doubts about the long-term safety and efficacy of DES. Both late occurring complications have been related to a marked inflammatory response against the non-degradable polymer-coated stent surface as well as an incomplete re-endothelialization [27].

There are several important design characteristics for a drug-eluting stent, which include:

- Biocompatible coatings that do not cause injury, toxic or immunologic reactions in the living tissue.
- Coating should not influence or interfere with blood flow in the artery or enhance clot (thrombosis) formation.
- Coating should not interfere with the performance of the stent. During the implantation process the coating should be stable (no cracks or blistering) and should not limit the stent dilatation process.
- Maximal drug loading capacity in the coating, in order to ensure that effective levels

of drug are reached

- Coating thickness should be optimized to ensure good coating adhesion to the stent surface especially during stent expansion and simultaneously not cause a diameter limitation in small vessels.
- Coating should be tailored to release the drug with optimal kinetics, so that drug concentrations in the affected tissue remains at optimal levels over the time frame required.

This work is focused on the development of long-term biocompatible and effective controlled drug-eluting stent systems to eliminate restenosis, and overcome the above mentioned limitations of DES.

2 Aim of the thesis and experimental setup

The motivation for this thesis is the still relatively high restenosis rate, especially in specific patient subsets such as the insulin-dependent diabetic patient or in challenging interventional scenarios, such as bifurcation stenting. On-site (in catheter laboratory) coating of stents immediately prior to implantation would enable the physician to choose the proper drug and drug dosage suitable for each patient.

Two main goals of the thesis are:

1. Evaluation of a novel coronary stent coating method which enables a customized coating just before stent implantation
2. Determination of the factors influencing drug release from coronary stents and investigation of drug elution

Based on the results found in literature, different coating techniques have been investigated to produce drug eluting stents, the spray – coating method being the most suitable coating technique. Chapter 7 describes the factors determined to influence the controlled drug release from coronary stents.

The following factors were investigated:

- stent surface modification
- kind and properties of biodegradable polymer matrix
- combination of both: modified surface and matrix properties
- drug and polymer ratio and concentration in coating solution

Further investigation and determination of drug transport in porcine coronary artery after drug-eluting stent implantation was performed. The obtained coatings were characterized and tested under in vitro conditions, as described in Chapter 6.

Experimental setup

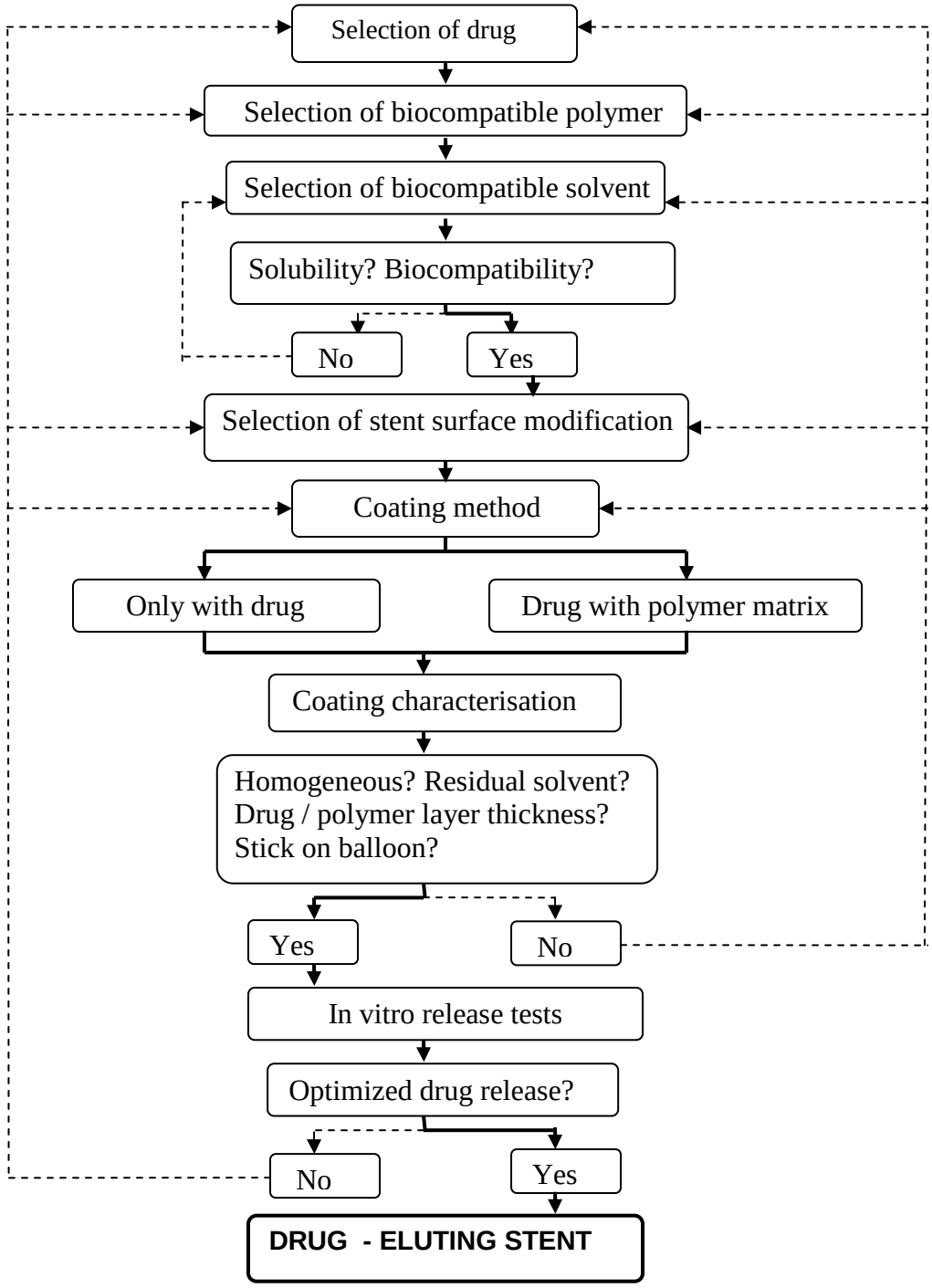

Fig.2.1: *Flow chart of the experimental strategy to obtain optimized drug-release stent. The most desirable route to reach the goal is labeled bold. If a level in the flow diagrams fails, it is necessary to go back and redo previous decisions (route labeled - - - -).*

3 Medical background

3.1 Restenosis and its therapies

A series of studies on coronary stents have demonstrated a lower incidence of angiographic restenosis when compared to PTCA alone in both simple and complex lesions, as well as in various patient subsets including acute myocardial infarction, total occlusions and restenotic lesions [16, 29, 30]. Recently the beneficial short– and long–term results of coronary stenting have resulted in a dramatic increase in stent utilization, accounting for more than 70% of coronary interventions [31].

Nevertheless the problem of restenosis which still occurs in at least 20 – 30 % of the patients undergoing stent implantation [32 – 34] has not been resolved and the need for new revascularization procedures exceeds 10% [8]. Especially in specific patient subsets, such as insulin-dependent diabetic subjects, or in challenging interventional scenarios, like bifurcation stenting, the rate of restenosis remains substantial at the present [35, 36]. In-stent restenosis (ISR) is considered to be the result of neointimal hyperplasia which is mainly due to intima-derived smooth muscle cells and extracellular proteoglycan matrix [9]. Several cellular and molecular events have been identified to occur sequentially after the vascular injury caused by stent implantation. Shortly after the procedure, fibrin deposition, platelet activation and thrombus formation take place. The process also involves acute inflammatory cells, granulation, tissue formation and the local release of a large number of substances, including chemotactic and growth factors, and oxygen-derived free radicals, which trigger a complex array of events that modulate matrix production and cellular migration and proliferation, ultimately leading to neointima formation [9-13].

To treat in-stent restenosis various techniques are used:

Repeated balloon dilatation and restenting. These revascularization procedures lead to repeated opening of artery occlusion after percutaneous coronary angioplasty using only balloon dilatation or implantation of new stent in the place of obstructive arterial lesions. The most difficult problem associated with PTCA and restenting is unexpected, abrupt

occlusion of lesion and as a consequence coronary artery bypass grafting should be performed [37, 41].

Techniques using removing of neointimal tissue (catheter atherectomy). Atherectomy is an endovascular interventional technique for excision and removal of obstructive arterial lesions. The atherectomy device has a small mechanically driven tool that either shaves, cuts, or breaks the plaque into small particles to remove the blockage from the lumen of the artery. After being shaved from the artery wall, this plaque is stored safely in the tip of the catheter and removed from the body [38, 40]. Common complications of atherectomy are the blood vessel injury, formation of new plaques, blood clots (hematoma), and bleeding at the site of device insertion. More serious but less frequent complications are blood vessel rupture, or reduced blood flow to the heart. Disruption and deformation of implanted stent during the atherectomy procedure have also been reported. Nevertheless, the scope of atherectomy is very limited and remains restricted to heavily calcified, inelastic or non-dilatable, and diffuse coronary lesions.

Coronary brachytherapy. Radiation therapy aimed to treat restenosis has two purposes: to treat the restenosis itself (by killing the cells that have re-occluded the stent), and to prevent further restenosis (by inhibiting tissue growth). This treatment is especially effective in patients with small vessels and a long stented area, and in patients with diabetes. Coronary brachytherapy consists in delivering beta or gamma radiation into the coronary arteries. This treatment is suitable for patients who have undergone stent implantation in a coronary artery and subsequently developed problems, such as diffuse in-stent restenosis. However, dose-dependent delay in stent endothelialization, edge restenosis, in addition to neointimal proliferation and negative remodeling, remains a serious limitation of vascular brachytherapy [42, 43].

Systemic drug therapy after stent implantation [8, 42]. Most drugs with systemic effects (antiplatelet agents, anticoagulants, anti-inflammatory agents, hypolipidemic agents, ACE inhibitors, calcium antagonists, antioxidants, etc) and a variety of mechanical devices mentioned above have failed to reduce restenosis [9, 43].The use of antiproliferative agents seemed to be the most efficient strategy to reduce in-stent restenosis. The limited efficiency of systemically administered agents may be related to inadequate drug concentrations at the site of stent insertion. Antiproliferative agents show in low doses limited effectiveness and in high doses systemic toxicity [44 – 49]. The

limited success of other drugs in decreasing the rate of in-stent restenosis, coupled with adverse side effects, has prompted the development of coated stents.

3.2 Stents to prevent restenosis

Stents can be classified according to their mechanism of expansion (self-expanding or balloon expandable), their composition (stainless steel, cobalt-based alloy, tantalum, nitinol, inert coating, active coating, or biodegradable), and their design (mesh structure, coil, slotted tube, ring and multi-design).

Intravascular stents, whether expanded using a balloon or autonomously, are delivered via the femoral or brachial arteries through the tortuous vessels of the cardiovascular system. The minimally invasive delivery of the stents poses many design challenges stents and catheter systems. To ensure an accurate placement of the stents, they must be visible under fluoroscopy and, as a result, the materials chosen for stents should be radiopaque. In addition, balloon-expanding stents have radiopaque markers on the proximal and distal ends of the balloon to aid positioning of the stents. To minimize in-stent restenosis, enable the delivery of a stent through a catheter, ensure accurate placement of a stent, and maintain long-term vessel patency after stent deployment, stents must fulfill the following design and material requirements.

DESIGN REQUIREMENTS

High radial strength: Stents require good radial support / structural strength to prevent vessel recoil and hence lumen loss post-stenting.

Good flexibility: Crimped stent on the delivery catheter must be flexible so that it can be delivered to the deployment site. The expanded stent must adapt to the tortuous artery geometry and should not straighten the vessel, since that would induce excessive injury to the vessel wall.

Good trackability: Trackability is a measure of the ability of a stent deployment catheter to follow a tortuous path to its ultimate destination.

Optimum scaffolding: A stent should provide optimum vessel coverage to ensure that the vessel tissue does not prolapse between the stent struts. However, a low artery-stent

contact surface area should also be maintained, because the foreign material of the stent can initiate an aggressive thrombotic response.

STENT MATERIAL REQUIREMENTS

Radioopacity: Stent materials need to be radioopaque to enable delivery, precise positioning, and evaluation of stents at checkups under the guidance of fluoroscopic imaging.

Biocompatibility: Stent materials must be biocompatible to prevent adverse foreign body responses.

Corrosion-resistance: Stent materials are specially designed to develop a passive oxide layer, which prevents corrosion in the long term.

Good fatigue properties: Cyclic stresses associated with blood flow can cause fatigue failure in stents.

All of these design requirements can be achieved by optimizing the following parameters:

- Material selection.
- Strut dimensions and cross-section.
- Number of circumferential and axial repeating units, and their geometry.
- The manufacturing process used to produce the stents.

3.2.1 Biodegradable stents with and without incorporated active agents

Currently there are two types of materials used for bioabsorbable stents: polymeric- and metallic-based biomaterials. Among the polymers suggested for absorbable stents are polylactic and polyglycolic acid based polymers and polycaprolactone [121]. Polymeric biodegradable stents have shown several limitations. Their mechanical strength is lower compared to metallic stents, which can result in early recoil post implantation. The polymer has a limited mechanical performance and a recoil rate of approximately 20% which requires thick struts that reduce their delivery capabilities, especially in small vessels. These stents are associated with a significant degree of local inflammation. The bioabsorption rate is relatively slow, and may still result in restenosis. These stents are

radiolucent, which may prevent accurate positioning and are difficult to deploy smoothly and precisely [50 – 53].

Bioabsorbable metals for stent include magnesium alloys. The biocompatibility of these stents depends on their design, solubility and their released degradation products. Their local toxicity is related to the local concentration of the elements over time. The tissue tolerance depends on their concentration in the tissue induced by corrosion. Animal studies show good biocompatibility of magnesium stents but the long-term clinical trials are not yet available [53]. Biodegradable metallic-based stents are still in the development phase [53 – 55]. Active agents incorporated into degradable stent can be released during the degradation process.

3.2.2 Stable metal (316 L) stents

As mentioned in the introduction, bare-metal stents show decreased restenosis rate compared to balloon dilatation but the target is to prevent restenosis.

Therefore numerous studies have been carried out investigating stent coatings with different materials:

- **Inert coatings** (carbon, gold, silicon carbide, phosphorylcholine, etc.). These coatings were thought to be less thrombogenic and inflammatory than baremetal stents and are thereby potentially able to reduce neointimal hyperplasia. Animal studies and some clinical trials did not show a significant reduction of in-stent restenosis when stents were coated with these materials [56 – 61].
- **Drug eluting coatings** (heparin, sirolimus, paclitaxel, etc.). The drug eluting coatings contain agents that inhibit thrombus formation, inflammation and cellular proliferation. Drug-eluting stents offer theoretical advantages over systemic pharmacotherapy such as higher drug concentration at the site of stent deployment and minimal systemic side effects [62]. Animal and human studies suggest that stents coated with anticoagulants and corticosteroids do not have a significant inhibitory effect on neointimal hyperplasia [63].

Recently, stents eluting antiproliferative agents have been shown to reduce significantly both the rate of in-stent restenosis and the need for subsequent revascularization procedures compared with bare-metalstents [64].

At present, these beneficial effects have been demonstrated mainly with Cypher (Cordis Corporation) and Taxus (Boston Scientific) stents. Various studies have shown that both drug eluting stents efficiently prevent both angiographic and clinical restenosis rates compared with bare-metal stents (Table 3.1) [65 – 68, 16]. The compounds used in Cypher and Taxus platforms are different: Cypher elutes sirolimus (rapamycin) and Taxus releases paclitaxel.

Study	**Drug**	**Restenosis [%]**	**Late lumen loss [mm]**
different studies	bare-metal stent	22 %	0.75 ± 0.17
REALITY	Sirolimus	7 %	0.09 ± 0.43
	Paclitaxel	8.3 %	0.31 ± 0.44
SIRTAX	Sirolimus	4.8 %	0.13 ± 0.37
	Paclitaxel	8.3 %	0.25 ± 0.49
ISAR DESIRE	Sirolimus	14.3 %	-
	Paclitaxel	21.7 %	-

Table 3.1*: Randomized prospective multicenter trials. Comparison of angiographic results and restenosis after a follow-up period of at least six months. The sirolimus-eluting Stent (Cypher) and the paclitaxel-eluting stent (Taxus) with bare metal stent. The results for the REALITY and SIRTAX studies were evaluated after 6 -8 months. ISAR DESIRE trials present long-term clinical results; here restenosis rate is significantly higher than in another studies. This difference could be caused by non-degradable polymer coatings* [16, 65 – 69].

The differences between Taxus and Cypher can be explained by the fact that sirolimus and paclitaxel are very different drugs with distinct mechanisms of action. Sirolimus is a macrolide antibiotic, whereas paclitaxel is the most widely used chemotherapeutic agent. Each drug affects a different stage of the cell cycle. Sirolimus arrest the cell before it enters the dividing cycle (phase G1), whereas paclitaxel interrupts cell division during the mitosis phase. Therefore sirolimus is regarded as a cytostatic drug and paclitaxel as cytotoxic [66].

But there are other factors which could influence the efficacy of drug-eluting stents in restenosis prevention. Before the application of drug-eluting stents, stent design was also

considered an important predictor for the rate of restenosis [67]. There are no studies available yet that compare different stent designs with identical coatings.

The presence and type of polymeric coating may also influence the rate of in-stent restenosis and stent thrombosis [68, 70, 71]. Polymers can be associated with ongoing vascular inflammation and delayed vascular healing [72, 73]. Especially non-degradable polymers can be dangerous since no long-term studies are available [74]. Little information is available concerning the detailed role of polymers used on Cypher and Taxus stents. Data from animal stent models suggest that both stents have an increased rate of ongoing vascular inflammation compared with bare-metal stents [75].

Considering the first long-time studies with non-degradable polymers, using biodegradable polymers as matrix for drugs seems to be a reasonable alternative to prevent restenosis. Biodegradable matrix can fulfill its assignment (controlling drug release) and degrade without toxic degradation products.

Another possibility to produce safe drug-eluting stents is to coat stents directly with the drug, without using polymer matrix.

These coatings have the following limitations:

- Insufficient adhesion of the drug to the stent surface, especially during the implantation procedure and stent deployment.
- Chemical stability of the drug. Stent coated only with the drug have a shortened storage life than stents coated with drug embedded in a polymer matrix.
- Ability of drug release controlling is limited.

A further novel method to coat stents and prevent restenosis is individualized drug dosage. Dose adjustments at the discretion of the interventional cardiologist to adjust the dosage of the compound on the drug-eluting stent may be desirable to enable an individualized dose adjustment for specific lesion or high risk patients, e.g. higher drug doses for diabetic patients.

4 Theoretical background

4.1 Controlled versus conventional drug therapy

Important factors in drug delivery are the therapeutic window and the therapeutic index of the drug. The therapeutic window (Fig.4.1) is the range of dosage of a drug or of its concentration in a tissue to provide a safe and effective therapy [77]. The therapeutic index is the ratio between the toxic dose and the therapeutic dose of a drug, used as a measure of the relative safety of the drug for a particular treatment [77]. Conventional drug therapy typically involves the periodic dosing (tablets, injections) of a therapeutic agent that has been formulated in a manner to ensure its stability, activity and bioavailability.

For most drugs, conventional methods of formulation are effective, but there are also drugs which require continuous administration [78], especially in cases when drugs:

- are unstable and / or toxic,
- have a narrow therapeutic range,
- exhibit extreme solubility problems,
- require localization to a particular site in the body,
- require strict compliance or long-term use.

In such cases continuous administration of the drug is desirable to maintain stable plasma drug levels and can be achieved by using an infusion pump or a polymeric drug delivery system. Controlled release denotes a system which can provide some control of a temporal or spatial nature, or both, during drug release in the body. The system is aimed to control drug concentrations in the target tissue or cells.

In general, controlled delivery attempts to:

- Sustain drug action at a predetermined rate by maintaining a relatively constant, effective drug level in the body with concomitant minimization of undesirable side effects.
- Localize drug action by spatial placement of a controlled release system (usually rate-controlled) adjacent to or in the diseased tissue or organ.

- Target drug action by using carriers or chemical derivatization to deliver drugs to a particular target cell type [79].

In practice very few of the applied systems fulfill all of these requirements. In order to maintain a constant drug level in either plasma or the target tissue, the release rate from the controlled release system should be equal to the elimination rate from plasma or target tissue.

Figure 4.1 shows comparative blood level profiles obtained from administration of conventional, controlled, as well as prolonged release dosage forms. The conventional tablet or capsule provides only a single and transient burst of drug. As long as the amount of drug is above the minimum effective concentration, a pharmacological response is observed. Problems occur when the therapeutic range is very narrow or when the peak of drug concentration is greater than the upper limit of this range.

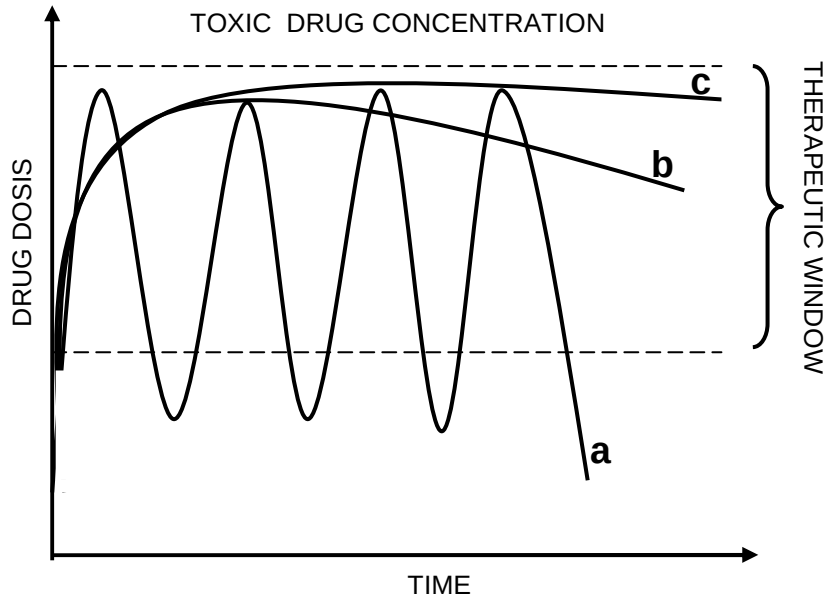

Fig.4.1: *Patterns of drug delivery. Plasma drug concentration – profiles for a) conventional tablet or capsule formulation, b) sustained release formulation and c) zero-order controlled release formulation. Curves b) and c) are examples of controlled drug release. Modified according to [78].*

One of the main purposes of controlled release is to improve safety and minimize side effects of the drug by reducing fluctuations in drug dosis. Prolonged release dosage forms

also reduce fluctuations in plasma drug levels by decreasing the adsorption rate as a result of a slower drug release rate [79].

Three types of therapeutic systems are available:

- passive pre-programmed
- active pre-programmed
- active self-programmed

Most rate-controlled release systems fall in the category of passive preprogrammed, in which the release rate is predetermined and is irresponsive to the external biological environment. The active preprogrammed systems adjust the release rate by a source external to the body e.g.: insulin pumps. The active self-programmed therapeutic systems modulate the release rate of the drug in response to information registered by a sensor on the changing dynamic biological environment such as blood sugar level in diabetes (membranes for insulin delivery).

4.2 Polymers in controlled release

The most popular drug delivery systems are polymeric systems made of degradable or non-degradable polymers. Polymeric matrices can protect drugs having short in vivo half-lives and improve the bioavailability of drugs having low aqueous solubility. Polymer-based drug delivery systems can be localized to a desired site reducing systemic toxicity and this localization can increase drug efficiency by over an order of magnitude.

These potential advantages must be viewed in light of the disadvantages that might be associated with the use of polymeric systems.

The implanted polymer must have the following features:

- biocompatibility
- no inflammatory response
- non-toxic degradation products of biodegradable polymers [80]

Chemical properties of a polymer determine many of the characteristics of the devices that are fabricated from it. Very important is the polymer structure and linkage type. Linear polymers are generally used in biodegradable drug delivery devices because cross-linking reduces matrix permeability and inhibits polymer degradation. The synthesis of the polymer is the key process which determines its chemical and physical properties. Any impurity in the monomer, use of additives or variation in the synthesis can result in a change in polymer composition and hence a change in matrix degradation and release characteristics.

Physical properties and morphology are also very important in drug release. Molecular weight is particularly important in determining the mechanical properties of a polymer as well as its capacity to be shaped and molded. Reduction in molecular weight can accelerate polymer degradation which sometimes is a desirable effect, but can also result in increased polymer crystallinity. During in vivo degradation polymer crystallites can be released from the device. The dimension of these crystallites is not predictable and can lead to unequal drug release as well as evoke undesirable foreign body reactions. To achieve a homogeneous drug delivery, the polymer matrix should be amorphous. Polymers for drug delivery can be separated into glassy and elastomeric ones, where the lower the glass temperature the higher the polymer permeability is. Elastomeric polymers have high permeability but occasionally lack mechanical strength.

Most delivery systems have been designed based on either a specific drug or a particular class of drugs. Specific chemical, physical and biological characteristics of the drug and the environment conditions are of primary importance in designing a delivery system. The drug and the matrix must be chemically compatible, e.g. the drug must be stable in the matrix and it must not interact with the matrix. Physical properties of the drug, including its molecular weight and solubility in biological fluids and in the polymer matrix, can affect the delivery rate of diffusion controlled devices by influencing the drug's diffusivity. Biological characteristics of the drug, such as efficiency, toxicity, and half-life, are critical in choosing a delivery vehicle. Finally, the target tissue and treatment duration directly affect the choice of a delivery system [78].

Implanted drug delivery systems can be classified into two groups (Fig. 4.2):

- Systems with an additional carrier material (e.g., polymer matrix) which controls drug release by appropriate selection of the polymer carrier.
- Systems without an additional carrier material. In these systems drug diffusion is controlled only by the implant geometry and by surface or structural patterns, i.e. pores.

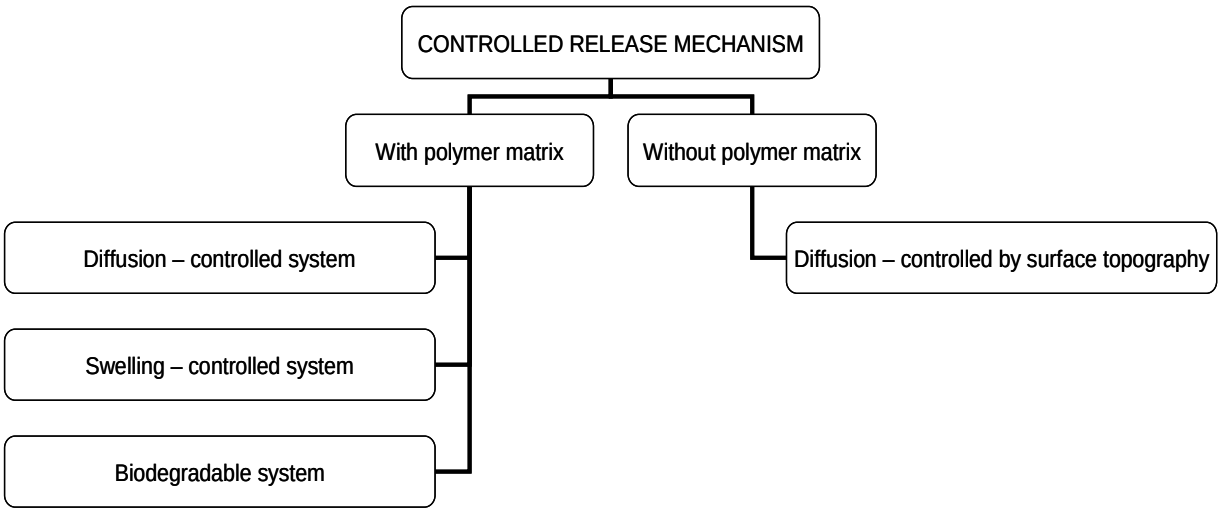

Fig. 4.2: *Overview of different drug-release mechanisms. Include classification of drug delivery devices with and without polymer matrices. Modified according to [81, 82]*

4.2.1 Classification of polymeric systems in controlled drug release

There are many possibilities to classify controlled release polymeric systems. One of the classifications suggested by Langer and Peppas [82] and later modified by Narasimhan [83] is based on the mechanism of drug release. According to this group delivery systems can be classified into the following categories.

1. **Diffusion-controlled systems** – diffusion of the drug through a polymer controls the release rate
   - Reservoir (membrane) devices
   - Monolithic (matrix) devices
2. **Swelling-controlled systems** – Swelling of the polymer and subsequent diffusion of the drug through the polymer controls the release rate.

3. **Chemically-controlled systems** – Hydrolytic or enzymatic cleavage results in polymer swelling, erosion, or release of covalently bonded drug by cleavage of a pendent chain.
4. **Osmotically-controlled systems** – Osmotic forces control the release of drug.
5. **Dissolution-controlled systems** – Dissolution of the polymeric carrier results in release of drug.
6. **Externally-controlled systems** – external stimuli results in release of drug.

- Magnetically-controlled systems
- Ultrasound-controlled systems

The rate limiting the step of the release process may be pure drug diffusion according to Fick's law (diffusion controlled systems), chemical reaction at the continuously depleted interface between the polymer and the dissolution medium (chemically controlled systems), or countercurrent diffusion of dissolution medium at constant penetration velocity in the polymer (swelling-controlled systems). Due to the complexity of polymer drug-release systems often two or more of these processes may take place.

Diffusion-controlled systems

Diffusion-controlled systems are the most widely used systems, and they are formulated in two basic configurations: reservoirs and matrices. For drug-eluting stents which have been approved for use in the USA or Europe, non-degradable polymers are used [84].

Reservoir systems

In reservoir systems a core of drug is surrounded by a swollen or non-swollen polymer film, and diffusion of the drug through the polymer is the rate-limiting step (Fig.3.3). There are many factors that affect the diffusion coefficient of the drug in the polymer, including the properties of the polymer (see Table 4.1) and the drug.

Polymer type	Factors affecting drug diffusion coefficient
semicrystalline polymers	- degree of crystallinity - crystallite size
swollen polymers	- degree of swelling - translational and relaxation behavior of the polymer
crosslinked polymers	- polymer networks - the degrees of crosslinking and mesh size (the distance between adjacent crosslinks)
porous polymers	- the porous structure - tortuosity affect

Table 4.1: *Polymer-dependent factors affecting drug diffusion in diffusion controlled systems.*

Properties of the drug, such as the drug's size and affinity for the polymer also affect diffusion coefficients. Typical values of diffusion coefficients (D_{12}) are $10^{-6} – 10^{-8}$ cm^2/s for elastomeric polymers and $10^{-10} – 10^{-12}$ cm^2/s for glassy polymers [83].

Monolithic systems

Matrix devices (Fig. 4.3) have a major advantage over reservoir devices because they are easy to formulate, provide a higher initial release rate than reservoir ones, and can be designed to release at a nearly constant rate. Monolithic devices are the ones in which a drug is either dispersed or dissolved in a polymer carrier.

Different modeling techniques have been used for different types of monolithic systems. The type of model used depends on whether the drug is dissolved or dispersed in the device and whether the device is porous or nonporous. Drug diffusion from porous systems can be very complex to model due to the random nature of the pore network and the dynamic nature of the pore structure that constantly changes during the course of the drug release. For many monolithic systems, the drug release rate is proportional to the half-life time of the drug. The release rate of drug decreases with time because there is no rate controlling membrane. The reason drug release decreases with time from matrix devices is because the drug is released from the surface layer having only a short distance to travel;

later on, the drug from deeper layers of the matrix is released having a longer distance to travel [81 – 83].

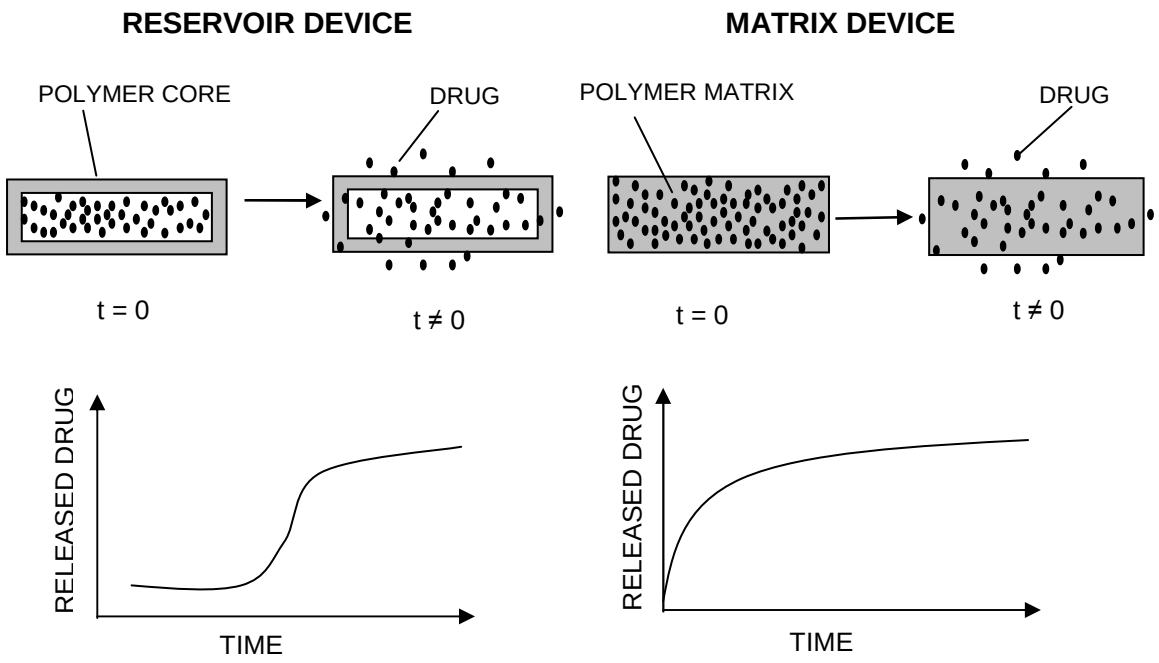

Fig.4.3: *Comparison of drug release from reservoir and matrix (monolithic) devices. Characteristic for reservoir device is that at the beginning of the release the drug elution process takes place slowly which is caused by drug diffusion through the polymer barrier. Matrix devices, in contrast, release the drug almost immediately at the beginning of the elution process and the desired level in the target spot is reached relatively quickly. Modified according to [82 – 84].*

4.2.2 Biodegradable polymers in drug release systems

Biodegradable matrix in drug-release systems

In this case drug release is caused by the biological degradation of the carrier material (polymer matrix). Drug release depends on the mesh size and the nature of the material and on the drug diffusion mechanism within the matrix [85].

According to the kind of degradation, the systems are differentiated into two categories:

- bulk degradable systems
- surface degradable systems (Fig.4.4)

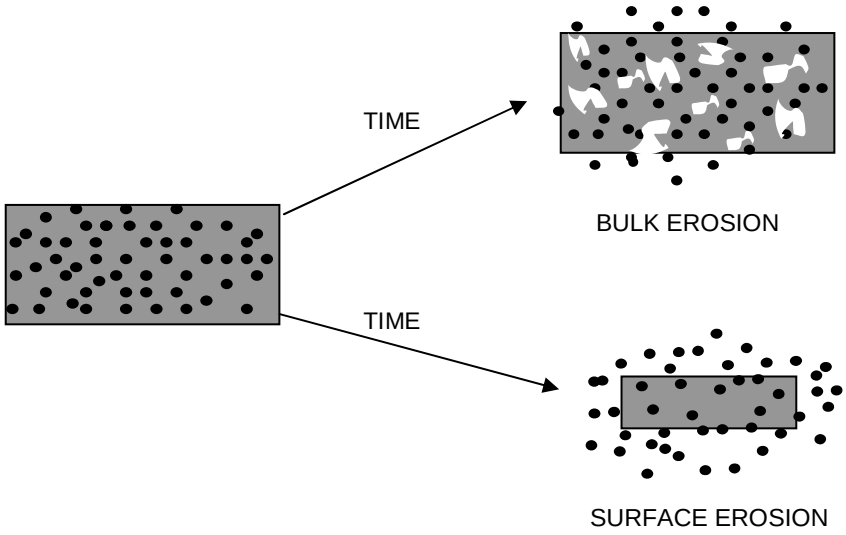

Fig. 4.4: *Biodegradable systems: bulk and surface erosion. Bulk erosion is characterized by a decreasing molecular weight of the entire polymer matrix, caused by diffusion of the medium into the polymer bulk. In surface erosion water (or another degradation medium) does not diffuse into the polymer bulk. Modified according to [81].*

The method of erosion depends on the diffusivity of water inside the matrix, degradation rate of the polymer's functional groups and matrix dimensions. Bulk degradation promotes the diffusion of water inside the polymer which is faster than polymer degradation. Decomposition occurs in the entire polymer matrix and a decrease of the molecular weight distribution (MWD) begins when the polymer reaches the so-called critical MWD. In bulk degradation the drug can be completely bound in the polymer matrix for a quite long time. When the polymer achieves the critical MWD and degrades, the drug release can be very rapid. In surface erosion small oligomers are separated from the polymer surface. Here rapid MWD lost can be remarkable. Rush polymer decomposition at relatively slow diffusion rate of solvent (water) into the bulk can be observed [81, 78].

4.2.3 Mathematical models of drug release from a polymer matrix

The most often used mathematical equation to describe the release rate of drugs from matrix systems is the so-called Higuchi equation published in 1961 (Eq.4.1).

$$\frac{M_t}{A} = \sqrt{D(2c_0 - c_s)c_s t} \qquad c_0 > c_s \qquad \text{(Eq.4.1)}$$

where:

M_t – cumulative absolute amount of drug released at the time t

A – area of the controlled release device exposed to the release medium

D – drug diffusivity in the polymer carrier

c_o; c_s – initial drug concentration and the solubility of the drug in the polymer, respectively

Equation (4.1) can be also expressed as:

$$\frac{M_t}{M_\infty} = K\sqrt{t} \qquad \text{(Eq.4.2)}$$

where:

M_∞ – absolute cumulative amount of drug released at infinite time (should be equal to absolute amount of drug incorporated within the system at time t = 0)

K – constant reflecting the design variables of the system [86, 87].

Initially valid for planar system only, the equation was later modified and extended to consider different geometries and matrix properties including porous structures [86]. Peppas pointed out that the classical Higuchi equation generally cannot be applied to real controlled release systems because it was derived under pseudo-steady state assumptions [88]. However, due to the simplicity of this equation, researchers have used it to model their systems in order to estimate the release mechanism. However, when applying Higuchi equation to controlled drug delivery systems, the following assumptions of this model should be kept in mind:

- Initial drug concentration in the system is much higher than the solubility of the drug

- Mathematical analysis is based on one-dimensional diffusion. Thus edge effect must be negligible.
- The suspended drug is in a fine state such that the particles are much smaller in diameter than the thickness of the drug release system.
- Swelling or dissolution of the polymer carrier is negligible.
- The diffusivity of the drug is constant [86].

It is evident that these assumptions provide a lot of limitations in using the Higuchi equation. Proportionality between the fractional amount of drug released and the square root of time can be derived as well from an exact solution of Fick's second law of diffusion for thin films of thickness δ under perfect sink conditions, uniform initial drug concentration with initial drug concentration smaller than the solubility of the drug in the polymer ($c_o < c_s$) and assuming constant diffusivities:

$$\frac{M_t}{M_\infty} = 4\left(\frac{Dt}{\delta^2}\right)^{1/2} = k'\sqrt{t} \qquad \text{(Eq.4.3)}$$

where:

M_t – cumulative absolute amount of drug released at the time t

M_∞ – absolute cumulative amount of drug released at infinite time (should be equal to absolute amount of drug incorporated within the system at time t = 0

D – drug diffusivity in the polymer carrier

k´ – constant

Thus, a proportionality between the fraction of drug released and the square root of time can also be based on these physical circumstances which are substantially different from those studied by Higuchi for the derivation of his classical equation. However, in both cases diffusion is the dominating mechanism and hence proportionality between the cumulative amount of drug released and the square root of time is commonly regarded as an indicator for diffusion-controlled drug release [89, 90].

A more comprehensive, but still very simple, semi-empirical equation to describe drug release from polymeric systems is the so-called power law:

$$\frac{M_t}{M_\infty} = kt^n \qquad \text{(Eq.4.4)}$$

Here M_t and M_∞ are the absolute cumulative amounts of drug released at time t and infinite time, respectively; k is a constant incorporating structural and geometric characteristics of the device and n is the release exponent, indicative of the mechanism of drug release [86].

As it can be seen, the classical Higuchi equation (Eq.4.1) as well as the above described short time approximation of the exact solution of Fick's second law for thin films (Eq.4.3) represent the special case of the power law were n = 0.5. Pepas and co-workers [91, 92] were the first to give an introduction into the use of the limitations of this equation. The power-law can be seen as a generalization of the observation that superposition of the two apparently independent mechanisms of drug transport, Fickian diffusion and second case transport, describes in many cases the dynamic of swelling and drug release from glassy polymers, regardless of the form of the constitutive equation and the type of coupling of relaxation and diffusion.

It is obvious from (Eq.4.4) that when the exponent n takes a value of 1.0, the drug release rate is independent from time. This case corresponds to zero-order release kinetics. For rectangular plates (slabs), the mechanism that creates the zero-order release is known among polymer scientists as case II –transport. Here the relaxation process of the macromolecules associated with the penetration of water into the system is the rate-controlling step. Water acts as a plasticizer and decreases the glass transition temperature (T_g) of the polymer. Once the T_g equals the temperature of the system, the polymer chains undergo a transformation from the glassy to the elastomeric state, with increasing mobility of macromolecules and volume expansion.

Thus, (Eq.4.4) has two distinct physical meanings in the two special cases:

- for diffusion controlled drug release $n = 0.5$
- for swelling-controlled drug release $n = 1.0$

Values of n between 0.5 and 1.0 can be regarded as an indicator for the superposition of both phenomena known as anomalous transport. These two extreme values for the exponent n are only valid for the slab device geometry. For spheres or cylinders different values have been derived and are listed in Table 4.2.

Exponent *n*			**Drug release mechanism**
thin film	**cylinder**	**sphere**	
0.5	0.45	0.43	Fickian diffusion
$0.5 < n < 1.0$	$0.45 < n < 0.89$	$0.43 < n < 0.85$	Anomalous transport
1.0	0.89	0.85	Case-II transport

Table 4.2: *Exponent n of the power-law and drug release mechanism for polymeric controlled delivery systems of different geometry. Modified according to [91, 92].*

Diffusion and chemical reaction based models

These models are based on the description of real physical processes involved in controlling drug release. For biodegradable systems, diffusion mass transfer and chemical reactions are important phenomena to be taken into account by mathematical modeling of the drug release. Heller and Baker [93] developed a mathematical model describing drug release from water-insoluble polymers which undergo hydrolytic degradation during which polymer chains are converted to water soluble monomers. They assumed that for polymer matrices undergoing bulk erosion, degradation can be described by first-order kinetics. Starting point for their mathematical analysis was the classical Higuchi equation (Eq.4.1) which can be written as follows:

$$\frac{dM_t}{dt} = \frac{A}{2}\sqrt{\frac{2Dc_0}{t}} \qquad \text{(Eq.4.5)}$$

where:

M_t – cumulative absolute amount of drug released at the time t

A – area of the controlled release device exposed to the release medium

D – drug diffusivity in the polymer carrier

c_o – initial drug concentration in the polymer carrier

In contrast to the assumption of Higuchi's original model, the permeability in biodegradable polymeric systems is not constant but increases with time. To calculate this phenomena Heller and Baker assumed the following relationship between D_t, the drug permeability at time *t*, and the initial permeability D_0*:*

$$\frac{D_t}{D_0} = \frac{initial\ \ number\ of\ \ bonds}{remaining\ number\ of\ \ bonds} = \frac{N}{N-Z} \qquad \text{(Eq.4.6)}$$

where:

N – number of initial bonds

Z – number of cleavages during the time interval [0 ; *t*]

From the assumption that polymer bonds are cleaved according to a first-order kinetic, it follows that:

$$\frac{dZ}{dt} = K(N-Z) \qquad \text{(Eq.4.7)}$$

K – first order rate constant

Integration and rearrangement leads to an expression (Eq.3.8) that quantifies drug release from thin, bulk eroding polymer films:

$$\frac{dM}{dt} = \frac{A}{2}\sqrt{\frac{2D_0 \exp(K \cdot t)c_0}{t}} \qquad \text{(Eq.4.8)}$$

In Fig.4.5 the drug release rates calculated from (Eq.4.8) that considers diffusion and erosion is compared with the purely diffusion-controlled release kinetics calculated from classical Higuchi equation (Eq.4.1).

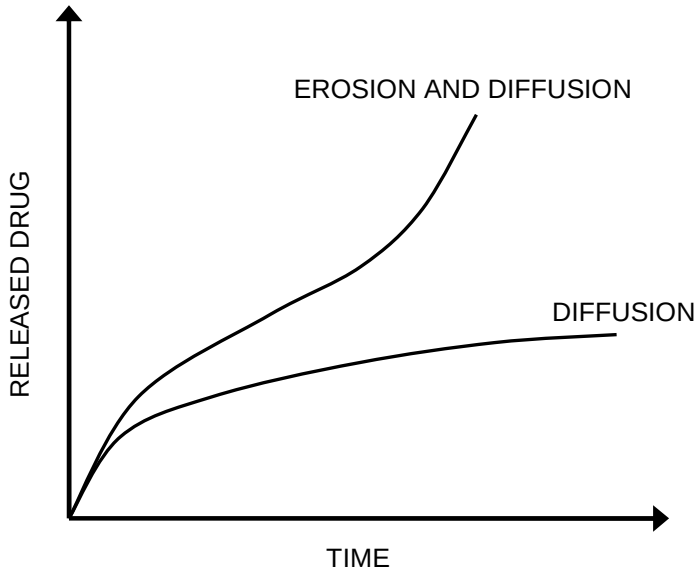

Fig.4.5: *Model of Heller and Baker [93] describing drug release from thin biodegradable polymer films undergoing bulk erosion or diffusion – controlled release kinetic calculated from Higuchi equation.*

This thesis is focused on non – polymeric and biodegradable polymeric drug delivery systems based on theoretical considerations and experimental results. As mentioned above the simulation and mathematical modeling of these systems are very complex and may fail whenever there is a need for taking specific physiochemical processes into account. Biodegradation of a polymer usually involves chemically or enzymatically catalyzed hydrolysis. Biodegradable polymers have both advantages and disadvantages when compared with the use of non-degradable polymers for controlled drug delivery. The major advantage is that biodegradable polymers do not require removal after delivering their dose. Additionally, adverse tissue reactions from the implanted polymer are ameliorated as the polymer degrades [61]. As mentioned in the introduction, non-degradable polymer stent coatings are presumed to be toxic and long-term studies showed that late thrombosis and late in-stent restenosis may lead to the patient's death [117, 122]. An alternative for stable polymer stent coatings could be coating with traceless degradable polymers or coating stents with the drug only.

5 Materials

5.1 Stents

For the drug release investigations, standard commercially available 316 L stainless steel stents (Translumina, Germany) were used (Table 5.1). Stents with two kinds of surface modification were provided: CURARE® with electropolished surface and YUKON® with sandblasted surface. Due to the complicated stents geometry some tests were performed on 1 cm x 1 cm plates made of the same material (316 L) and modified in the same way as the stents.

Element	Fe	Ni	Cr	Mo	Mn	Si	C	P	Cu	N	S
Weigth [%]	62.7	14.72	17.33	2.75	1.8	0.36	0.017	0.018	0.08	0.076	<0.002

Table 5.1: *Chemical composition of 316 L stainless steel used for stents and plates. According to supplier, Translumina Inc.*

5.1.1 Surface modification

Stent surface was modified to investigate the influence of surface properties on drug release. The following modification processes were performed: electropolishing, etching and sandblasting. Electropolishing is a chemical process where a special acid mixture is used to achieve a smooth metal surface. This method provides a particle free, corrosion – resistant surface. Another electrochemical modification of stent surface is evaluated in our Institute. This technique, called metal grain boundary etching described in detail in [94]. After the etching procedure drug depots in the stent surface with average size of ca. $10\mu m^3$ were formed. Sandblasting is a mechanical method to modify the metal surface. During this process the stent surface is bombarded with a granular medium (corundum A220, avg. grain size: 40 - 70µ) for a 20 seconds with pressure 1.6 bar to increase surface roughness without deep depots. Each surface modification method was reproducible. The stents with surface modifications are shown below (Fig. 5.1)

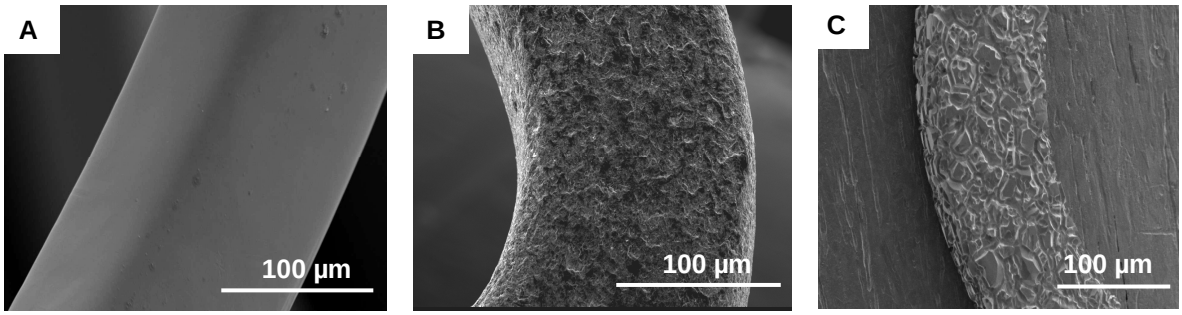

Fig.5.1: *Scanning electron micrographs: Figures show different modifications of metallic stent surfaces A – electropolished, B - sandblasted and C - etched surface.*

5.2 *Drug (rapamycin)*

Rapamycin, also called sirolimus, is a natural macrocyclic lactone with potent immunosuppressive action which was approved in 1999 as an immunosuppressive drug in renal transplant recipients. The drug is produced by cultured *Streptomyces hydroscopicus*. Rapamycin ($C_{51}H_{79}NO_{13}$) is a white crystalline solid. Due to its lipophilic character rapamycin is soluble in methanol, ethanol, acetone, chloroform, dimethyl sulfide and minimally soluble in water (2,6 µg/ml). It is sensitive to light and particularly susceptible to degradation in plasma. In basic solutions it undergoes fragmentation and water addition reactions [122]. Sirolimus blocks cell-cycle progression and expression of inflammatory cytokines, thus inhibiting cellular proliferation.

The mechanism of action of sirolimus is distinct from other immunosuppressive agents since it acts solely by inhibiting DNA synthesis. Up regulation of FK506-binding protein 12 (FKBP12) has been observed in human neointimal smooth muscle cells. The sirolimus FKBP complex binds to a specific cell cycle regulatory protein, the mammalian target of rapamycin (mTOR), and inhibits its activation. The inhibition of mTOR ultimately induces cell-cycle arrest in late G1 phase and consequently arrests smooth muscle cell growth. Its low toxicity, anti-inflammatory effects, and potent cytostatic action place sirolimus at the top of the list of anti-restenotic agents for local drug delivery [95 - 100]. For this study 99.8% rapamycin was purchased from Oskar Tropitzsch GmbH, Germany. The purity and chemical composition of rapamycin were confirmed by FTIR and HPLC measurements.

5.2.1 Rapamycin labeling with anthracene carboxylic acid (rapamycin – ACA)

In order to carry out quantitative examinations of the coatings and determine drug diffusion into the artery wall, it was necessary to label rapamycin.

A common strategy for labeling substances is the use of a fluorescence marker to make the desired molecule visible by irradiating it with ultraviolet light. A simple route leads to the coupling of the alcohols with an acid derivate of a small molecule with a sufficient delocalized π-electron system with adequate absorption and emission characteristics.

Anthracene, with absorption at 380 nm and emission at 450 nm, seems to be a perfect candidate for this purpose. For the condensation of anthracene carboxylic acid with the hydroxyl group of the drug, DCC (N,N'-dicyclohexylcarbodiimide) and 4-(dimethylamino)pyridine DMAP were chosen, as a coupling agent (see Fig. 5.2).

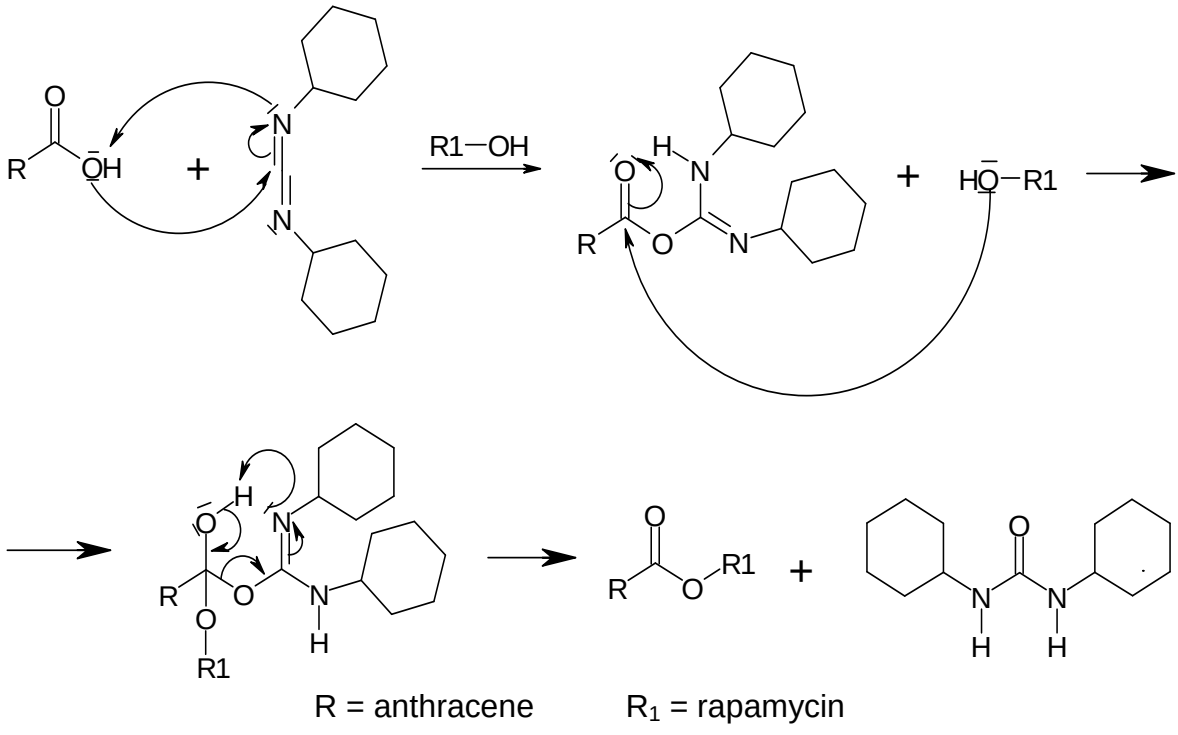

Fig. 5.2: *Reaction mechanism of coupling anthracene carboxylic acid with the alcohol using DDC as a coupling agent.*

The reaction gave the main product (*a*, Fig. 5.3) in good yield (65%). The main product and the by-product *b* were obtained in a 6:1 ratio with no multiple substitutions, as seen in the mass spectrum. Given that the main goal was to label the molecule, both products can be used in further experiments. In addition, the other by-products derived from the DCC and DMAP as well as remaining reactants are, in contrast to the nonpolar rapamycin-ACA (R_f = 0.9 *a*, 0.8 *b* in H/EA: 50/50), very polar molecules (R_f = 0-0.1 in H/EA: 50/50), which guarantees a fast and clean purification if aliphatic solvents are used. Overall, the reaction can be performed in a single reaction vessel and the purification could be shortened by using a plain simple glass tube filled with silica gel.

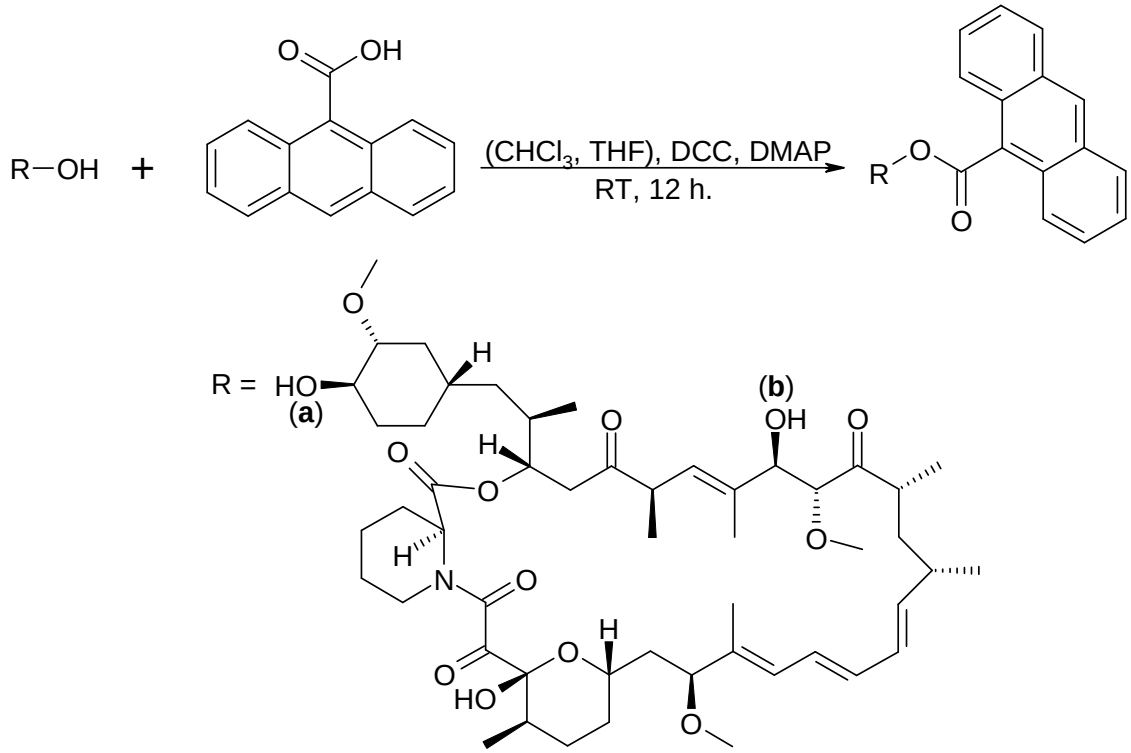

Fig. 5.3: *Schematic reaction of rapamycin labeling with anthracene carboxylic acid.* ***(a)****-substitution place for main product,* ***(b)*** *– substitution place for by-product. a / b ratio 6:1*

5.2.2 Toxicity tests of labeled rapamycin

Determination of the uptake of labeled rapamycin into cells was performed by using Human Umbilical Vein Endothelial Cells (HUVEC). As a reference for these tests, non-labeled rapamycin was used. Concentrated solutions in PBS were made of both labeled and non-labeled drugs at concentrations of 1 mg/l, 10 mg/l, and 100 mg/l. These solutions were added to the medium in cell culture plates. Cells were investigated by fluorescence microscopy at increasing incubation times of 30 min, 60 min, 90 min and 24 hours. To visualise anthracene carboxylic acid labeled rapamycin a DAPI filter was used – luminescence in blue light spectrum.

For toxicity tests cell nucleus staining using Calcein and Ethidium homodimer were performed. Observations of live/dead tests were performed using fluorescence microscopy with a FITC filter. Labeled HUVEC showed a similar metabolic activity as the control, indicating preserved cell viability and function.

5.3 Polymers

There is a number of biodegradable polymers used as matrices for controlled drug release. The polymer chosen depends on the place of release and polymer properties. Polyesters based on the lactic acid have shown their safety as suture materials. The great advantages of these polymers are their degradation by simple hydrolysis of the ester backbone in an aqueous environment, such as body fluids. Finally, the degradation products are metabolized to carbon oxide and water [140].

Polyesters generally degrade in four major stages:

1. Polymer hydration causing disruption of the primary and secondary structure by altering hydrogen bonding and van der Waals forces
2. Strength loss caused by the rupture of covalent bonds in the polymer backbone
3. Loss of mass integrity resulting in initiation of absorption
4. Loss of mass resulting in polymer dissolution and phagocytosis [101].

The hydrolysis rate depends on the physical properties of the matrix. Widely used biodegradable polyesters are polylactic acid and polyglycolic acid. Polylactic acid is generally synthesized from dilactide, the cyclic diester of lactic acid by heating under vacuum in the presence of a catalyst. Poly(d,l-lactic acid) is an amorphous polymer with a T_g of 57ºC while poly(l-lactic acid) is highly crystalline [102]. The crystallinity of poly(l-lactic acid) can be reduced by copolymerizing it with either its D-enantiomer or with another hydroxyl acid such as glycolic acid. This is often done to increase its permeability toward hydrophobic drugs [103].

Molecular weight is an important property of biodegradable polyesters. The rate of in vivo degradation of polylactic acid matrices has shown to be inversely proportional to the polymer molecular weight. Polylactic acid has uncritically low toxicity and sufficient biocompatibility. When implanted in animals it is not retained in any vital organ [102, 104]. In this thesis medical grade poly(d,l-lactic acid), polyglycolic acid and their copolymers (Boehringer Ingelheim, Gremany) were used (Table 5.2)

Name	**Art of polymer**	**Inherent Viscosity [dl/g]**	**Molecular weight [k Da]**
Resomer L 210 S	Poly(l-lactic acid)	3.3 – 4.3	483 -788
Resomer R 202 S	Poly(d,l-lactic acid)	0.16 – 0.24	6 – 16
Resomer R 202 H	Poly(d,l-lactic acid)	0.16 – 0.24	6 – 16
Resomer R 203 S	Poly(d,l-lactic acid)	0.25 – 0.35	16 – 30
Resomer R 207 S	Poly(d,l-lactic acid)	1.3 –1.7	195 – 270
Resomer RG 502	Poly(d,l-lactic-co-glycolic) 50:50	0.16 – 0.24	5 – 12
Resomer RG 503	Poly(d,l-lactic-co-glycolic) 50:50	0.32 – 0.44	24 – 34
Resomer RG 504	Poly(d,l-lactic-co-glycolic) 50:50	0.45 – 0.60	35 – 63

Table 5.2: *Index of polymers used and their selected properties. Data from Boehringer Ingelheim*

5.4 Solvents / chemicals

When selecting solvents for drugs and polymers aimed for clinical application it is very important to pay attention to its biocompatibility and the ability of the solvent to evaporate immediately after coating. In the coating method used based on spraying the drug solution onto the device directly before implantation, the residual solvent in the implant is also an important consideration in this work. Solvents were carefully selected according to their biocompatibility and ability to evaporate quickly and traceless.

As a solvent for rapamycin pure ethanol was used. Due to its very good biocompatibility and relatively high affinity for both water and a great range of organic compounds, ethanol has many pharmacological uses as a solvent. According to the “European pharmacopoeia” ethanol belongs to a group of solvents with insignificant toxic effect. The permitted daily exposure (PDE) range is 50 mg per day.

As a solvent for rapamycin and poly(d,l – lactide) ethyl formate was used. According to the “European pharmacopoeia” ethyl formate belongs to a group of solvents with low toxic effect. The permitted daily exposure (PDE) range is 20 mg per day. Moreover another advantage of ethyl formate is its relatively low boiling point. After coating, the ethyl formate evaporates very quickly and produces a homogeneous drug / polymer coating on the stent surface.

6 Methods

6.1 Stent surface characterization

Due to their complex geometry, stent further characterization is rather difficult to perform applying standard analytical methods. For some investigations 1cm x 1cm plates of 316 L stainless steel were used as model material. The surfaces of these plates were modified in the same way as the stent surfaces. Optical and mechanical methods were used to quantitatively compare the surface finish.

6.1.1 Surface finish and roughness

Microscopy

The observation of stents using light microscopy was difficult due to their reflective metallic surface and relatively poor resolution. One of the best methods available to investigate the surface of metal stents (coated and uncoated) proved to be scanning electron microscopy (SEM). The SEM offers a large depth of field, which allows a large amount of the sample to be in-focus at one time. The SEM also produces images of high resolution, which means that closely spaced features can be examined at high magnifications. The preparation of the samples with a metallic coating is relatively easy since SEM requires the sample to be conductive.

Scanning electron microscopy (S – 3500 N, -Hitachi Science Systems, Tokyo, Japan) was used for stent surface and coating topology analysis. For all SEM investiagations, the samples were coated with gold (10 – 20 nm thickness) by using a sputter-coater (SCD 005, BAL-TEC AG, Balzers, Lichtenstein) under high vacuum with a current range of 40 - 60 mA and different sputter times.

Roughness of modified surfaces

Using SEM, differences between surface modifications were well visible but quantification of surface roughness was not possible.

The surface roughness of the modified stents was determined using three different methods:

- perthometry
- atomic force microscopy (AFM)
- white light confocal microscopy.

Roughness was determined for stents and also for 316L plates modified using the same methods to produce the same surface geometry.

Perthometry

For roughness measurements of stent surfaces a perthometer was used. This is a mechanical method in which a metal pin scans the surface, registers its topography and the resulting depth profiles are plotted on the integrated printer. The accuracy of this method is limited to the geometry of the scanning needle (Fig. 6.1).

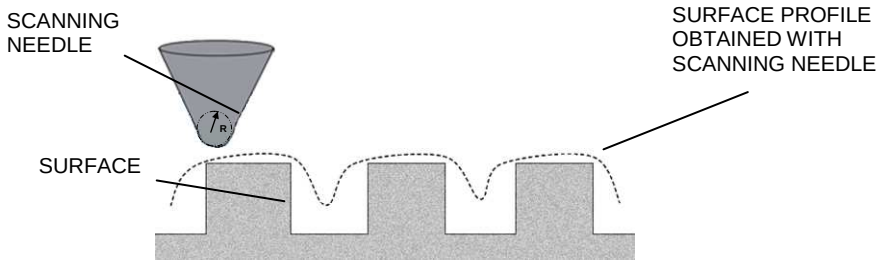

Fig. 6.1: *Roughness measurements using perthometer. Comparison of surface geometry profile and scanning needle. The resolution obtained with this method is limited by the geometry of the scanning needle.*

This method approximates the surface roughness and shows differences between the various modified surfaces (Fig. 6.2).

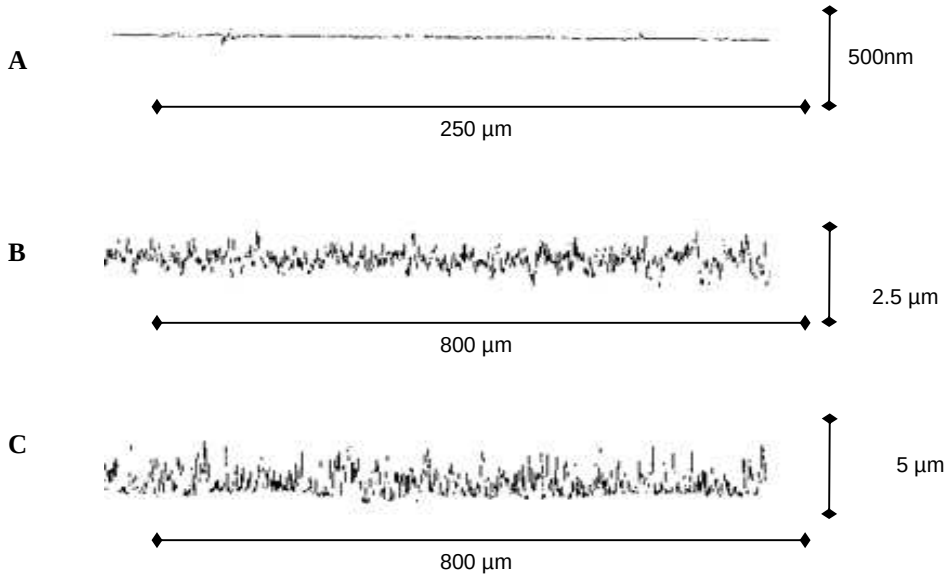

Fig.6.2: *Perthometer measurements of modified surfaces; A: polished, B: sandblasted and C: etched surfaces.*

Each surface modification (electropolished, sandblasted and etched surfaces) was investigated on three different specimens. For each specimen a minimum of three different areas were investigated to improve accuracy. Data from all following investigations were presented as the route mean square (RMS) according to the German standard DIN EN 180 4287.

Atomic force microscopy (AFM)

Despite following the same measurement principle (needle/cantilever) atomic force microscopy is considerably more accurate than the perthometer. Surface topography and a quantitative measurement of roughness were determined by using two different atomic force microscopes (AFM). First the AFM JSPM-5200 from JEOL Ltd. with UltraSharp™ silicon contact cantilevers (CSC 12/3) with spring constant 0.03 N/m was used. Measurements were performed in contact mode over a measurement area of 19.8 µm x 19.8 µm. Surface roughness was evaluated with the JEOL software. Due to the short spring constant and the small specimen chamber only 316 L plates were used for these measurements. Stents could not be investigated using this device.

The MFP-3D™ from Asylum Research was the second AFM device used for topography inspection. Here stent investigation was possible using a silicon cantilever with a spring constant of 2 N/m and using an AC–Mode. This device provided better results due to its larger measurement area of 90 µm x 90 µm for plates, and 20 µm x 20 µm for stents. The sampling area of the stents was smaller due to strut bending and geometry constraints.

A comparison of depth profile and plot of the modified surfaces is shown in Fig. 6.3 – 6.5

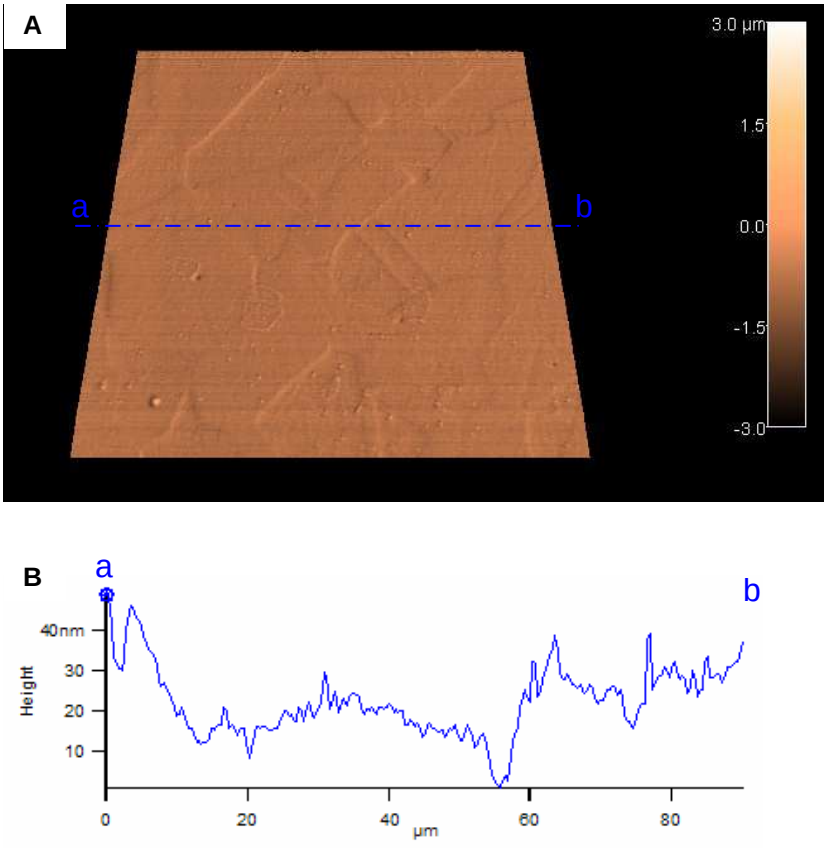

Fig. 6.3: *AFM picture (A) with depth profile (B) of electropolished surface*

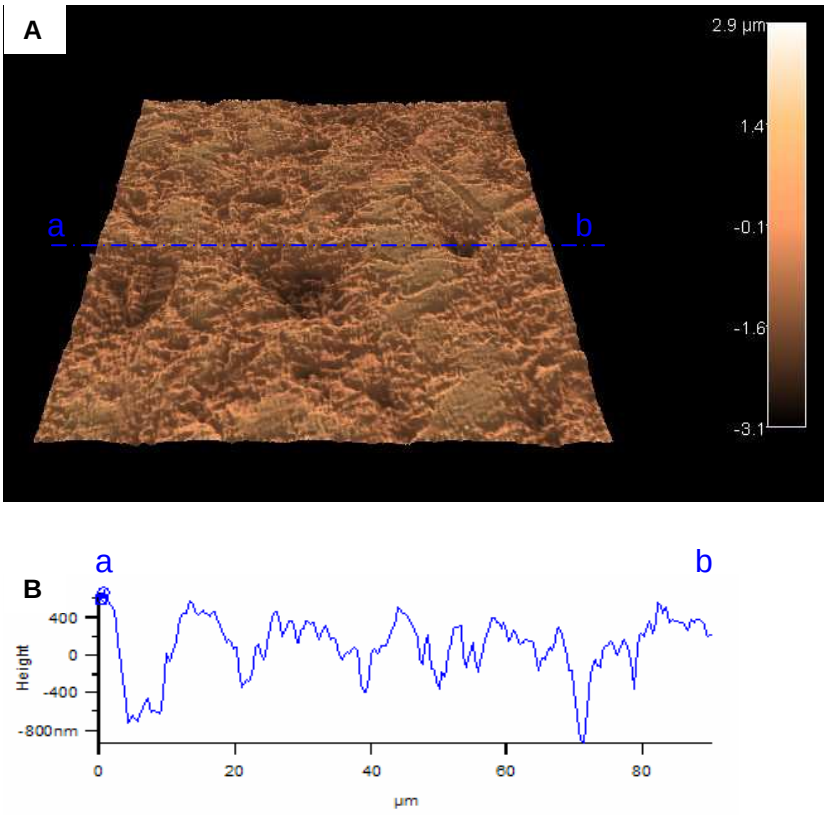

Fig. 6.4: *AFM picture (A) with depth profile (B) of sandblasted surface.*

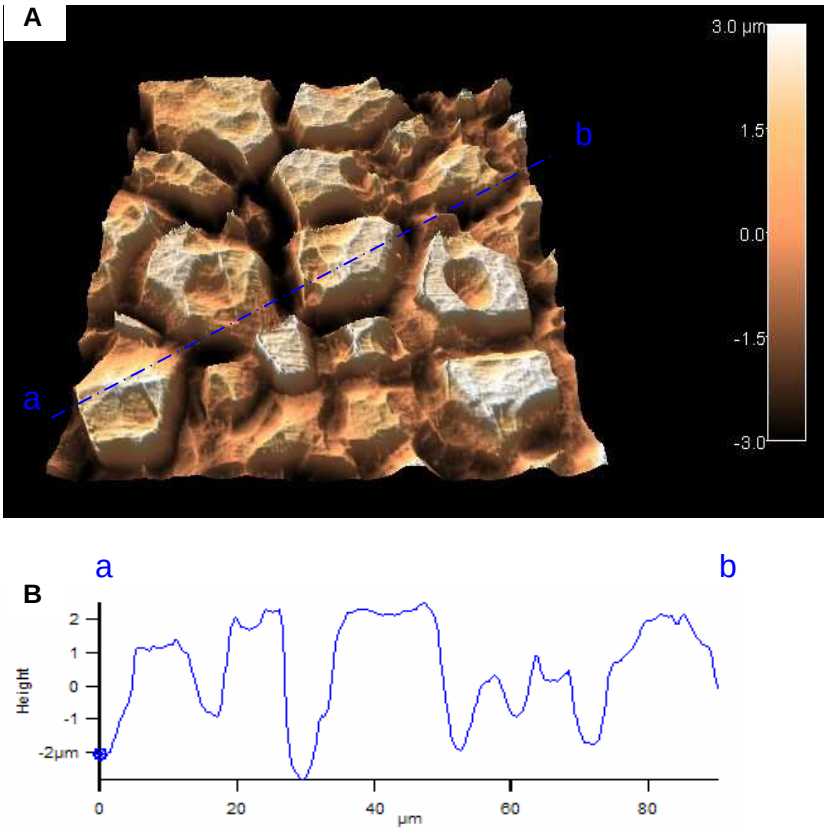

Fig. 6.5: *AFM picture (A) with depth profile (B) of oxalic acid etched surface.*

Confocal microscopy: µ-Surf® device (NanoFocus, Germany)

The best accuracy in roughness measurements was obtained by confocal white light microscopy. Surface topography is determined optically without the use of a mechanical needle, and surface penetration is performed using light. This method allows the determination of the surface topography and surface magnification v_r developed during etching and sandblasting.

Sequences of slices with the same height level were collected using a xenon lamp which highlighted the surface of the specimen and light reflections were detected on a CCD chip. The special aperture filters the reflection from out-of-focus plane. This process allows measurement points to be collected from only one plane at a time and the surface profile from each plane can be collected on the detector and can be used to generate a three dimensional picture of the surface.

For stents and plates measurements, objectives providing 20, 50 and 100 fold magnifications were used. Surface analyses were performed using the computer program Surface Analysis Module, SAM 2.6.

A

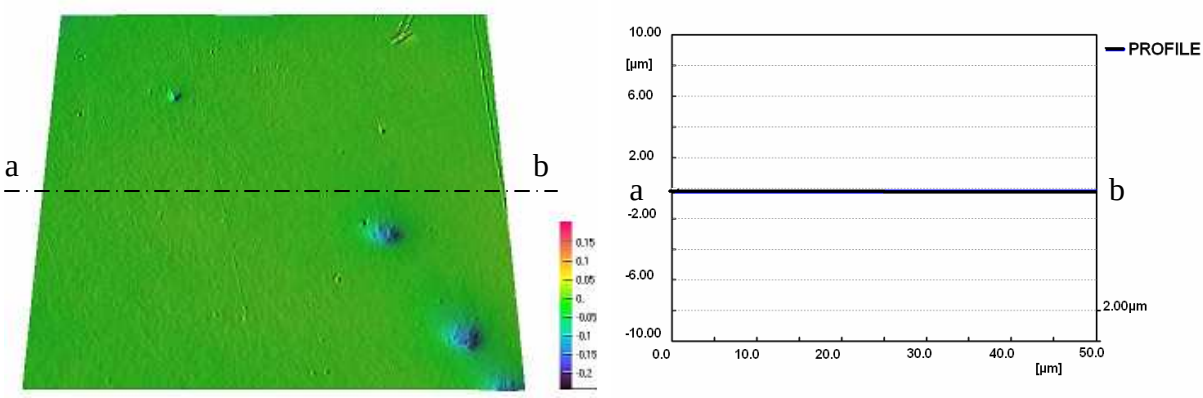

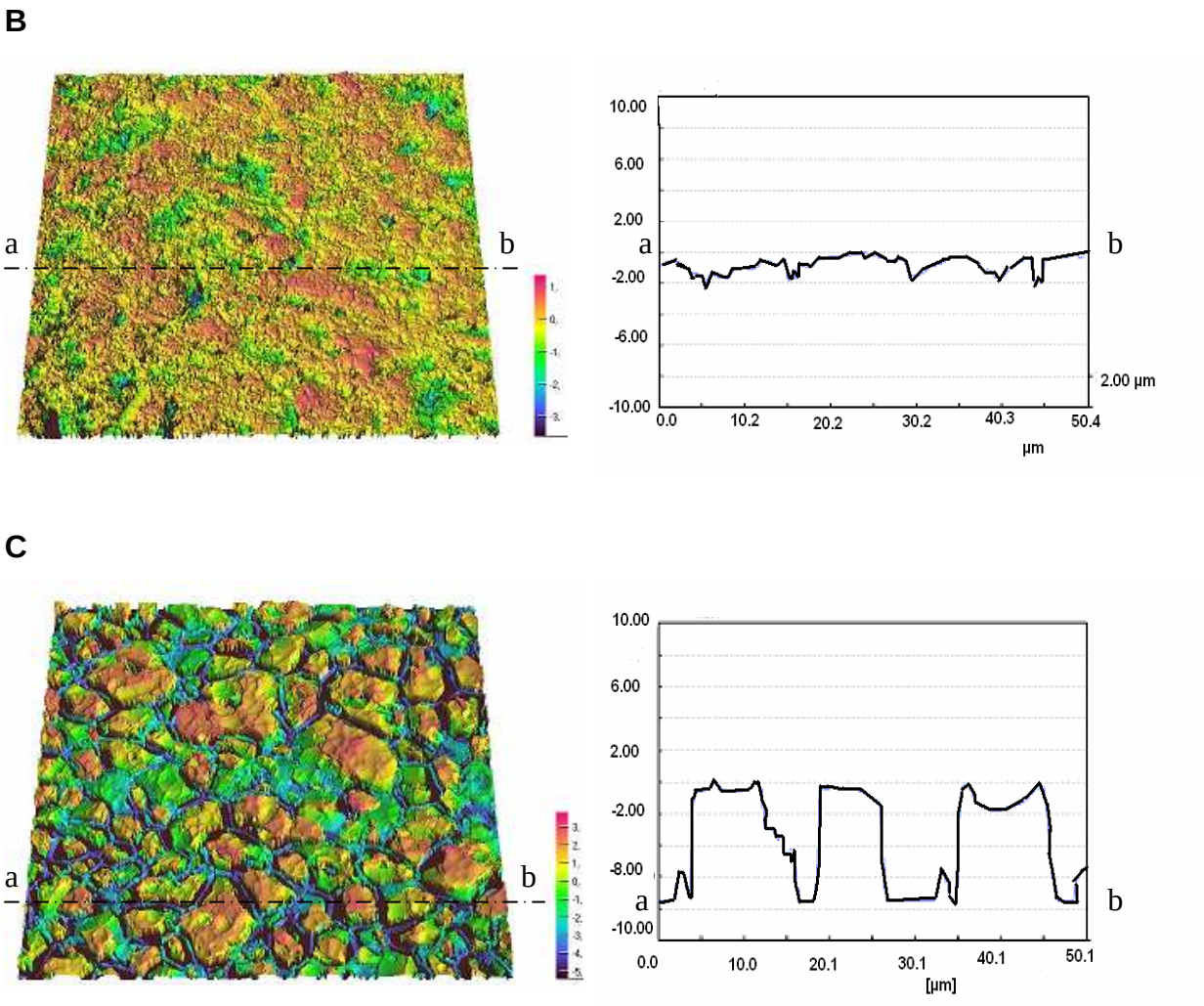

Fig. 6.6: *Topography of modified surfaces imaged using confocal microscope: A – electropolished, B – sandblasted, C – oxalic etched surface. The increasing of surface roughness from the electropolished to the oxalic etched surface is revealed as a color change in the left picture or in the profile picture shown right.*

6.1.2 Surface tension properties and surface wetting

These measurements allowed the determination of the contact angle of a liquid on the stent surface. This value is very important to determine the proper coating parameters and coating solution. On extremely hydrophilic surfaces, a water droplet will completely spread (an effective contact angle of 0°). This occurs for surfaces that have a large affinity for water (including materials that absorb water). On many hydrophilic surfaces, water droplets will exhibit contact angles of 10° to 30°. On highly hydrophobic surfaces, which are incompatible with water, a large contact angle (70° to 90°) is observed. The contact angle thus directly provides information on the interaction energy between the surface and the liquid (Fig. 6.7). If the contact angle of the substance on the surface is greater than 70°, the coating cannot cover the whole surface homogeneously.

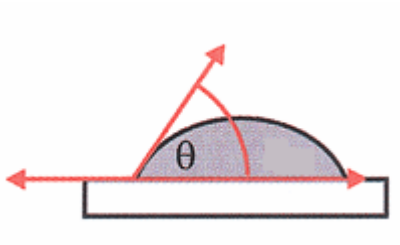

Fig.6.7: *Principle of contact angle measurements. In contour analysis the angle θ of the tangent of the drop contour is determined by using a video measurement technique.*

Contact angle measurements of different substances on modified 316L surfaces were performed using the contact angle device G10 connected with a video camera G1041 (Kruess, Germany). As test method “sessile drops” were used. The profiles of the drops on the surface were determined using tangent calculations with the software “DSA Drop Shape Analysis”. The common cone equation allowed the determination of the drop profile and the contact angle could be determined by differentiation of the equation on the base line.

To determine surface tension properties, common contact angle measurements on polished 316 L surface were performed. As test liquids distilled water and diiodomethane, which is a nonpolar liquid, were used. 10 µl were spread on the

surface at a rate of 10 µl / 60 s using an integrated needle. Pictures of the drops were taken always after a constant time interval of 60 seconds.

The wetting behaviour of stents with different surface modifications (sandblasted, electropolished and etched surfaces) was tested. For each surface modification a minimum of three different specimens were investigated. As the test liquid coating solutions of rapamycin in ethanol and PLLA or PLLA – rapamycin in ethyl formate were used. Due to the low boiling point of the solvents used, drops of coating solutions spread and evaporated very quickly from the surfaces. Thus, the equilibration of the drop on the surface was difficult to establish. To estimate the best position of the drop a sequence of videos were taken and the contact angle was measured 300 ms after the drop came in contact with the surface. To confirm the accuracy of these measurements, tests with a high speed camera were performed and each drop was filmed with 1800 frames per minute. The contact angle was determined using a Young-Laplace Fit from the DSA 10 software.

6.2 Stent coating

A new Stent Coating Machine (SCM) was developed within the framework of the ISAR (**I**ndividualized **S**tent system to **A**brogate **R**estenosis) Project (supported by a research grant AZ 504/02 from the Bayerische Forschungstifftung Munich, Germany) together with industrial partners Translumina GmbH, Hechingen, Germany and Seleon GmbH, Heilbronn, Germany. This coating system was especially designed to provide the physician with greater flexibility during drug selection and dosage. The process of stent coating takes place directly before implantation in the Catheter Laboratory making it possible to adjust the treatment depending on the patient's requirements. In this machine stents are coated using the spray coating method [127-129].

During coating a mobile spray nozzle moves along the stent which is fixed in a special housing (Fig. 6.8). The coating solution is placed in a reservoir and transported during the coating process by compressed air into a nozzle and sprayed onto the stent.

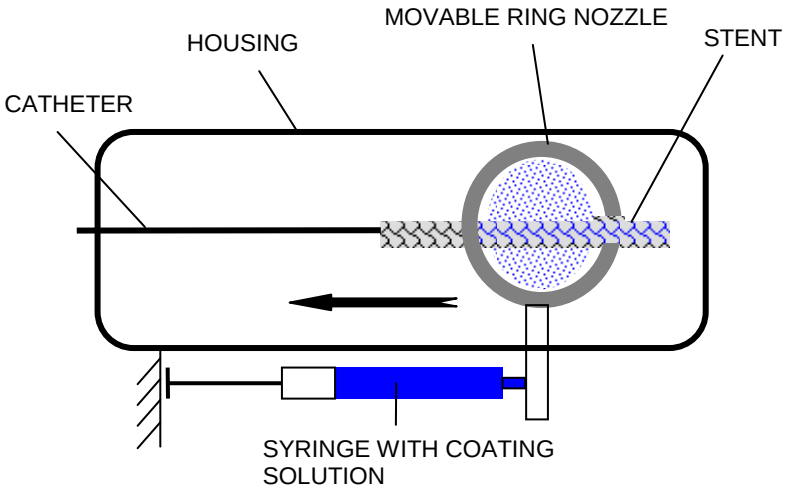

Fig. 6.8: *Schematic drawing of the stent coating machine developed to customize coatings in the catheter laboratory directly before implantation. The arrow indicates the motion of the ring nozzle along the stent during the coating process.*

There are a few important parameters which need to be taken into account during coating: air pressure, coating speed, and drying process. The selected parameters depend on the properties of the coating solution. To coat the stent only with the drug, different solutions of rapamycin in ethanol were prepared and the standard SCM was used. To coat the stent with the drug polymer solutions a special prototype of SCM was required due to the high viscosity of the polymer. In this machine parameters such as coating speed, air pressure and drying process are programmable on-site. For coating stents with polymer drug solutions the housing and the nozzle should be optimized.

This coating method allows to investigate the influence of drug concentration on the release kinetic, which requires coatings with different concentrations of rapamycin solutions. Stents with different modified surfaces were coated with the same rapamycin concentration and then compared with each surface.

Quantitative tests were performed to prove if the machine enabled homogeneous and customized coating to be applied directly before implantation, and also to show if there is any dependency between the drug concentration in the coating solution and drug amount bound onto the modified surfaces. Investigations should prove if the surface modification has any influence on the uptake of the drug.

Three different stent surface modifications were investigated: electropolished, sandblasted and etched surfaces. Each surface has a different surface roughness: the electropolished one is smooth, the sandblasted one is lightly porous, and drug depots are available in the etched surface. The total surface area increased due to these chemical or mechanical modifications.

For quantitative studies, after coating with rapamycin, each stent was expanded with 16 bar pressure and washed with 2 ml ethanol. The rapamycin amount in ethanol solution was determined using UV-Vis spectrometry.

6.3 Investigation of coating properties

Stents were coated with rapamycin and rapamycin polymer solutions using different drug concentrations and drug polymer ratio.

The first step after coating was to investigate the following coating properties:

- homogeneity
- thickness
- residual solvent
- adhesion to stent surface
- drug release kinetic

6.3.1 Optical characterization

After coating, stents crimped on the catheter were observed under SEM to analyze the coating homogeneity. It is crucial to investigate the condition of the coating after stent implantation and expansion. Because during implantation the stent has to travel through a long and very tortuous path along the circulatory system. Afterwards, during expansion, the metallic stent undergoes plastic deformation and the coating is exposed to tensile stress. Forces acting on the coating may trigger cracks to develop. To examine the coating finish and quality, SEM investigation was performed. To measure the coating thickness, both 316 L plates and stents were coated with all investigated substances and their mixtures, gold sputtered and embedded in epoxy resin in order to produce polished sections. The coating thickness was measured using SEM. Due to the significant material inherent tensions achieved during the embedding process of the three mm thick 316 L plates this method could only be applied for stents. To measure the coating thickness of the plates confocal white light microscopy (µ-Surf® device) was used.

6.3.2 Determination of the coating parameters

The spray-coating method (described in 6.2) was used to coat stents. To determine the coating parameters, it is necessary to first gain knowledge about the viscosity of the coating solutions, which in turn gives information about the permissible drug and polymer concentration and solvent amount in the coating solution. Viscosity and solvent amount in the coating solution then determine the necessary coating parameters: speed, air pressure in nozzle and drying time.

Viscosity of coating solutions

Because solution for spray coating should easily go through coating nozzle to ensure homogeny coating the viscosity of the polymer solutions is one of the most important parameters. The viscosity of polymer solutions was determined using a rheometer (C–VOR 120, Malvern, Germany) and compared with the viscosity of ethanol for which

the Stent Coating Machine was designed. The viscosity measurements of polymer solutions were performed using a double slit test system (DG 40/50) at 20 °C. The shear stress was fitted for each solution to prevent the development of turbulent flow. At very low solution viscosities it is very difficult to obtain a constant value, therefore for each test 100 -150 data points were collected before averaging.

Solvent residues in coating (thermo-gravimetric method)

Residual solvent in the coating determines the biocompatibility of the device. As mentioned above (see Chapter 5.4) the Permitted Daily Exposition is high for the solvents used in these investigations. To determine solvent residues in the stent coatings directly after the coating process, samples were investigated using the simultaneous thermogravimetry method (STA Netzsch Apparatus, Germany) in nitrogen atmosphere at a constant temperature of 40˚C untill the weight stabilized (3 hours). The weight loss observed was approximately 300 µg for ethanol and 400 µg for ethyl formate. Both values are within the permitted daily dosage range according to the “European pharmacopoeia”.

6.3.3 Chemical characterization of the stent coating

Gel Permeation Chromatography (GPC)

To investigate the degradation of polymers during release tests and assess changes in the molecular weight distribution (MWD), measurements using Gel Permeation Chromatograpy were performed (600E, Waters; with a refractive index detector, Waters 410, Eschborn, Germany). These tests were preformed at 40°C using high resolution (HR) columns, and as an eluent tetrahydrofuran (THF) HPLC grade was used. The system was calibrated with polystyrene standards. All samples were filtered with 0.45 µm a hydrophilic polypropylene membrane filter (Acrodisc 13GHP, Waters).

Stents coated with polymers and polymer-rapamycin mixtures were immersed in Ringer solution and drug release was observed as a function of time. At fixed time

intervals coated stents were taken from the solution and the substance remaining at the stent surface was washed off with THF, filtrated and investigated in GPC.

High Performance Liquid Chromatography

Solutions from release and quantification tests were analyzed with High Performance Liquid Chromatography (HPLC) system (600 E LC, Waters GmbH, Eschborn, Gremany) with a 717plus Autosampler, Jetstream column oven and a 2487 dual UV Absorbance detector. HPLC was calibrated with pure methylene dianiline standards (from Waters, Germany).

All samples were filtrated with 0.45µm Waters filters. The rapamycin solution was separated with a Waters Atlantic C18 column (5µm, 4,6 mm x 150 mm). HPLC grade water 10-%vol (LiChrosolv, VWR Darmstadt, Germany) and 90-%vol methanol (LiChrosolv, VWR Darmstadt, Germany) were used as the mobile phase compounds with a flow rate of 2 ml/min. Each test lasted five minutes and the rapamycin peak was detectable after nearly two minutes. The Waters Empower software was used to acquire and process data.

UV-Vis Spectrometry

To quantify the drug amount on the stent surface before and after placement in the Ringer solution during release measurements, photometric analysis was conducted using a UV-Vis spectral photometer (Specord -210 Jena Analytik AG, Jena, Germany). The generated data were evaluated using the WinAspect software. UV–Vis analyses were performed by determining the absorbance at the specified wavelength for rapamycin (277 nm). Calibration graphs of rapamycin in ethanol were established by measuring the absorbance of a set of standards of drug in ethanol in the 0 – 0.4 mmol/l concentration range. The rapamycin-ACA complex is very well soluble in ethanol and the anthracene group does not change the absorption maximum of rapamycin. The UV-Vis measurements of rapamycin-ACA were evaluated using the calibration curves from the rapamycin-ethanol solutions.

6.3.4 Coating adhesion

To investigate adhesion forces of coating on different surfaces two series of tests were performed:

- simulation of stent implantation in an artificial blood circuit (ABC)
- laboratory physical test: laser shock adhesion measurement.

Measurements in ABC were performed on stents coated with the drug only. The second method, laser shock adhesion tests (LASAT) were used to determine the adhesion of the polymer drug coatings on the stent surface.

6.3.4.1 Artificial blood circuit (ABC)

The ABC was designed to simulate the implantation of coronary stents. It allows to reproduce the conditions to which the stents are subjected to from the point of insertion (arteria femoralis) to the location of the stenosis (coronary arteries, Fig.6.9 – 6.10). The model also allows a simulation of the expansion of stents in the stenosis. As a heart equivalent, a roller pump (Stoecker, Germany) was applied. Medical grade silicon and PVC tubes with appropriate diameter were used as substitutes for arteries. In this circuit four pressure gauges and four flow meters are placed to monitor and control solution parameters. The circuit allows reproducing the environment of the human circulatory system.

The aim of these procedures was to detect the adhesive strength of the drug coating on different stent surfaces. To simulate human blood circulation all parameters such as the pressure in the tubes, fluid flow and also fluid composition were adjusted to fit the human parameters. Ringer solution (RL) was used as blood substitute [106]. Ringer solution is an aqueous solution containing the chlorides of sodium, potassium and calcium that have the same osmotic pressure as blood and is used to prevent dehydration and in physiological experiments as a medium for in vitro preparations (Table 6.1).

Substance	Amount	Concentration [mmol/l]
sodium chloride	8.6 g Na^+	147
potassium chloride	0.3 g K^+	4.0
calcium chloride	0.33 g Ca^{2+}	2.25
pH	5.0 – 7.0 Cl^-	155.5

Table 6.1: *Chemical composition of Ringer solution from Delta Select Company.*

The ABC was filled with Ringer solution from Delta Select Company (Germany) and heated to 37º C using a heat exchanger. Coated stents were introduced into an artificial coronary artery (silicon tube), expanded (balloon pressure 16 bar) using a standard expansion device, removed after one minute and washed with ethanol. The drug amount remaining on the stent surface after the implantation procedure was determined using UV-Vis spectrometry.

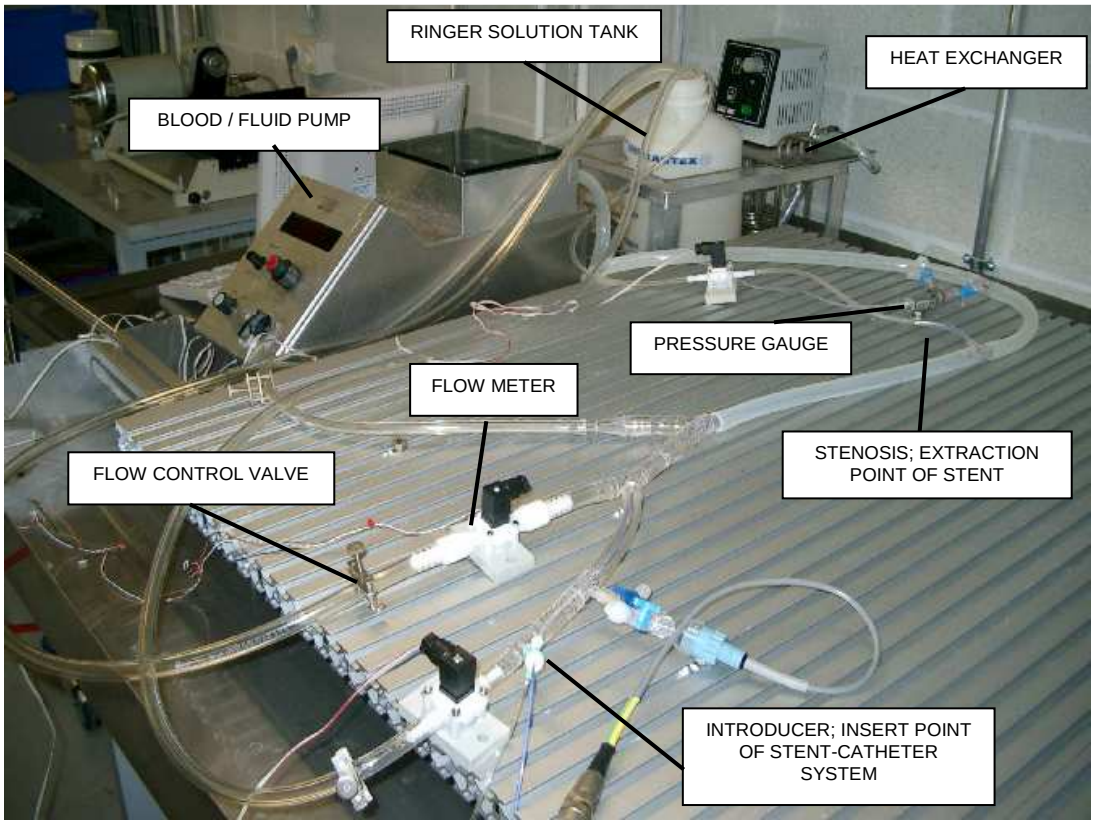

Fig. 6.9: *Artificial blood circulation, build to simulate bodily conditions during stent implantation. Silicon tubes make up for blood vessels and as a heart equivalent a roller pump was applied. The system is equipped with flow meters and pressure sensors to ensure physiologic conditions.*

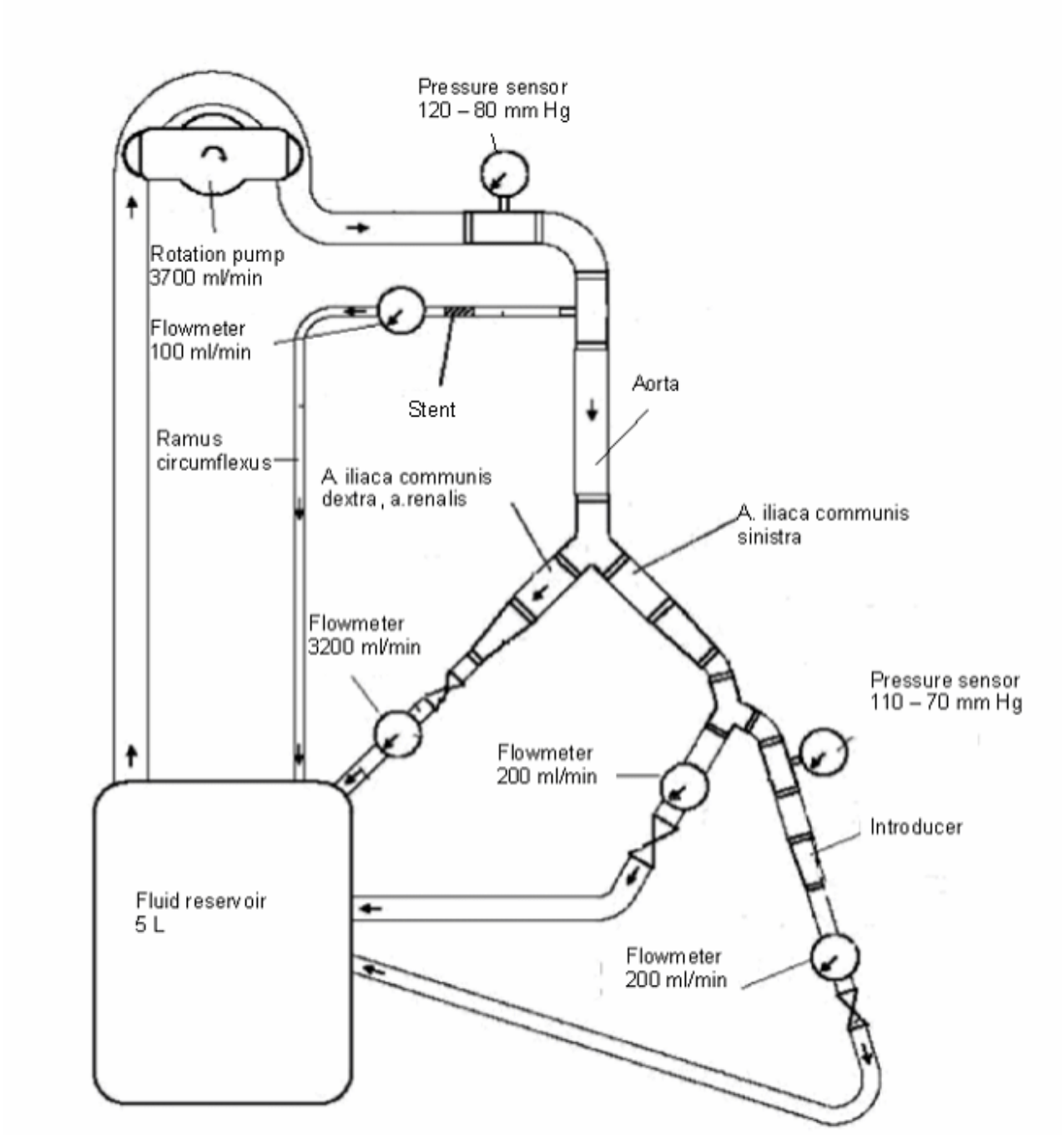

Fig. 6.10: *Sketch of artificial blood circuit. Apparatus developed to simulate mechanical conditions of coronary stent implantation.*

6.3.4.2 Laser shock adhesion test (LASAT)

This method allows the determination of the adhesion strength of coatings on different surfaces, e.g., epoxy resin or ceramic coatings on metal or ceramic substrates [107]. In this work the LASAT method had to be modified due to the elastic properties of the polymer coatings. The adhesion of polymer coatings on metal substrates was tested.

The general principle of this method is to pulse with a laser beam on the uncoated side of the specimen in order to create a shock wave in the substrate which leads to the separation of the coating from the substrate (Fig. 6.11).

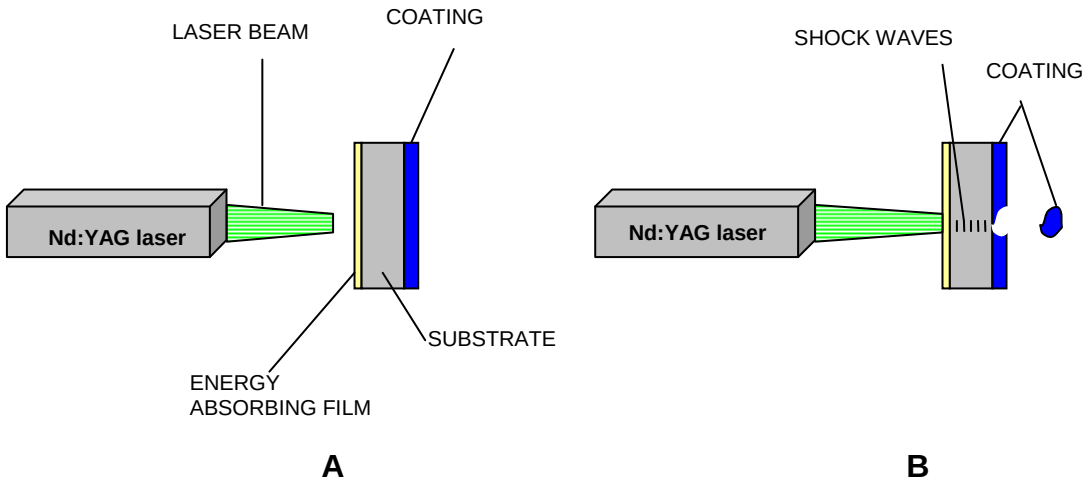

Fig. 6.11: *A – Principle of the laser shock adhesion test. Cross-section of stainless steel substrate coated with polymer. B – Laser beam pulse focused on the uncoated side of the substrate leads to the creation of shock waves in the substrate which causes the coating to dettach from the substrate.*

To observe the adhesion strength between a pyrolitic graphite substrate and metallic coatings (Al, Nb, Cu, Cr…) Gupta et al. used a high-energy laser pulse of three ns duration from an neodymium-doped yttrium aluminium garnet (Nd:YAG) laser [108]. Nd:YAG lasers are optically pumped using a flash lamp or laser diodes. They are one of the most common types of laser.

In this work the Nd:YAG laser system PL2043A/20 installed with a special mirror and lens construction was successfully used to quantify the adhesion strength of the polymer coating on the metallic substrate (Fig. 6.12). A laser beam was emitted

through the mirror to the lens and focused on the uncoated side of the substrate. An oscillator created single pulses with 20 ps length. A beam chopper superimposed four single pulses to form one 80 ps length pulse which was passed through an amplifier and transmitted as a square light pulse of 50 - 60 ps. The energy of a pulse of 532 nm wave length was 50 mJ. The focus diameter was adjustable and varied from 70 µm to 230 µm. The absorbing film played an important role and for this test gold coating seemed to be the best material for the laser used (532 nm) due to its large thermal extension coefficient.

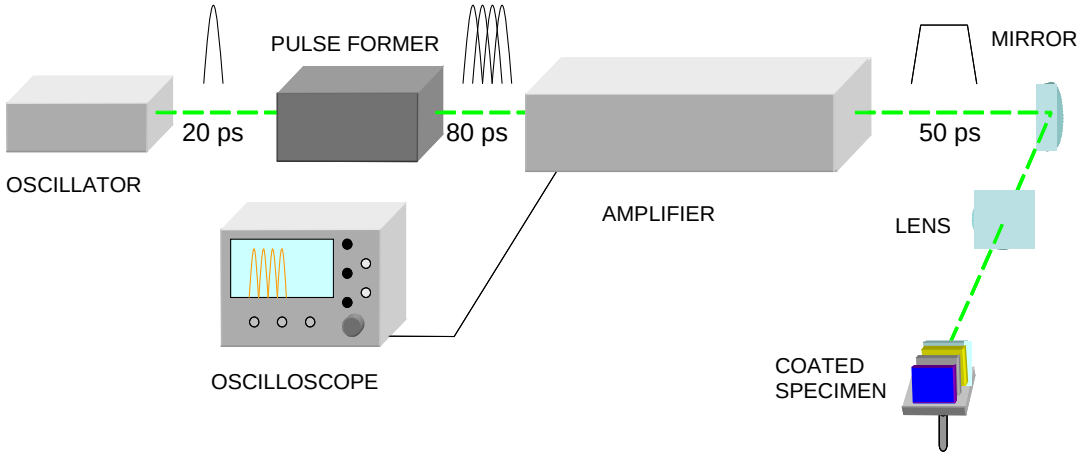

Fig. 6.12: *Laser shock adhesion test. Measurement system Nd:YAG laser. An oscillator creates single pulses with 20 ps length. A beam chopper superimpose four single pulses to form one 80 ps length pulse which is passed through an amplifier and transmitted as a square light pulse of 50 - 60 ps and a laser beam emitted through the mirror to the lens is focused on the uncoated side of the substrate.*

6.4 Release tests

Release measurements of coated stents were performed in vitro. To select the proper release kinetic of rapamycin to abrogate restenosis, in vivo tests are desirable. Aim of this study is to find and define different ways of controlled drug release. Two different mechanisms were investigated: release controlled by surface geometry and release controlled by a polymer matrix.

For these investigations stents with different modified surfaces were used:

- electropolished,
- sandblasted,
- etched using inorganic acids

For the coatings two different rapamycin solutions were used:

- rapamycin dissolved in ethanol in concentrations of 10 mg/ml and 20 mg/ml,
- rapamycin mixed with biodegradable polymer (PLA) dissolved in ethyl formate

Due to the suitable molecular weight and viscosity properties of the polymer matrix, Resomer 202H (16 kDa) and Resomer 203S (32 kDa) were chosen (see Table 6.2). After performing coating tests to establish the most homogeneous coating on the stent surface, a 1:1 ratio of rapamycin to polymer was chosen for the coating solution.

To simulate blood flow in the arteries coated stents were placed in 50 ml containers with SBF, placed inside a shaker and stored inside an incubator at 37˚C (Fig 6.13). The shaker was rotated at 30 rotations per minute.

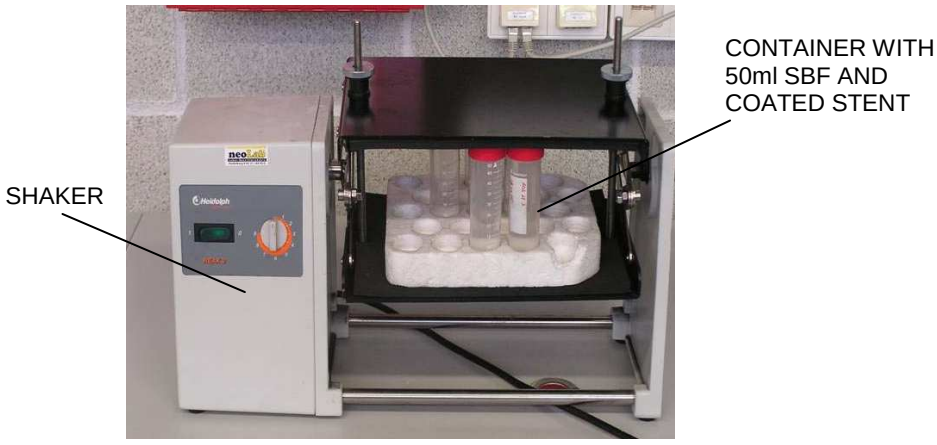

Fig. 6.13: *Shaker for drug release test. To protect rapamycin from degradation in the light and to simulate bodily conditions the shaker was placed inside an incubator.*

Release tests of stents coated only with rapamycin lasted approximately four weeks until the entire amount of drug was released. For stents coated with a polymer-rapamycin mixture the tests were run for three months. The immersion solution was

investigated and refreshed after certain time intervals. The rapamycin released into SBF was detected by UV–Vis spectrometry.

6.5 Drug diffusion into coronary artery wall

In vitro experiments with porcine coronary arteries were performed to measure the diffusion of rapamycin into the coronary artery wall and to contrast the results obtained in the drug release test performed with the shaker approach (see Chapter 6.4 and 7.1.4).

6.5.1 Simulation of in vivo conditions

Porcine coronary arteries were excised from fresh porcine hearts and used immediately. To maintain the vital functions, the excised arteries were placed in a perfusion bath. The perfusion bath obtained from the Hugo Sachs Company was used to simulate the heart environment: pressure, temperature, pH, extra- and intraluminal flow.

Krebs Hanseleit solution (KHS), a modification of Ringer solution (developed in the early 1930´s by Hans Krebs and Kurt Henseleit) was used as blood substitute in the perfusion bath [109]. The solution used in this work was obtained from Sigma Aldrich (Germany) and was modified by addition of 2 g/l glucose as an energy substrate for cells (Table 6.2).

Substance	Concentration [g / l]
D-Glucose	2.0
Magnesium sulphate	0.141
Potassium phosphate	0.16
Potassium chloride	0.35
Sodium chloride	6.9
Calcium chloride	0.373
Sodium bicarbonate	2.1
1N HCl or 1N NaOH	for pH adjustment

Table 6.2: *Composition of Krebs-Hanseleit solution (KHS) from Sigma-Aldrich Company.*

6.5.1.1 Coronary artery tissue

Human and porcine heart share similar dimension and anatomy. Thus, porcine hearts were used for in vitro tests of drug diffusion and uptake into the coronary artery wall. Fresh hearts were transported from a slaughterhouse into the laboratory and coronary arteries were dissected. The porcine ramus interventricularis paraconalis corresponds to a human anterior interventricular artery and the porcine ramus interventricularis subsinosus corresponds to a human left circumflex artery (Fig. 6.14).

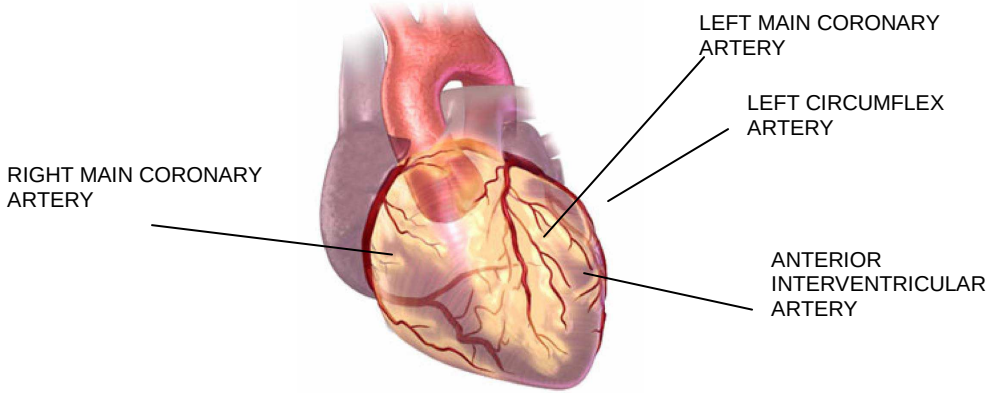

Fig. 6.14: *Coronary arteries of the human heart [medmovie.com, Lexington,USA].*

6.5.1.2 Perfusion bath

To determine rapamycin diffusion into the coronary artery wall, a fresh porcine ramus interventrcularis paraconalis was dissected from porcine heart and placed in a perfusion bath. This is a special device suitable for tests on hollow organs simulating in vivo environment (Fig. 6.15 – 6.16). Individual solutions can be used for intraluminal perfusion and extraluminal superfusion. The effective intraluminal perfusion is generated by an adjustable load control system. A differential pressure transducer is used to measure the intraluminal pressure difference at the proximal and distal end of the organ. The tissue bath is a water-jacketed plexiglas bath. The holder for the cannulae can be removed from the main bath during the cannulation of the segment of tubular organs. The cannulae are fixed on sliding holders to optimize the distance between the cannulae to accommodate for variations in the length of the specimen, thus avoiding any slackness in the tissue. The unit is supplied with four different interchangeable adapters for vessels with diameters of 1.5, 2.5, 3 and 4 mm.

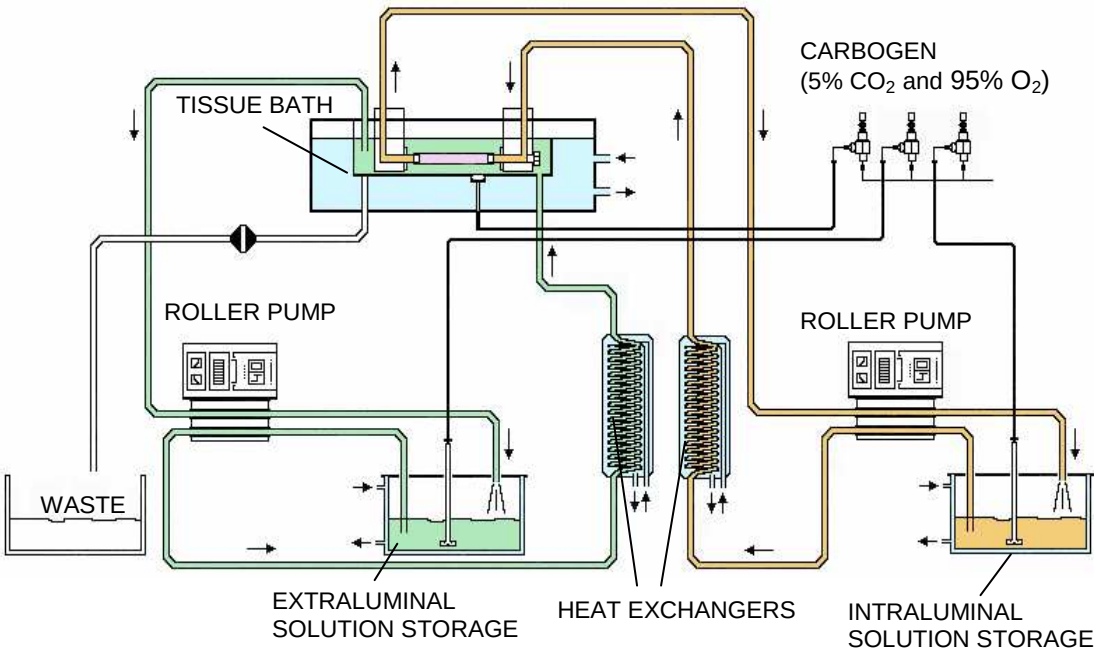

Fig. 6.15: *Schema of perfusions bath operation. Perfusion bath is the device suitable for investigations of hollow organs in simulated in vivo conditions. There are two separate circulations: intraluminal marked yellow and extraluminal perfusion marked green.*

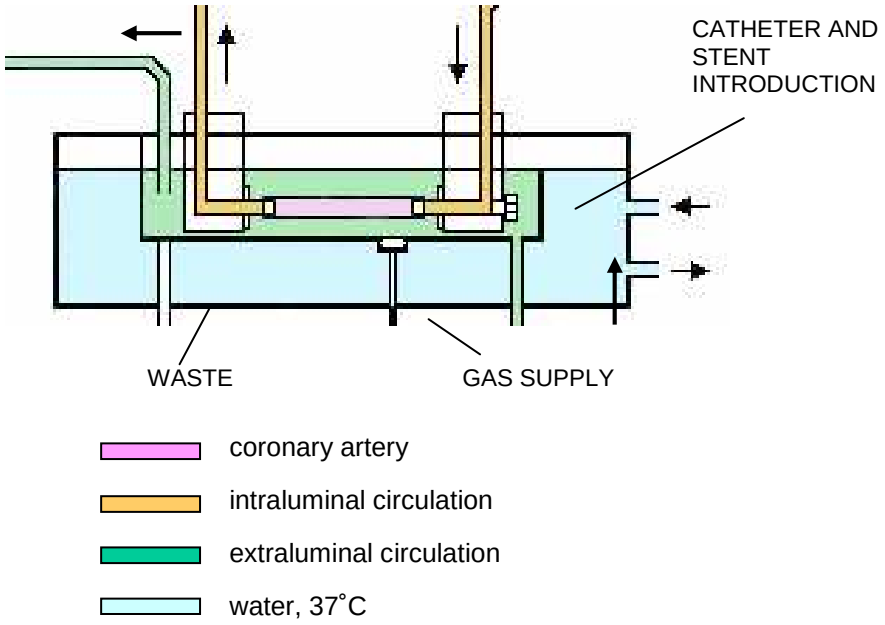

***Fig. 6.16**: Schema of perfusion bath operation: Magnification of tissue bath. The hollow organ (here artery) is placed in a water-jacked Plexiglas bath filled with water heated to* 37˚C

Coronary arterial flow was simulated in the intraluminal circulation of the perfusion bath. The flow of the KHS fluid was controlled by a peristaltic pump and fixed at 40 ml/min. This value does not agree with the physiological flow in coronary arteries which approaches 100 ml/min. The lower flow rates used in the measurements were unavoidable due to the state of the dissected arteries. There was no tissue around the artery and arborisations of artery had to be sewn. Too high flow rates caused the artery rupture in the perfusion bath. The circulating medium was heated to 37 ºC using an external thermostat. Extremely important for preserving the artery functionality in vitro is the pH of medium (which should be maintained at 7.4) and suitable glucose level. The pH value was regulated with carbogen gas (5% carbon dioxide and 95% oxygen) supply [110].

6.5.1.3 Evaluation of integrity and functionality of the coronary artery

Examination of functionality of coronary arteries after incubation in a perfusion bath

To estimate the appropriate investigation period of diffusion tests and to assess the integrity and the functionality of arteries over time in the perfusion bath, the following two tests were carried out:

- histological evaluation
- vasoactivity tests

Histological evaluation

For the histological evaluation, coronary arteries were incubated in the perfusion bath containing the Krebs-Hanseleit solution for 12h, 24h and 48h. Cylindrical sections of the arteries were cut and embedded in paraffin immediately after perfusion. Histological slices were prepared with a microtome and mounted on glass slices. For histological evaluation all specimens were stained with the Hämatoxilin-Eosin-staining and observed with the microscope.

To study the effects of perfusion time ($t_p \neq 0$) on the artery segment, a sample from the same artery with perfusion time $t_p = 0$ was studied as a reference. After 12 hours perfusion exposure, the structure of the artery wall remained unaltered. After 24h first defect in the structure can be observed. Only a mild swelling of the media could be observed. After 24h the swelling of the media was much more evident and after 48 h the integrity of the artery wall was severely disrupted with the development of big vacuoles and crevices in the media (Fig. 6.17).

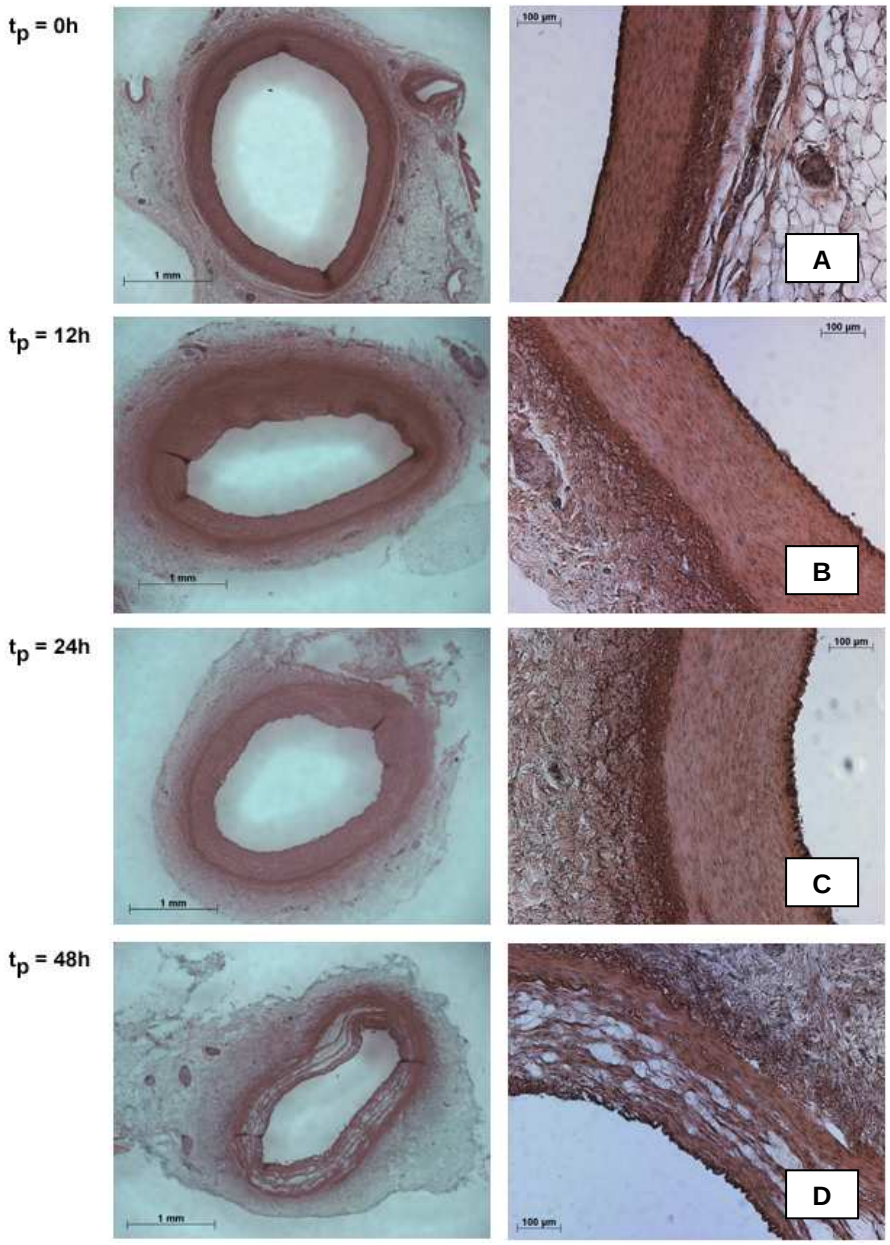

Fig. 6.17: *Exemplary histological cuts of porcine coronary arteries. Complete cross section (left) and detail (right). Perfusion time is given in hours. A: intact arterial wall with a dense structure of intima and media. B: after 12 h of perfusion artery layers are still intact with a mild swelling of the media C: a diffuse swelling of the media could be observed. D: destroyed architecture of the artery layers with development of vacuoles and crevices.*

Vasoactivity tests in organ bath

To amend the results obtained from the histological evaluation vasoactivity tests were performed on fresh arteries as well as on arteries perfused for 24h in the organ bath.

For the vasoactivity tests a special device composed of eight separate, parallel operated organ baths was used. Each bath was connected to a force transducer and the signals were software based monitored (Fig. 6.18).

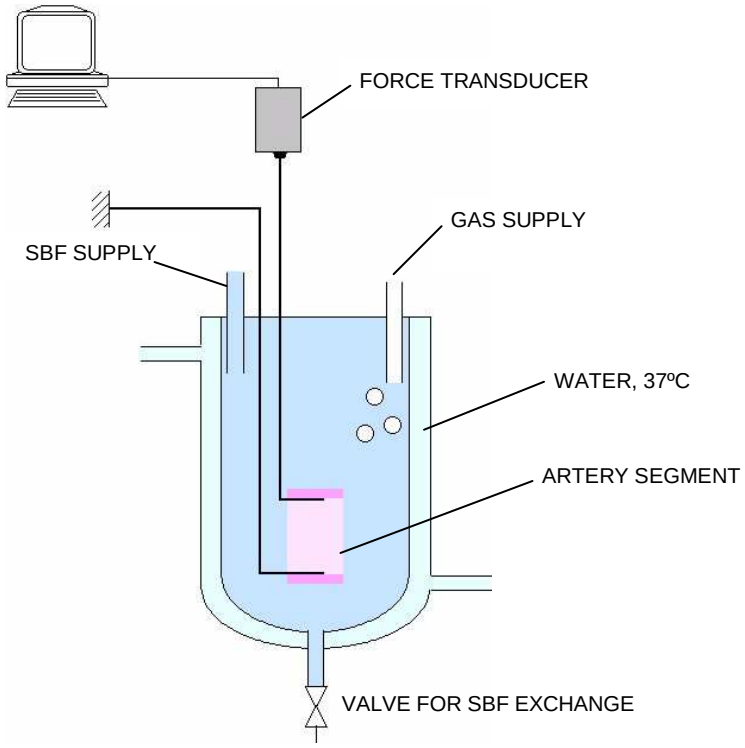

Fig. 6.18: *Scheme of one of the eight organ baths. A segment of the coronary artery is placed in the organ bath, positioned between two arms and connected to a force transducer which registers tension or relaxation of the artery segment.*

Each organ bath, containing 5ml Ringer solution was tempered at 37 ºC using an external water bath. The artery segment (approx. 2 mm long) was fixed between the two arms, where one arm was permanent fixed to the device and the second arm was movable and connected to a force transducer. Addition of vasoactive substances caused contraction or dilatation of the coronary artery segments indicating functional integrity of the artery. These movements were registered by the force transducer and analyzed by the software.

In our experiments the following vasoactive substances were used:

- Potassium chloride (KCl): causes contraction of the arteries [134]
- Norepinephrinhydrochloride (NE): causes contraction of the artery and activates α_1-receptors [137]

- Stable Thromboxan AB2B analogue (U46619): causes contraction of the artery and activates thromboxane receptors [135]
- Acetylcholinchloride (ACh): causes relaxation of the artery, activates muscarinic receptors [136]. Fresh arteries react to ACh with relaxation and endothelium damage reveals contraction.

Reaction of artery segments to NE, ACh and U46619 give information about receptors functionality and KCl about membrane functionality (Fig. 6.19 - 6.20) [137].

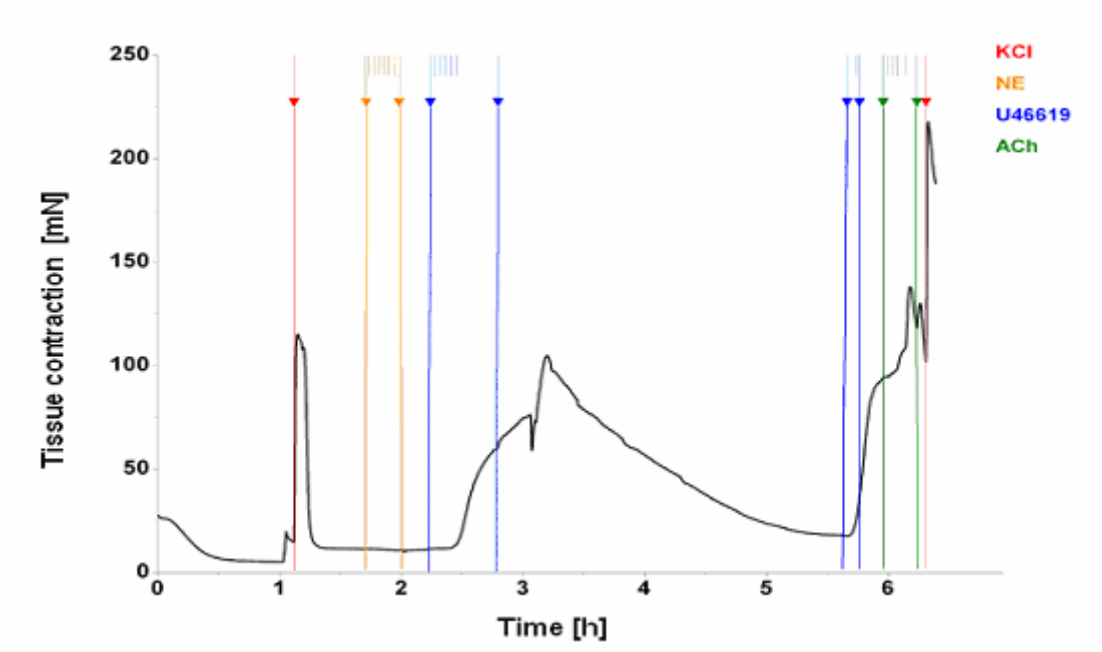

Fig. 6.19 *Diagram of vasoactivity test on freshly dissected artery segments. Reactions after addition of vasoactive substances are coded as follows: red KCl, yellow NE, blue U46619, and green ACh. KCl caused contraction of the artery segment that indicates integrity of cells membranes. NE did not evoke any arterial response but U46619 – another receptor activating substance caused artery contraction. ACh caused also artery contraction what indicating damage of the endothelium.*

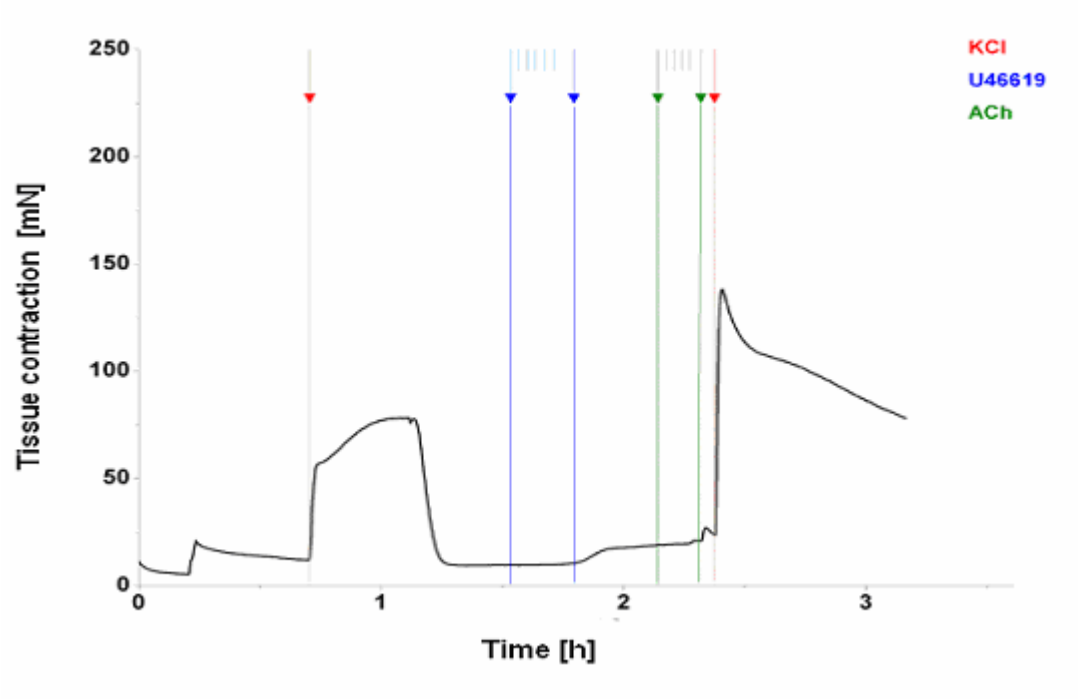

Fig. 6.20: *Diagram of vasoactivity test on artery segments after 24 hours perfusion. Reactions after addition of vasoactive substances are coded as follows: red KCl, blue U46619, green ACh. Tests with NE were not performed due to lack of reaction with fresh artery segments. In general responses of artery segments after 24h perfusion on the vasoactive substances were similar but weaker as fresh ones.*

In comparison to the fresh artery, the 24h perfused artery showed weaker and delayed reaction on the receptor dependent substances (U46619 and ACh) which indicates slight receptors damage after 24h perfusion. Concerning ACh it should be mentioned that for both perfused and fresh arteries the expected dilatation did not occur. This can be explained by the damage of the endothelium which probably arose during preparation of the artery.

In summary, after 24h perfusion a time lag and reduction of artery answer on the vasoactive substances was observed probably caused by a slight receptor damage. However this slide receptor defects can not be regarded as crucial factors for the drug transport into artery wall. It was shown that after 24h perfusion the artery wall integrity and the functional response of vasoactive substances were still present. This indicates that 24h perfusion time is an applicable time for diffusion tests of drugs into artery wall [138].

6.5.1.4 Stenting

After determination of the in vitro environment which allowed the artery to stay vital, diffusion tests of rapamycin into the coronary artery were performed.

Stents with modified surfaces were coated with different amounts of rapamycin or rapamycin–ACA and implanted into dissected coronary arteries fixed in the perfusion bath (Fig. 6.21). After a certain time of perfusion arteries were carefully removed from the chamber, sectioned longitudinally and frozen at -80ºC for further investigations.

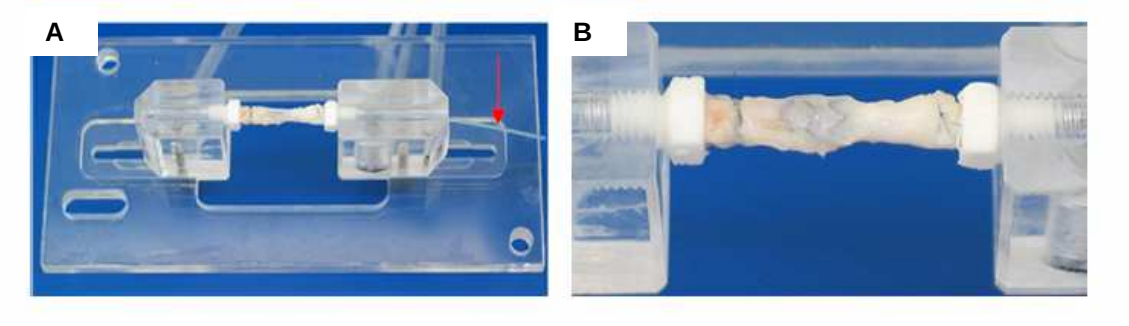

Fig. 6.21: *Perfusion bath: Magnification of coronary artery holder and stenting procedure. A: introduction of balloon catheter (red arrow) with crimped stent; B: stented coronary artery.*

6.5.2 Applied methods to investigate rapamycin diffusion into porcine coronary arteries

To quantitatively and qualitatively evaluate the diffusion of rapamycin into coronary arteries the following tests were performed:

- optical methods for investigations of radial and lateral drug diffusion from the stent into the artery wall
- chemical methods to quantify the amount of drug released into the artery wall.

Optical inspection of the arteries, was performed by labeling rapamycin with an UV active substance (anthracene carboxylic acid – ACA, see Chapter 5.2.1).

6.5.2.1 Optical methods

Quantitative assessment of radial and lateral drug release from stents into the coronary arteries was performed by using different techniques of fluorescence microscopy (Fig. 6.22). Surface inspection of the lumen of stented arteries gave information about lateral drug distribution on the vascular intima (directly in the contact area between stent and tissue). The optical detection of rapamycin – ACA on the tissue surface was carried out using conventional fluorescence microscopy. Investigations on the radial diffusion of the drug into the vascular tissue were possible using fluorescence microscopy with the ApoTome system or two photons laser scanning microscopy. Examination of rapamycin – ACA penetration into the artery wall using the ApoTome system is a relatively simple method that scans a set of plane sections through the fluorescent specimens. Achieved axial resolution enables the reconstruction of three dimensional images which are composed of these single scans. The fluorescence from other levels are filtered out during the scanning of a given plane section.

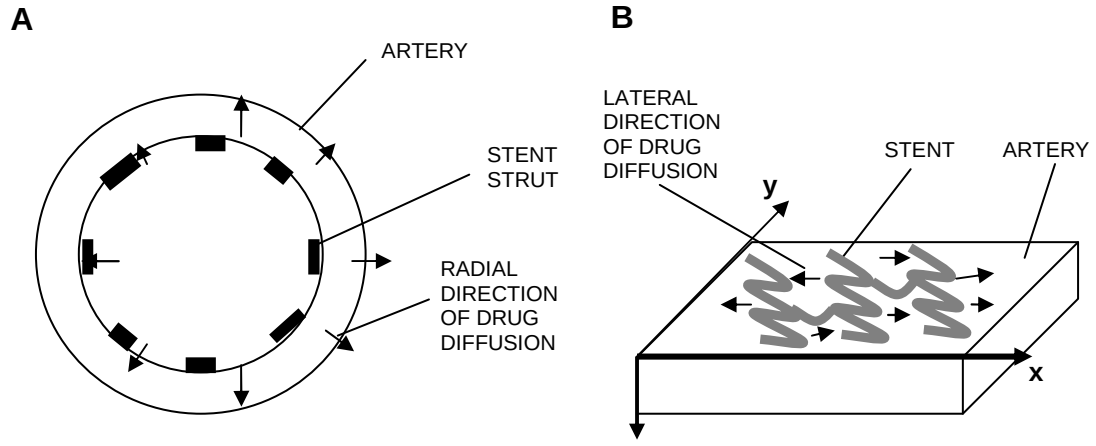

Fig.6.22: *Directions of drug diffusion from stent struts into the coronary artery. A – radial diffusion: from the strut towards normal direction of artery, B- lateral direction: from struts towards the adjactent luminal surface of the artery.*

Another method use for investigations on drug penetration into artery walls is two photons laser scanning microscopy (2PLSM). In contrast to conventional fluorescence microscopy, where the fluorescence molecule is activated using UV radiation, here the molecule is activated by simultaneous absorption of two photons. Each photon possesses the half energy which is required for molecule activation. It means that for

anthracene carboxylic acid UV radiation is not required and the molecule can be activated using near-infrared radiation.

6.5.2.2 Chemical methods

To investigate the amount of rapamycin–ACA into the artery walls homogenization of the arteries was performed. At indicated time intervals the stented arteries were carefully removed from the perfusion bath, sectioned longitudinally, and the stents were carefully removed from the artery surface. The arteries were stretched and pinned down onto special pads and frozen at -80°C. Directly before homogenization, the arteries were weighed, transferred to round bottom tubes (Falcon #2059) filled with 0.5–1 ml PBS and mechanically fragmented using a mixer (Miccra D-8 #10753). After this procedure to open the cell wall, specimens were frozen three times at - 70°C and thawed on ice. Subsequently, specimens were centrifuged for 20 minutes at 13 000 rpm at 4°C, and the rapamycin–ACA amounts in the arteries were determined using UV-Vis spectrometry and HPLC.

To investigate the diffusion of rapamycin-ACA into the coronary arteries the following tests were performed:

Stent surface	Sandblasted				Oxalic etched
Coating	Rapamycin-ACA 0.5%		Rapamycin-ACA 1%		Rapamycin-ACA 0.5%
Perfusion time	12h	24h	12h	24h	24h

Table 6.3: *Schema of measurements in perfusions bath. Diffusion of rapamycin into artery wall was investigated for both sandblasted and oxalic acid etched surfaces coated with 0.5% and 1% drug solution. To investigate if time has an influence on drug diffusion direction arteries after 12 hours and 24 hours perfusion were tested.*

Diffusion of labeled rapamycin was investigated microscopically using common fluorescence microscope with the ApoTome unit, confocal microcopy and two photons laser scanning microscopy. The quantitative detection of drug diffusion into the coronary artery was performed using HPLC.

7 Results

The aim of the thesis was to investigate different mechanisms to control drug release from coronary stents, and to demonstrate if the coating can be applied directly before implantation (customized coating for the patient).

This work is focuses on two mechanisms of drug release control:

1. Modification of the device surface topography by generation of drug depots within the surface with special properties which enable controlled release (geometry control).
2. Controlling drug release by a use of biocompatible polymer matrix. Polymer properties such as molecular weight, crystallinity and degradation time can control the elution of the embedded drug.

To investigate the possibilities of controlled drug release from coronary stents, special attention was addressed to the following aspects:

- Factors influencing the adhesion of drug or polymer-drug mixture to stent surface
- Coating method and quality of the coating

Coating adhesion on the surface is a very important parameter which determines the quality of the coating and the drug release from coronary stents. Drug release can only be controlled when the coating adheres well on the surface. If coating adhesion is poor, investigation of drug release is impossible due to the uncontrolled coating behavior during mechanical stressing of the device. Adhesion depends on both substrate surface characteristic and coating quality and properties.

7.1 Control of drug release by surface modifications

Surface modifications serve to improve the adhesion of the coating to the stent, and moreover the surface seems to have an influence on restenosis and artery recovery after implantation. Studies in the porcine restenosis model demonstrate that the use of the microporous stent system is associated with a significant reduction in neointima proliferation when rapamycin is used as the active antiproliferative compound [112].

Two different modifications of electropolished stent surface were investigated: microporous (sandblasted) and chemically etched.

Stent surface characterization

Optical analysis of stent surface was performed using scanning electron microscopy (SEM). Differences in modified surfaces topography were visible at 50 x magnification (Fig.7.1 – 7.3).

ELECTROPOLISHED SURFACE

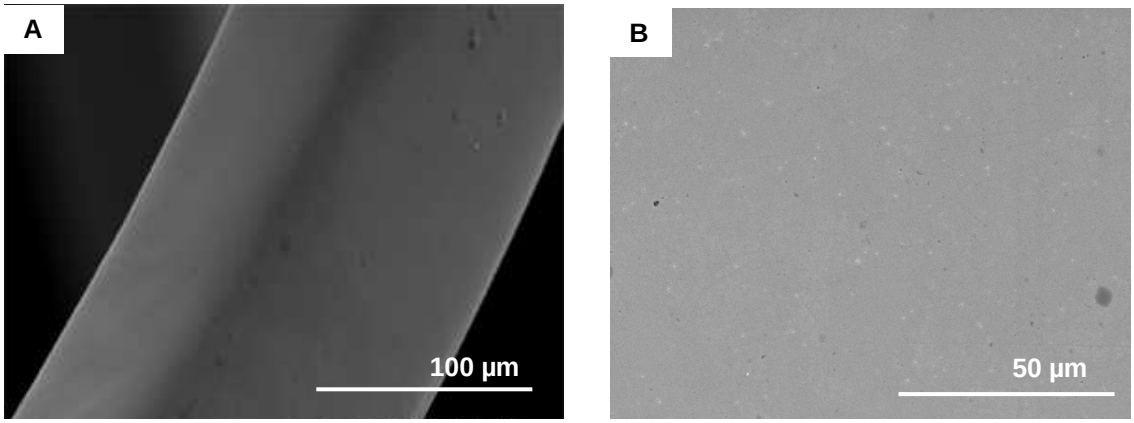

Fig. 7.1: *SEM pictures of electropolished stent; A: 500x magnification, B: Detailed figure, magnification 1000x. Surface is smooth and cannot ensure sufficient adhesion for crystalline drug (rapamycin).*

Chemical polishing or electropolishing, instead of mechanical polishing, are recommended for the attainment of metallic surface polishes without the introduction of contaminants or tensions in the surface layers of the metal. The fundamental difference between the chemical and electrochemical polishing processes is that in the latter anodic

currents/potentials are used to help in the dissolution and passivation of the metal. The electropolishing process modifies surface properties of metals without affecting their bulk properties. 316L stainless steel becomes more corrosion resistant, smoother, and cleanable after this treatment [130].

SANDBLASTED SURFACE

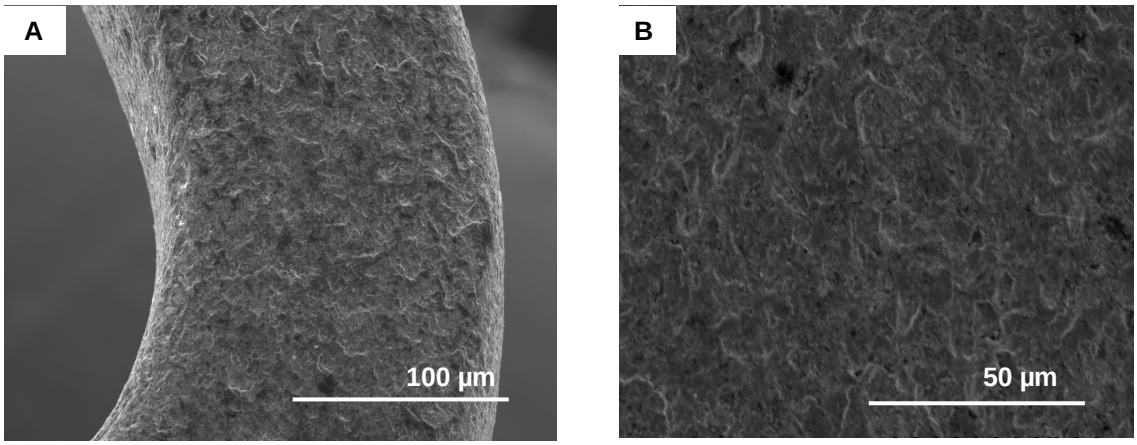

Fig.7.2: *SEM pictures of sandblasted stent. Rough surface with numerous small cavities can be observed. These cavities can serve as drug depots. A: 500x magnification, B: Detailed figure, magnification 1000x.*

Stents are sandblasted for increasing surface roughness. These can result in two main advantages in comparison to the smooth surface: improving the adhesion properties and ensure favored basis for cell growth [131, 132]. Sandblasting ist often applied for permanent implants which requires suffcient ingrowth into a living tissue e.g. bone implants [132, 133].

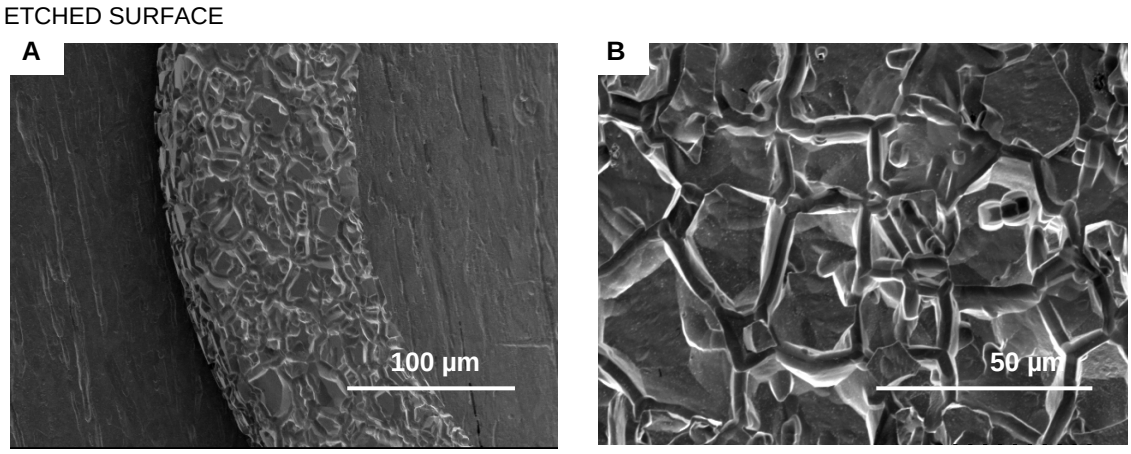

Fig.7.3: *SEM pictures of an etched stent. The cavities in the surface obtained by etching are much larger than those obtained by sandblasting. These cavities can serve as drug reservoirs to enable a controlled drug release. A: 500x magnification, B: 1000x magnification.*

Oxalic acid etched surface was obtained in two step process [94]. The first etching was performed using nitic acid to create a grid of evenly distributed depots. The second step this is etching with oxalic acid. The aim is here to broaden the grain boundary furrows generated by the first step so that larger, wider depots without sharp cerevices are created [94].

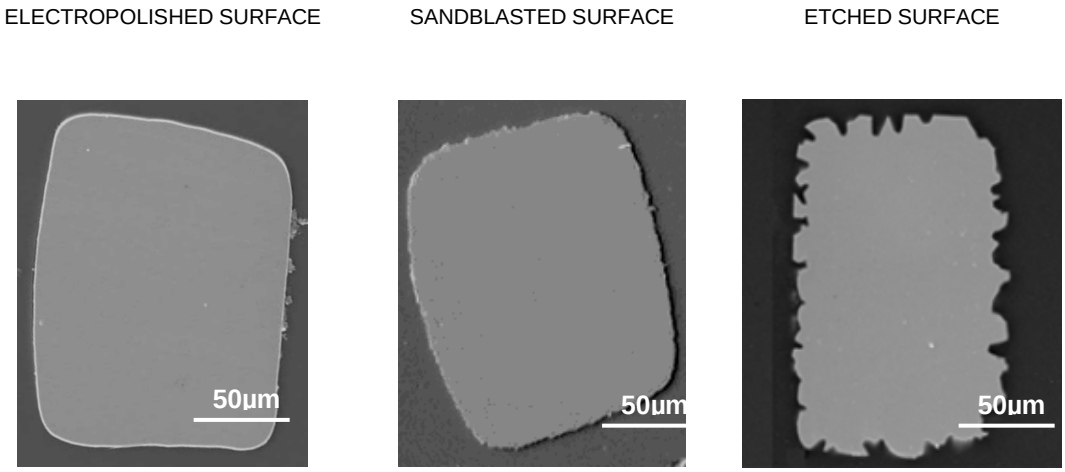

Fig. 7.4: *SEM pictures of the cross section of a stent strut. There are no significant differences between pictures of the cross section of electropolished and sandblasted surfaces. The etched surface shows a significant increase in the size of cavities available for storing the drug.*

The pictures in Fig. 7.4 show clearly the differences between the surface topography obtained after surface treatment and how the surface topography can affect the drug

amount bound onto the surface after the coating. The electropolished surface is significantly smoother compared to the sandblasted and etched ones. Sandblasting develops a rough surface with fine structures and etching results in the creation of visible depots.The etched surface is not as rough as the sandblasted one. Depots are present but the surface between them is relatively smooth.

7.1.1 Surface roughness and surface enlargement

The roughness of modified surfaces was analyzed using three different methods. Two of these methods, perthometer and AFM, are mechanical in nature and the third method, confocal light microscopy, is optical (see Chapter 6.1.1).

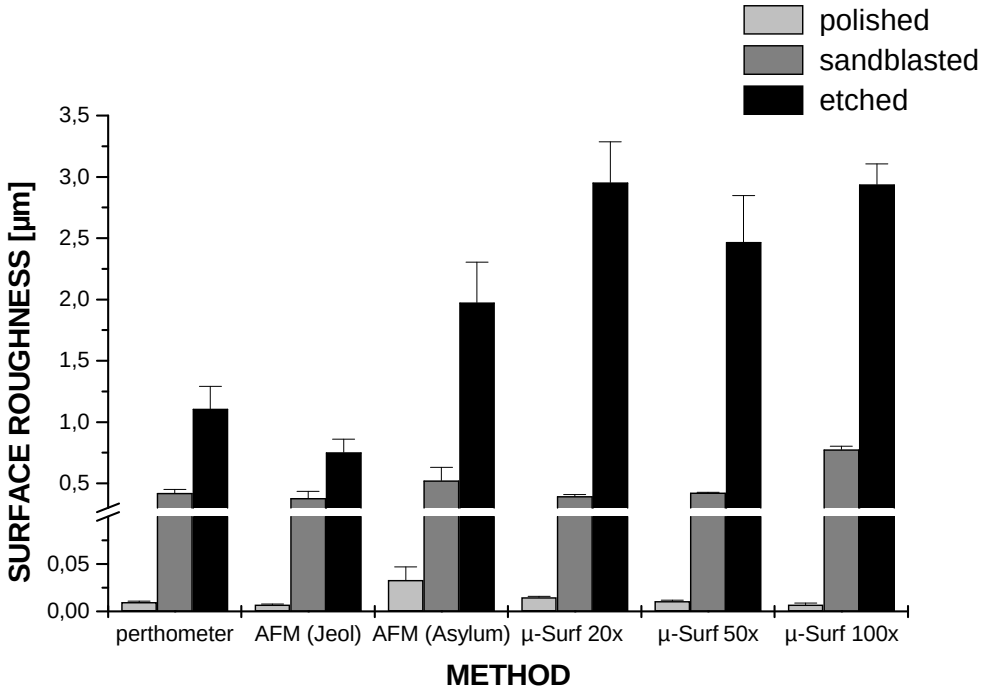

Fig. 7.5: *Comparison of methods of surface roughness measurements.The most accurately method for surface roughness measurements is the optic one (µ-Surf). Due to limitations of mechanical methods (pethrometer and AFM) mentioned in Chapter 6.1.1 the increase in effective surface area for modified surfaces was measured using confocal with light microscopy.*

The surface roughness could be measured most accurately using the optical method. These measurements confirmed that modification of the surfaces results in different topography and also gives an opportunity to vary the amount of drug on the stent surface and to control drug release (Fig. 7.5).

The increase in effective surface area was measured using confocal white light microscopy (Table 7.1). This is an important parameter for estimating coating adhesion [111]. Increasing the total contact surface area between the coating and the metal can be directly correlated to an increase in the number of interactions within the contact region. If no other additional surface modifications have occurred, e.g. changes in the chemical composition, roughening the surface can cause an increase in the adhesion strength proportional to the surface area enlargement factor $v_{r.}$

surface area enlargement v_r		
electropolished surface	**sandblasted surface**	**oxalic acid etched surface**
1.0 ± 0.0	2.7 ± 0.14	3.8 ± 0.28

Table 7.1: *Surface area enlargement was calculated from data obtained from µ-Surf measurements by means of the Surface Analysis Program (SAM 2.6). The electropolished surface was used as the reference material and set as 1.0.*

These investigations show that sandblasting and oxalic acid etching result in a considerable increase in surface area enlargement. Following tests confirm that on modified surfaces more coating can be deposited and that the adhesion on a rough surface is clearly stronger than on a smooth one.

7.1.2 Drug amount on different surfaces

Stent coating only with rapamycin (surface geometry control)

One of the possible ways to control drug release from coronary stents is to coat modified surfaces directly with various amounts of drug. Control of drug release could be achieved

in two ways: by changing the surface structure and creating drug depots, and secondly, by changing the coating thickness on the modified surfaces. The most important parameter is the elasticity of the coating and coating adhesion, due to the tensile stress which occurs during implantation and expansion of the stent in the human body, as mentioned previously in chapter 6.3.4.

Quantification of the drug amount on different stent surfaces

Results show that the rapamycin amount on the stent surfaces increases linearly with increasing the concentration in the coating solution (Fig 7.6). In these tests, the following solutions were investigated: two different drug concentrations of 10mg and 20mg rapamycin in 1ml ethanol, respectively.

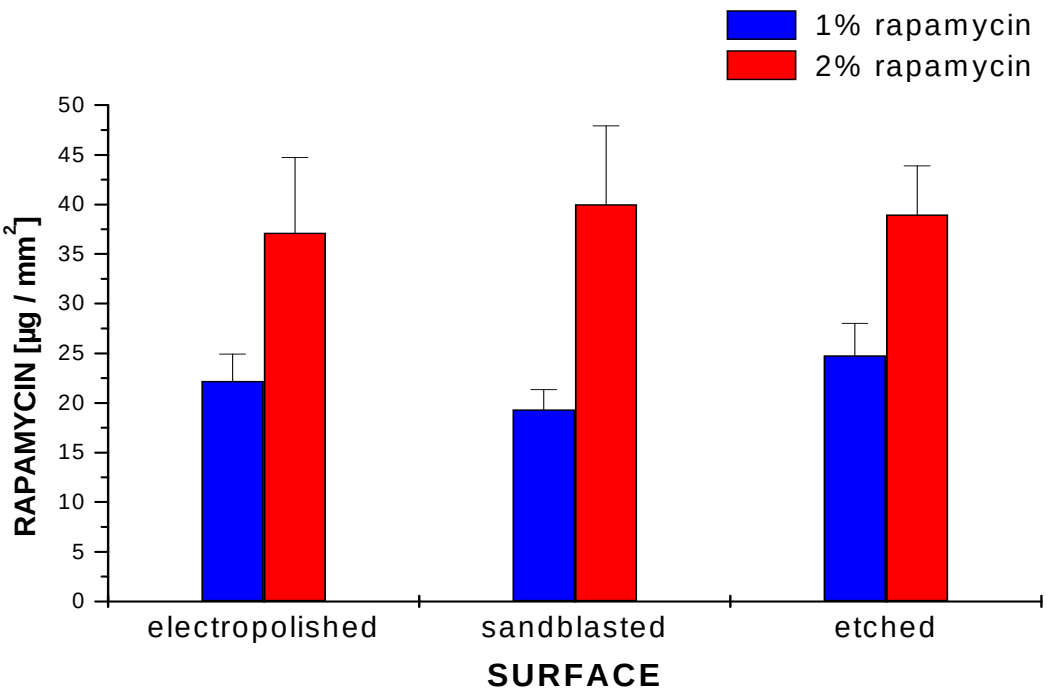

Fig. 7.6: *Quantitative comparison of three surface modifications and different drug concentrations in the coating solution.*

There are no significant differences observed between the binding of rapamycin on the electropolished and sandblasted surfaces. Both surfaces take up approximately 100% more drug if coated with the 2% rapamycin solution than with the 1% solution. Only the oalic

acid etched surface shows a slight tendency to bind more rapamycin on the surface and in the depots. Here coating with the 1% drug solution results in about 20% more drug coated on the stent than on the electropolished one. This can be attributed to the increase in surface area obtained and the binding capacity of the drug in the depots. Although the etched surface has depots the surface is relatively smooth and these surfaces do not take up as much drug as expected in comparison to the two other surfaces. For the 2% coating solution the amount of drug bound on the stent is for all surfaces almost the same. Only the electropolished surface bounds slightly less drug than the another two surfaces probably due to the poor drug adhesion to the smooth surface.

For each kind of surface modification studied, 10 stents were coated with the same drug solution. These tests proved that the coating method, using the spray machine, is reproducible. The variability observed in the drug amount deposited on the etched surface could be caused by variations in the depot volume. As this modification method depends on grain boundary etching, the size and distribution of grains on the surface are not always the same and can result in a variation of the depot distribution. On the electropolished surface a lot of rapamycin could be lost during stent expansion in the human body (see Fig. 7.7). Scanning electron microscopy (SEM) was used to investigate the coating homogeneity after stent expansion (rapamycin is crystalline and the coating can flake off). These tests showed differences between the modified surfaces. On the smooth electropolished surface, the coating flakes off and exhibits cracks and areas where whole “plates” have been peeled away. There are also some cracks observed in the coating on the sandblasted and etched surfaces but there are no signs of flaking and the coating is homogeneously distributed (Fig. 7.7).

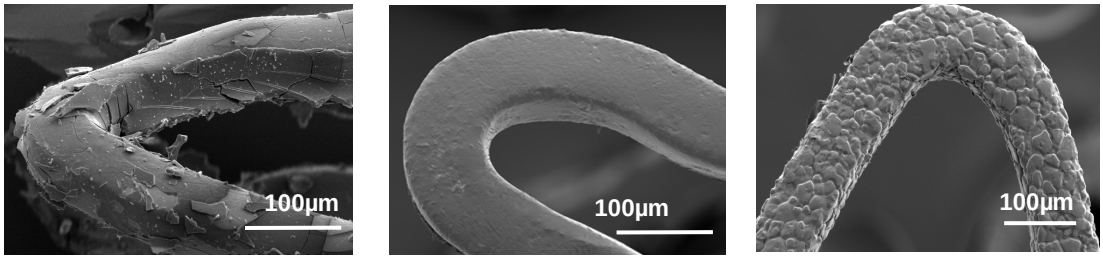

ELECTROPOLISHED SURFACE | SANDBLASTED SURFACE | ETCHED SURFACE

Fig 7.7: *SEM of expanded stents coated with 1% rapamycin solution. Comparison of surface modification.*

7.1.3 Drug adhesion on the stent surface

Adhesion tests in the artificial blood circuit

Due to the inhomogeneity of the coatings observed under SEM, adhesion tests in an artificial blood circuit were performed. For each surface modification three stents were tested. Data were collected using a UV-Vis spectrometer. The rapamycin lost during implantation is showed in percent values. The amount of drug at the surface of the expanded stents evaluated during the quantitative tests was taken as 100% and the amount of drug on the stent surface remaining after implantation was calculated in terms of percent of the amount found at the onset (see Appendix A2). The differences between these two numbers have been plotted on the graph below (Fig. 7.8).

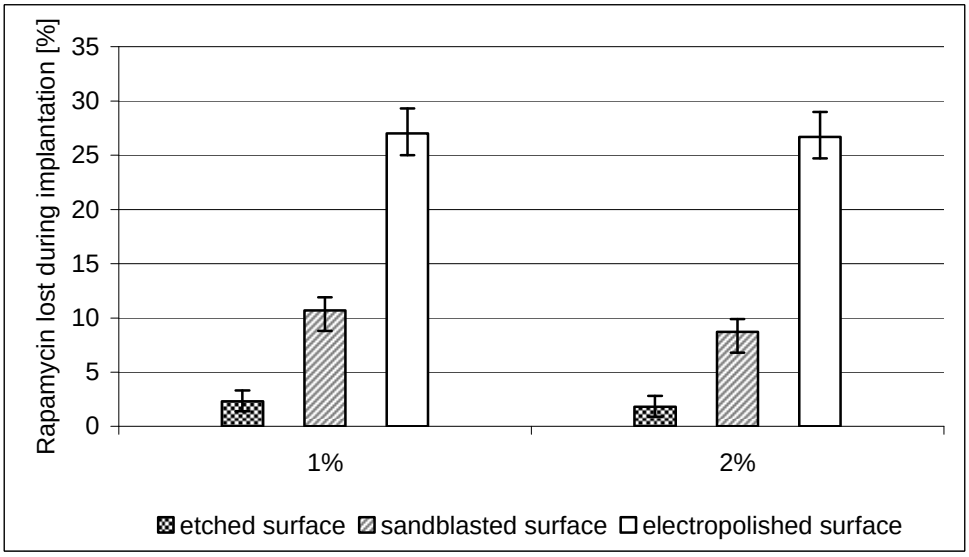

Fig. 7.8: *Adhesion tests of rapamycin in the model of human blood circulation. Stent surface topography has an enormous influence on the drug adhesion, the smallest lost of drug ensured oxalic etched surface which is the most rough from all investigated surfaces*

These tests showed that the surface modification has an enormous influence on drug adhesion to the stent surface. The most stable coating is observed on the sandblasted and etched surfaces. The coating adhesion to the surface can be explained by two mechanisms: an enlargement of the effective contact surface and/or mechanical adhesion due to the surface topography, so-called anchor effect.

The anchor effect is observed when the adhesive performs the function of an anchor, a nail, or a wedge after it has spread into the small openings on the surface and adheres and solidifies there (Fig.7.9). This kind of adhesion can be observed in porous material [114 – 116].

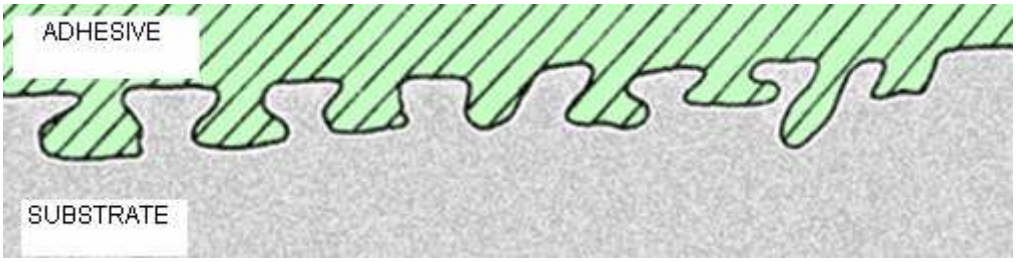

Fig. 7.9: *Sketch of mechanical interlocking of coating on the metal substrate. So called anchor effect occurs if cavities on the surface during the coating allow the adhesive to spread into these openings and solidify there creating interlocking.*

As mentioned before, rapamycin is a crystalline substance with low elasticity. Only by coating directly before stent implantation the problem of losing substance from the stent surface and storage of the drug under proper conditions can be solved. Commercially available stents are coated with drug-polymer solution by the manufacturer. The function of the polymer is to protect the drug from mechanical and chemical damage during implantation and storage in a hospital.

Rapamycin lost from the coating process until implantation was investigated to assess the reproductbility of the coating method and to evaluate wheter further addition of a polymer is necessary. (Fig. 7.10)

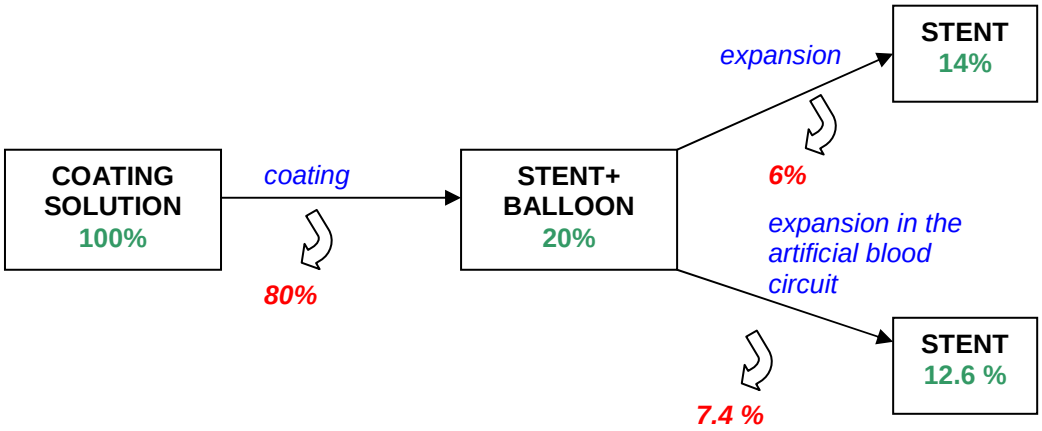

Fig. 7.10: *Rapamycin lost from the coating process until stent expansion. The first and the most lost of drug happens during coating using spray method. The next step: due to mechanical stress of stent surface during stent expansion further 6% (for expansion in the air) or 7.4% for expansion in simulated bodily conditions. The values shown are for the sandblasted surface. For mathematical explanations see Appendix.*

On the stent surface after implantation only 12.6% of the drug remains. Thus 87.4% of the initial rapamycin amount is lost during this procedure. It is caused by mechanical stress to which the surface and the coating are exposed to during stent implantation and expansion.

The next investigations of stents with different surfaces coated with rapamycin were in vitro drug release tests.

7.1.4 Release tests

Influence of drug concentration in the coating solution on drug release from sandblasted surfaces

Tests were performed with stents coated using the standard stent coating machine (SCM) with pre-programmed parameters (see chapter 6.2). For each concentration 10 stents were coated. Amounts of drug released per time interval are shown in Fig. 7.11.

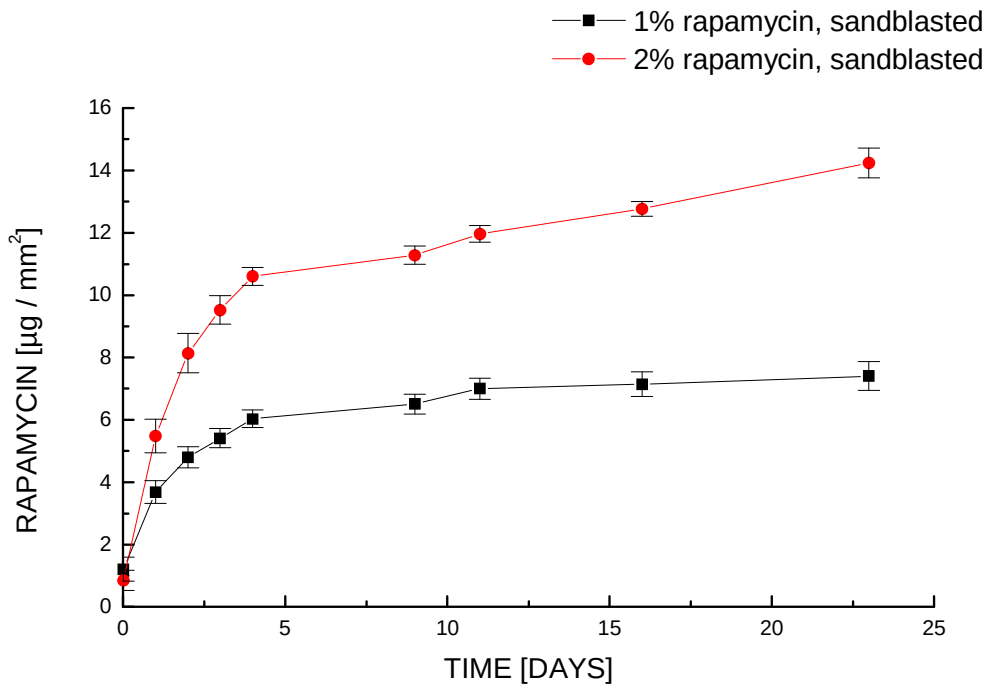

Fig. 7.11: *Influence of the coating solution concentration on the cumulative release concentration of rapamycin relased from sandblasted surface.*

Results show that the drug concentration in the coating solutions has no significant influence on the length of the release time (Fig. 7.11). Stents coated with 1% rapamycin solution as well as those coated with 2% solution released about 37% of the drug stored on the stent surface over the same time period (approx. 23 days). At the end of the release test each stent was washed in ethanol to determinate the drug amount remaining on the surface: for the 1% coating the remaining drug on the surface was insignificant, so the spectrum of

rapamycin could not be evaluated, and for the 2% coating a release of 0.11 ± 0.03µg/mm^2 was obtained. On both surfaces the percentage of the drug remaining after release tests is due to negligible amount is not relevant for further conclusions and can be omit.

If the total amount of drug released (plus drug amount remaining on the stent surface after 23 days of release tests) is compared with the amount of rapamycin determined from quantitative tests, only 37% of the rapamycin is accounted for (see Table 7.2). The loss of more than 50% of the total drug amount could be due to rapamycin degradation in solution during release tests and / or due to inaccuracy of measurement methods.

Drug concentration of the coating solution	**Coat**	**Release**
1%	20µg (100%)	7.4µg (37%)
2%	38µg (100%)	14 µg (37%)

Table 7.2: *Comparison of drug amount on the sandblasted stent surface directly after coating and expansion (coat) and total amount of drug detected during an after release tests (release). Numbers in parentheses correspond to % of total amount of drug stored on the stent surface after coating and expansion.*

As mentioned in Chapter 4.2.3 the release kinetic of a drug from a device in the human body can be described using various equations. One of the simplest equations describing drug release kinetic is the Higuchi equation:

$$\frac{M_t}{M_\infty} = K\sqrt{t} \qquad \text{(Eq.7.1)}$$

This equation does not separately consider the device geometry and the properties of materials used in the device to influence drug release. Only one constant which is specific for each device is given, namely *k*. The factor *k* determines the drug release trajectory gradient and for both concentrations of rapamycin in coating solution (1% and 2%) is almost the same in the time intervals investigated.

A significant difference between stents coated with the 1% and 2% rapamycin solutions is the initial amount of drug released per unit time. The amount of eluted drug during the first four days for the 2% coating solution was 30% more than on the 1% solution (Fig 7.12). After four days the rate of drug release was almost the same when considering non-cumulative results. It confirms that the amount of drug on the stent surface does not influence the release kinetic which is dependent on chemical properties of the drug and the immersion medium. Only at the beginning the drug amount does have an influence on the amount of released drug. During the first four days most of the drug is still present on the stent surface – proportional to the drug concentration in the coating solution. The strong initial drug release can be associated with the mechanical stress affecting the coating.

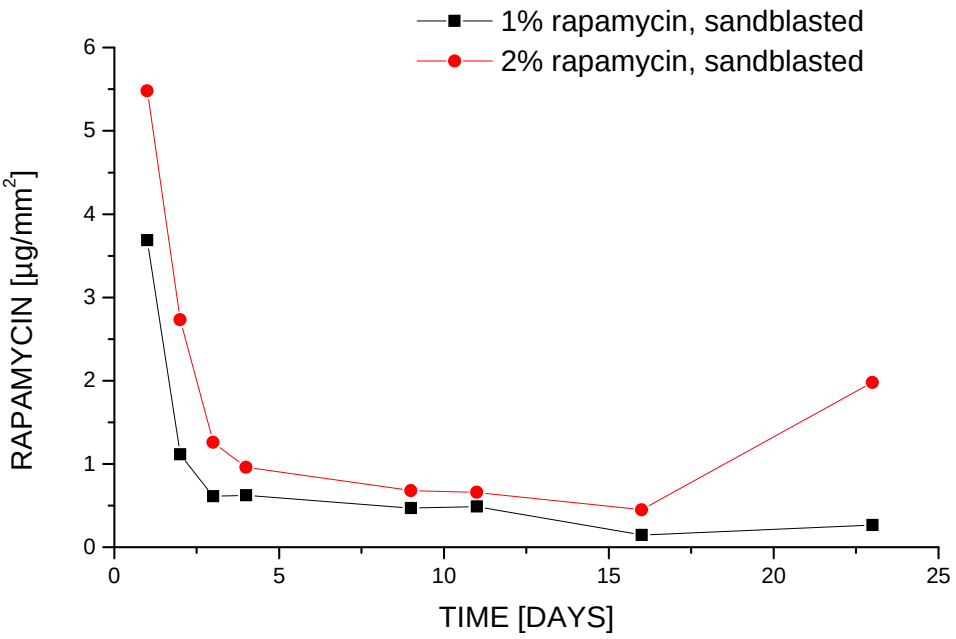

Fig.7.12: *Influence of the coating solution concentration on the non-cumulative release concentration of rapamycin from sandblasted surface*

There is no time elongation of drug release and no significant differences in release kinetic between coatings with different concentrations. Only the drug amount released in the first few days after stent implantation can be controlled by using different concentrations of coating solutions.

Influence of drug concentration in the coating solution on drug release from oxalic acid etched surfaces

On the etched surface the release phenomena are similar to that observed for the sandblasted surfaces. The amount of drug released is proportional to the drug amount on the stent surface; the greater the amount of drug on surface, the higher the drug amount released in a given time unit. However, the release kinetic is not affected by the concentration of the drug (Fig. 7.13).

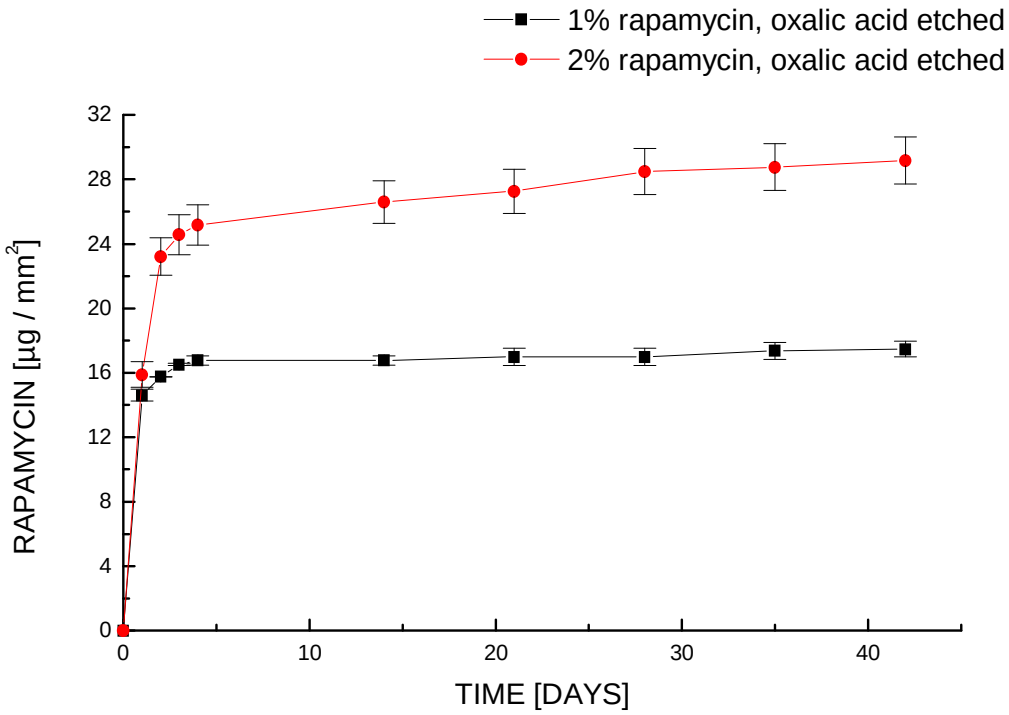

Fig. 7.13:*Influence of the coating solution concentration on the cumulative release concentration of rapamycin from oxalic acid etched surface.*

The kinetic behaviour is not affected by variations of the drug amount in the coating solution. During 42 days of in vitro investigations the release of drug from oxalic acid etched surface is not continuous. Within the first day almost the same drug amount is released for both drug concentrations in the coating solution. However subsequential drug release in the following days depends on the drug amount on the stent surface, which can be explained by the specific of surface geometry, i.e., presence of depots.

Rapamycin coating on the oxalic acid etched stent could be divided into two parts:

- the external layer of drug, which results in a rapid release of drug from the surface at the start of testing
- the drug located in depots, which causes slow release of drug from the deeper depot levels (Fig. 7.14)

Increasing the drug concentration in the coating solution results in increasing the coating thickness and in the same time interval the amount of rapamycin released is doubled but only at the beginning of the tests. After the external layer of drug is depleted there should be no concentration influence, as the depots have a defined volume and only a defined volume of drug can be stored in it.

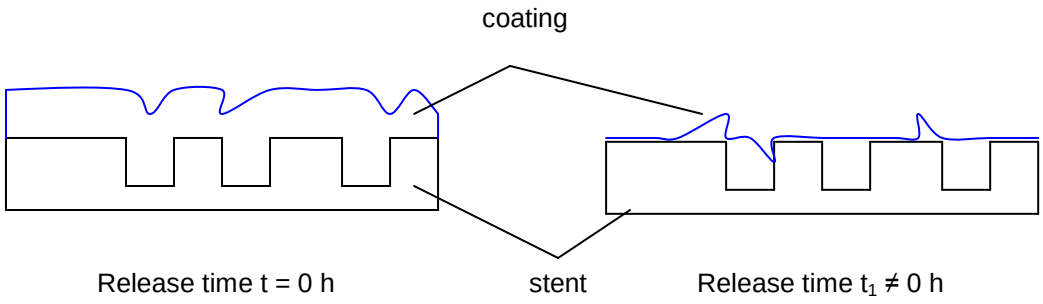

Fig. 7.14: *Schematic representation of drug release from oxalic acid etched surface. A special software[126] was developed to estimate the time when the drug from the surface has been released and the drug from depots start releasing (t_1).*

During the first days, the drug is released from the surface of the stents but not from the depots (see Fig. 7.14). To estimate the time during release when the drug starts to be released from the depots, special software has been developed [126].

Statistical information over the spatial arrangement and size of the depots in oxalic acid etched stent surfaces can be made by examining the depot surfaces in two-dimensions by SEM and extrapolating the results to three-dimensions. Polished micrograph sections of stent struts (Fig. 7.15) served for the analysis.

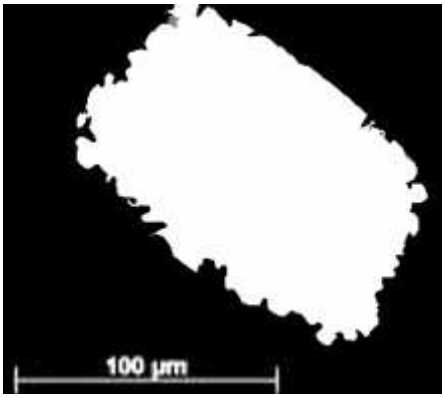

Fig. 7.15: *Cross section of oxalic acid etched stent strut. SEM picture prepared for software to evaluate the depots depth.*

To establish the rapamycin amount which can be stored in the depots the following equation was used:

$$R_D = D_d \cdot \rho_R \qquad \text{(Eq.7.2)}$$

where:

R_D – rapamycin amount stored in the depots

D_d – depot depth, obtained from SEM pictures of cross sections of stent struts

ρ_R – rapamycin density

The rapamycin density was determined using equation x and was calculated to be 1.04 g/cm^3.

$$\text{Rapamycin density} = \frac{W(a) \cdot \rho(fl)}{W(a) - W(fl)} \qquad \text{(Eq.7.3)}$$

where:

W(a) - rapamycin weight

W(fl) - weight of water

ρ (fl) - density of water

For etched surfaces the average depot depth provided by the software was 2.2±0.16µm, thus yielding about 2.3 µg/mm^2 rapamycin that can be stored in the depots (Eq.7.2).

This shows that for 1% coatings the drug started to be released from the depots after three to four days. In contrast for 2% coatings, the coating layer which covers the depots is much thicker and needs more time to be released. Therefore due to the coating thickness drug is released from the depots only after 14 or 21 days respectively (Fig 7.16).

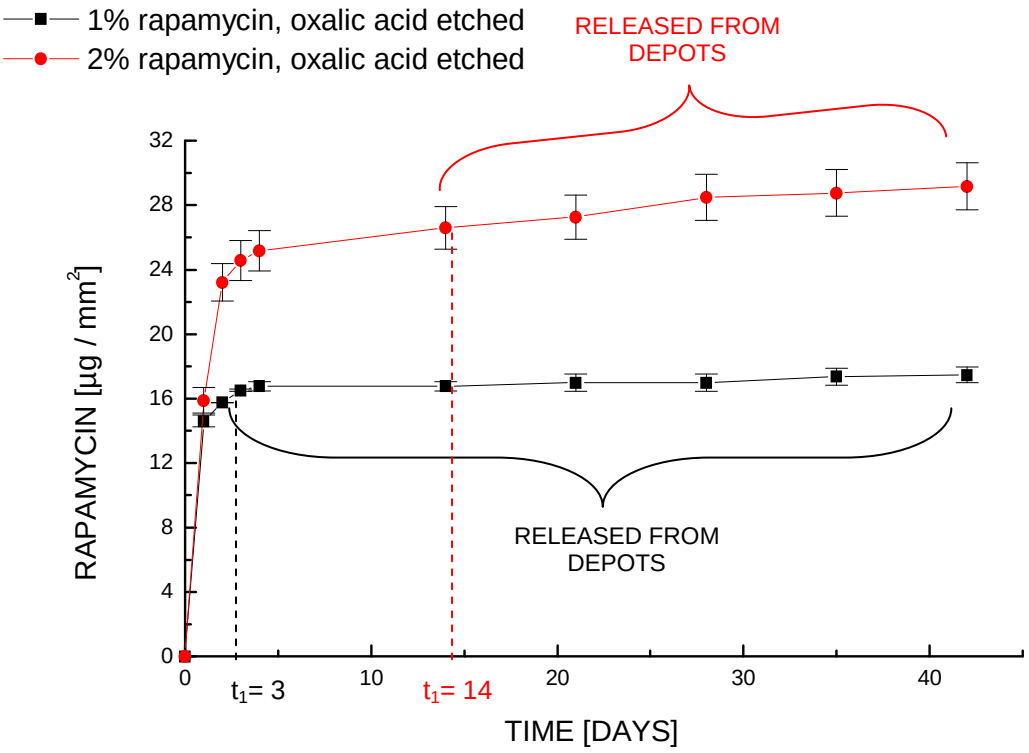

Fig. 7.16: *Influence of the coating solution concentration on the release of rapamycin from depots in oxalic acid etched surfaces. For the 1% coating the value t_1 = 3 days (t_1 – time, when drug start to be release from surface depots, see Fig 7.14) and for 2% coating t_1= 14 days. The 1% coating gives thinner coating on the stent surface than the 2% one what results in later drug release from depots for 2% coating.*

If there is less drug present in the depots, the release is slower than for more drug. The drug stored in the surface depots is released much faster for 2% coating solution, which took 28 days, than for 1% coating solution, which took 38 days (Fig. 7.16). This effect can be caused by the ability of rapamycin to aggregate due to its crystalline character (when sufficient amount is available).

Influence of the stent surface modification on drug release

For these tests three different stent surface modifications were used: electropolished, sandblasted and oxalic acid etched. Due to poor adhesion of the coating on the electropolished surface, only the 1% rapamycin solution which gives a thinner coating than 2% one was investigated. For the other two surfaces tests with 2% coating solutions were also performed.

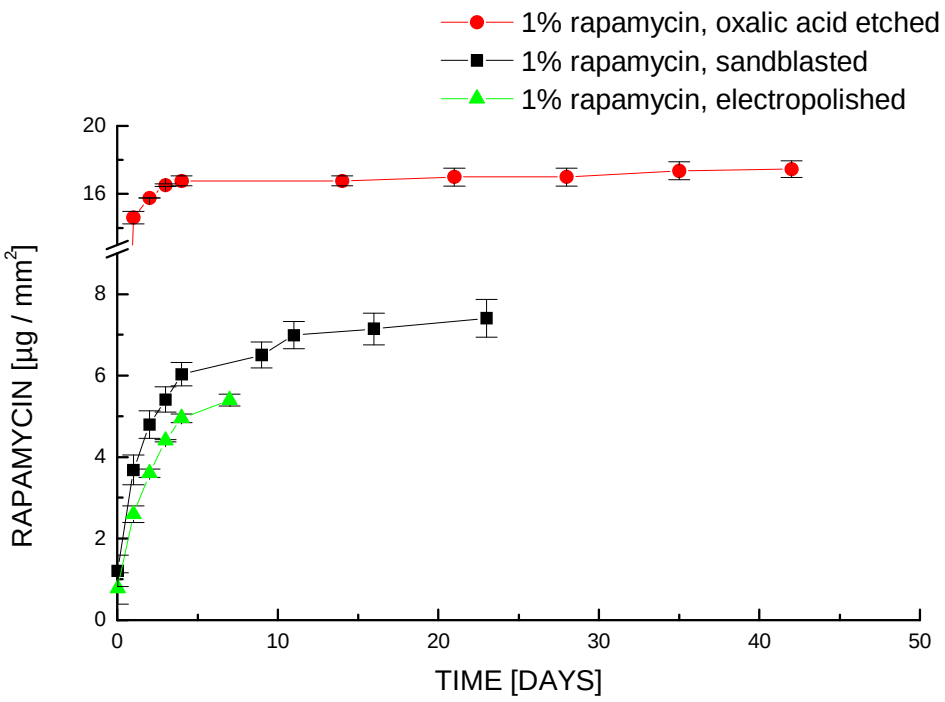

Fig. 7.17: *Influence of the surface modification on the cumulative release concentration of rapamycin from the 1% coating solution. Comparison of etched, sandblasted and electropolished surfaces. The release duration is different for each surface modification. This phenomena correlate with the surfaces ability to bind the drug. There is more drug on the sandblasted and etched surface after coating than on the electropolished one. From the smooth electropolished surface drug release is faster due to better release medium penetration than on the rough ones.*

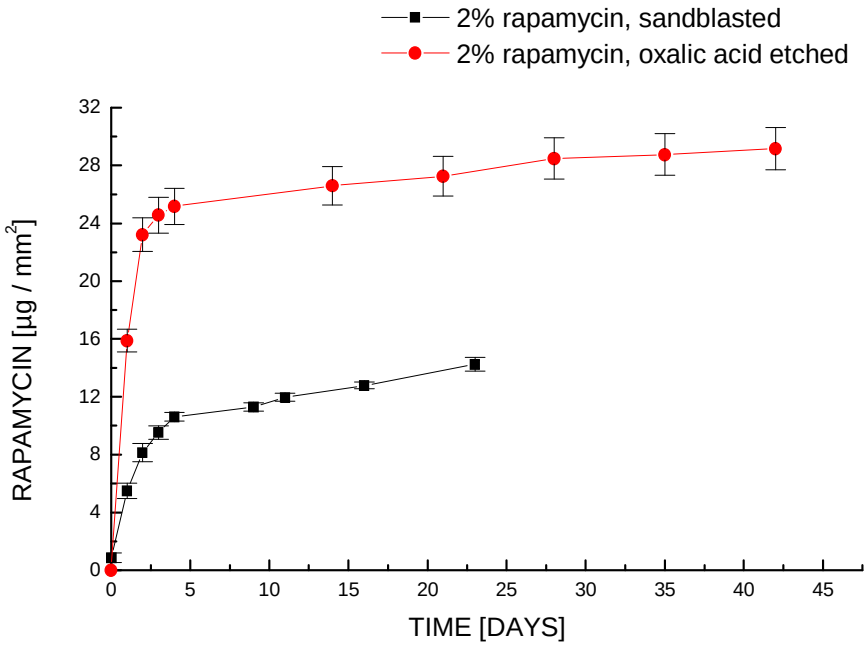

Fig. 7.18: *Influence of the surface treatment on the cumulative release concentration of rapamycin from the 2% coating solution. The same release tendency as for the 1%coating can be observed (compare Fig. 7.17).*

At a given surface treatment aspect the concentration of the drug in the coating solution has no significant impact on the drug release. The tendencies are the same for both 1% and 2% concentrations (compare Fig. 7.17 and 7.18). The statistical spreads of the values measured are larger for oxalic acid etched surface than for the sandblasted one, which can be attributed to differences in the metal microstructure. Oxalic acid etching is a grain boundary etching and depots are located there.

Etched surfaces take and release more drug than the two other surfaces and show a sustained release compared to sandblasted and electropolished surfaces (Fig. 7.17).

The release of rapamycin from the etched surface exhibits a strong release at the beginning of the measurements (first four days) and then the remaining drug amount is released continuously in small doses.

The sandblasted and electropolished surfaces produce a more continuous release of rapamycin from the beginning but there is no depot effect and all the drug is released from the surface in a shorter period (21 days and 7 days, respectively) than for the etched

surface (42 days). Surface modifications have shown a significant effect on the release kinetic of the drug; the greater the surface roughness, the more drug stored on the surface and the longer the release time.

Many different approaches have been used to characterize the drug delivery from stents, and the duration of the drug delivery has been varied [21]. It has been suggested that vascular smooth muscle cells start proliferation only a day after the injury resulting from balloon angioplasty or stent deployment and up to about two weeks [124]. Thus it is believed that antirestenotic drugs need to be delivered for at least three weeks [125]. In the case of sandblasted surfaces almost 30% of the total drug amount is released during the first three days increasing to 40% after three weeks. Etched surfaces release rapamycin over 42 days but at the beginning about 80% of total drug is released.

7.2 Investigation of rapamycin diffusion into porcine coronary artery wall

To verify if in vitro and in vivo tests are comparable and to estimate the time from which the modified surface starts to have an influence on drug release and its diffusion into the coronary artery wall, in vitro tests on porcine arteries were performed.

Special techniques were applied or modified to investigate the diffusion of rapamycin labeled with anthracene carboxylic acid into the coronary artery wall (see chapter 6.5).

Radial and lateral diffusion of the drug into the innermost layer of the artery (see Fig. 6.22) was investigated in a perfusion bath on freshly dissected porcine arteries (see chapter 6.5).

Based on the evaluation of histological sections after perfusion for 12, 24 and 48 hours and comparing with non treated samples a first estimation of the optimal perfusion duration for the porcine coronary artery under given perfusion conditions could be determined and was found to be 24 hours. Artery functionality tests on freshly prepared samples and on

samples after 24 hours perfusion allowed a more objective assessment on the optimal parameters on a cellular level.

After 24 hours perfusion, temporal delays as well as a decrease of the response to vasoactive substances were observed. However, cell vitality as well as membrane integrity could be clearly shown to be decisive for the drug transport. Parameters for a perfusion period of 24 hours were reasonable.

Two methods were used to investigate drug diffusion into the coronary artery wall:

- optical: fluorescence microscopy and two photons laser scanning microscopy
- chemical: high pressure liquid chromatography (HPLC).

In the following section the superficial (surface) view of the artery intima is performed by conventional fluorescence microscopy with ApoTome system as well as two photons laser scanning microscopy (2PLSM) for the evaluation of the lateral drug diffusion. A schematic picture for better understanding of the optical cuts is presented below in figure 7.19.

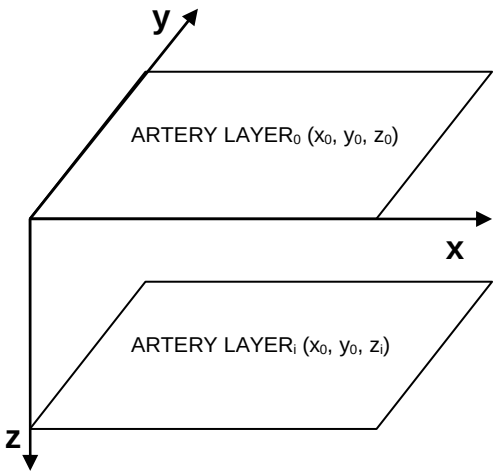

***Fig. 7.19**: The levels relevant for microscopy photographs to the investigation of the lateral as well as radial drug release outgoing from the artery intima (x_0, y_0, z_0) into more deep-seated vascular layers (x_0, y_0, z_i).*

Evaluation of lateral drug release was accomplished using microscopic methods. The following picture made by using fluorescence microscope, shows on the artery intima the imprint of a stent coated with labeled rapamycin (Fig. 7.20).

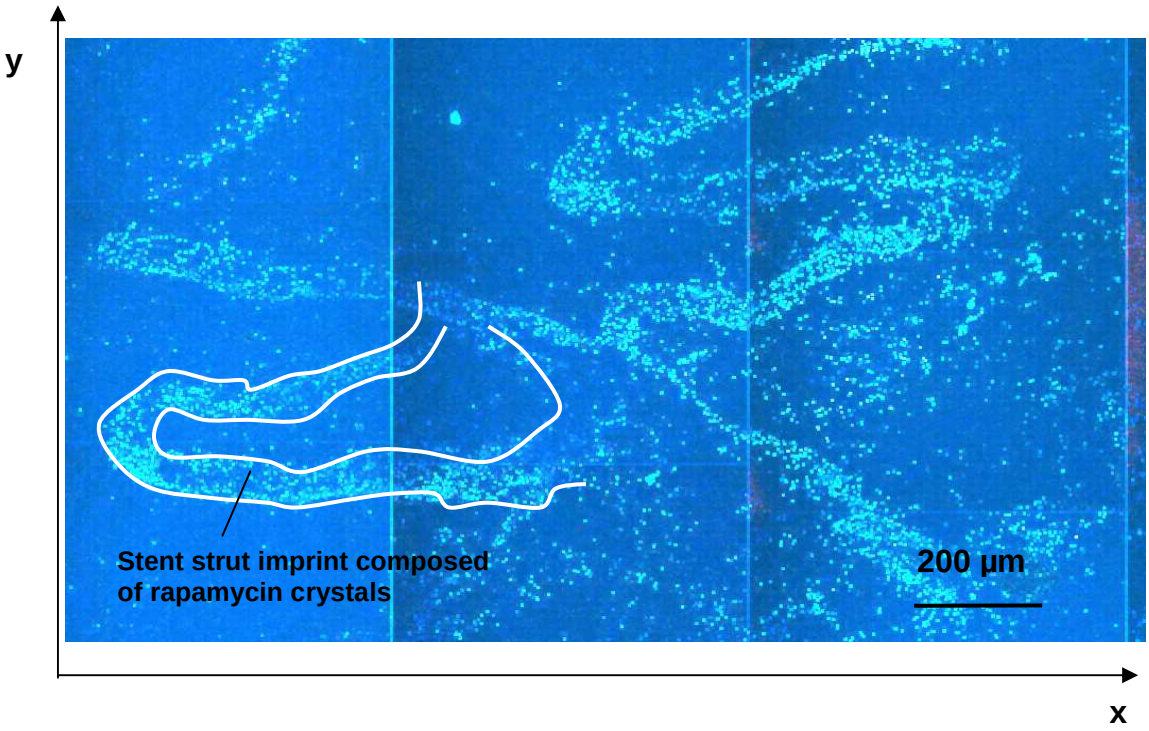

Fig. 7.20: *Fluorescence microscopy image of the intima (artery layer x_0, y_0,, z_0, see Fig.7.19) of a stented porcine coronary artery. In the picture the imprint of the stent coated with rapamycin is clearly visible due to fluorescent labeling of the drug (highlighted with white line). Blue background is due to the autofluorescence of the artery. x and y axes show the considered area and layer.*

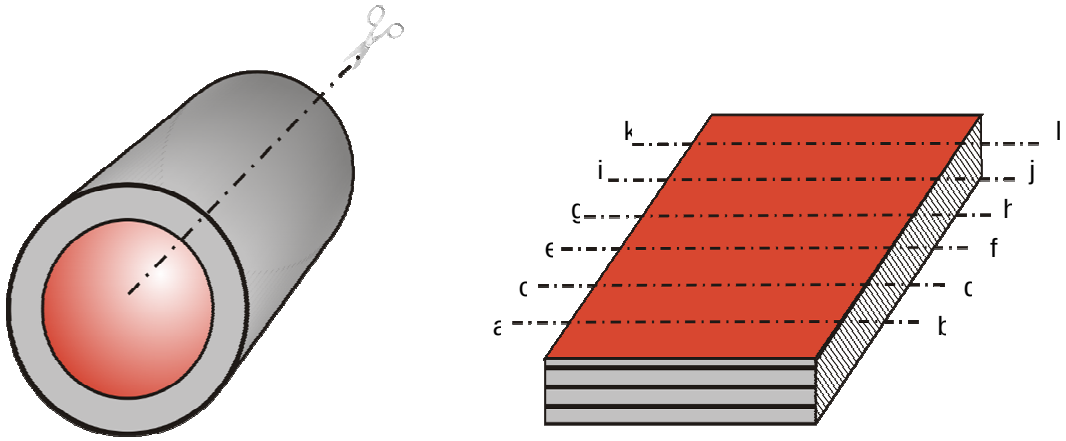

Fig. 7.21*: Three-dimensional artery location, the intima is marked red. Left: coronary artery segment, direction of cut is marked. Right: artery is longitudinally cut and unfolded; location of sections* a-l *is indicated and relate to Fig. 7.22.*

Subsequently, imaging of the radial drug release into artery wall with the ApoTome system as well as two photons laser scanning microscopy (2PLSM) took place. In these studies optical sectioning from deeper artery layers of the x-z plane was possible (Fig. 7.22).

a  b

Cross section of the part of the artery which had direct contact with stent strut coated with 0.5% rapamycin; 12h perfusion,

c  d

Cross section of the part of the artery which had direct contact with stent strut coated with 0.5% rapamycin; 12h perfusion,

e  f

Cross section of the part of the artery which had direct contact with stent strut coated with 0.5% rapamycin; 24h perfusion

g  h

Cross section of the part of the artery which had direct contact with stent strut coated with 0.5% rapamycin;24h perfusion

i  j

Cross section of the part of the artery which had direct contact with stent strut coated with 1% rapamycin; 24h perfusion

k 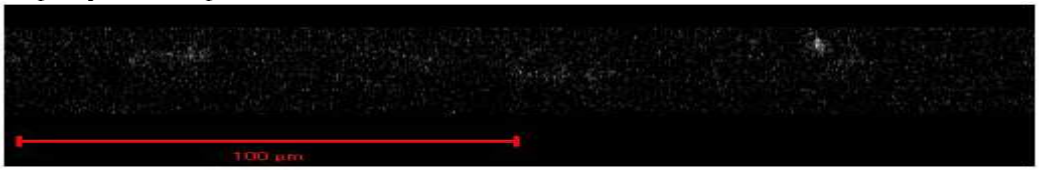 l

Cross section of the part of the artery which had no direct contact with stent strut coated with 1% rapamycin;24h perfusion,

Fig. 7.22: *Diffusion of rapamycin (white crystals) into the coronary artery wall. Pictures were made using two photons laser scanning microscope. For these illustrations, pictures of the artery in x-z direction (compare Fig. 7.19 and Fig. 7.21) were made.*

The diffusion of rapamycin is clearly not homogeneous in the radial and lateral directions (Fig. 7.20, Fig. 7.22). For the 0.5% drug concentration in the coating solution the same diffusion tendency as for the 1% concentration could be observed. Two photon laser scanning microscope allowed identification of the endogenous structures of the artery as elastic fibres. Hwang and colleagues have already shown with Paclitaxel that these structures (elastic fibres) show a higher number of unspecific connection sites in the artery wall for hydrophobic drugs [35]. The non-uniform drug binding within the artery wall can be explained with the nonuniform structural construction of arteries [55]. It is suggested that the artery structure is also the reason for a varying number at hydrophobic connection sites which in the intima and the adventitia [37]. These unspecific connections serve as a reservoir for rapamycin and cause an increase of local drug concentration. It can be observed in Fig. 7.22.

Besides the concentration variations the connection sites also cause a decrease in the drug transport through the artery [37]. This can help to explain the fact that on a microscopic level the different perfusion duration has no considerable influence on the penetration depth of rapamycin.

For the quantitative evaluation of rapamycin diffusion into the coronary artery the following values were determined using mechanical procedure to homogenize the tissue:

- m_{RG} [µg]: drug amount in tissue
- m_G [ng rapamycin / mg tissue]: drug amount in tissue related to artery weight

These tests were performed on two modified stent surfaces: sandblasted and oxalic acid etched. Results of measurements with sandblasted surface are presented in Table 7.3 and comparison of surface modifications in Table 7.4.

Parameter	0.5 % / 12h	0.5 % / 24h	1 % / 12h	1 % / 24h
$m_{R,G}$ [µg]	2.61 (± 0.31)	2.67 (± 0.24)	2.41 (± 0.05)	2.38 (± 0.05)
$\frac{m_{R,G}}{m_G}$ [ng/mg]	13.2 (±1.06)	11.0 (±2.9)	19.0 (±7.8)	15.8 (±3.4)

Table 7.3: *Quantitative evaluation of rapamycin diffusion from sandblasted stent surface into the coronary artery wall. Following data were obtained for both 0.5% and 1% rapamycin solutions and perfusion time of stented artery: 12h and 24h: $m_{R,G}$ - drug amount in the whole artery segment; $m_{R,G}$ / m_G - drug amount in artery tissue related to 1mg of the tissue. There is no significant difference in results concerning time of perfusion. Only concentration increasing of drug in coating solution results with more drug detected in artery tissue.*

Parameter	0.5 % / 24h / sandblasted surface	0.5 % / 24h / oxalic acid etched surface
$m_{R,G}$ [µg]	2.67 (± 0.24)	2.31 (± 0.01)
$\frac{m_{R,G}}{m_G}$ [ng/mg]	11.0 (±2.9)	12.05 (± 2.8)

Table 7.4: *Quantitative evaluation of rapamycin diffusion into the coronary artery wall; comparison of surface modification influence: sandblasted and oxalic acid etched stent surface.*

There is no significant difference between diffusion of rapamycin from sandblasted and etched stents surfaces during 24 h perfusion in the organ bath (table 7.4). At the beginning directly after stent implantation the type of surface modification has no influence on the drug release. As shown in the in vitro measurements without arteries, drug release from the surface depots occurred after a few days of coated stent immersion into Ringer solution. Due to histological and vasoactivity tests it is not possible to perform tests longer than 24h using dissected coronary arteries. For detailed studies of the effect of surface depots in vivo studies are required.

The consideration of the drug amount found in the tissue suggests that the release within a 24 hours period is independent on both the drug concentration in the coating solution and the stent surface. Possible explanations for this behaviour would be the presence of a

temporary saturation in the tissue or the initial dominance of the drug crystals released from the stent surface during balloon dilatation. Both explanations support the conclusions reached in the qualitative investigation. This is in agreement with the conclusion of Levin and colleagues [55].

Since within the first 24 hours only the outermost drug layer is in direct contact with the surrounding tissue, the different reservoirs present in both stent surfaces investigated (sandblasted and etched) have no influence on the drug release within the period examined.

The evaluation of the drug amount stored in the tissue related to the respective weight of the surrounding tissue provided an average value of ≈ 14 ng/mg, which nearly corresponds to the results obtained from investigations in vivo [112]. In this study the maximum drug amount released into the artery wall was observed during the second and third day after stent implantation [112]. The time lapse from the insertion of the stent to the achievement of the equilibrium is only about 60 hours [55]. This implies that, at earliest only after this time point different drug concentrations as well as reservoirs in stent surfaces may become relevant. The uncertainties could be solved in the ideal case with the help of an optimization of investigation methods as well as the realization of a large number of trials. However, the statement can only be applied to healthy tissue, but not for stenotic vessels with sclerosis which pose an additional barrier for drug transport.

Clinical studies were performed to prove that sandblasted stents coated with rapamycin directly before implantation in catheter laboratory are capable to reduce neointima formation in vivo [112]. These studies have shown that despite high loss of drug from the stent surface during implantation procedure (see Fig. 7.8 and Fig. 7.10) the effectiveness of rapamycin eluting stents compared with bare metal stents is high (Fig.7.23). Rapamycin eluting sandblasted stents coated with increasing amounts of drug significantly inhibit in-stent neointima formation [112].

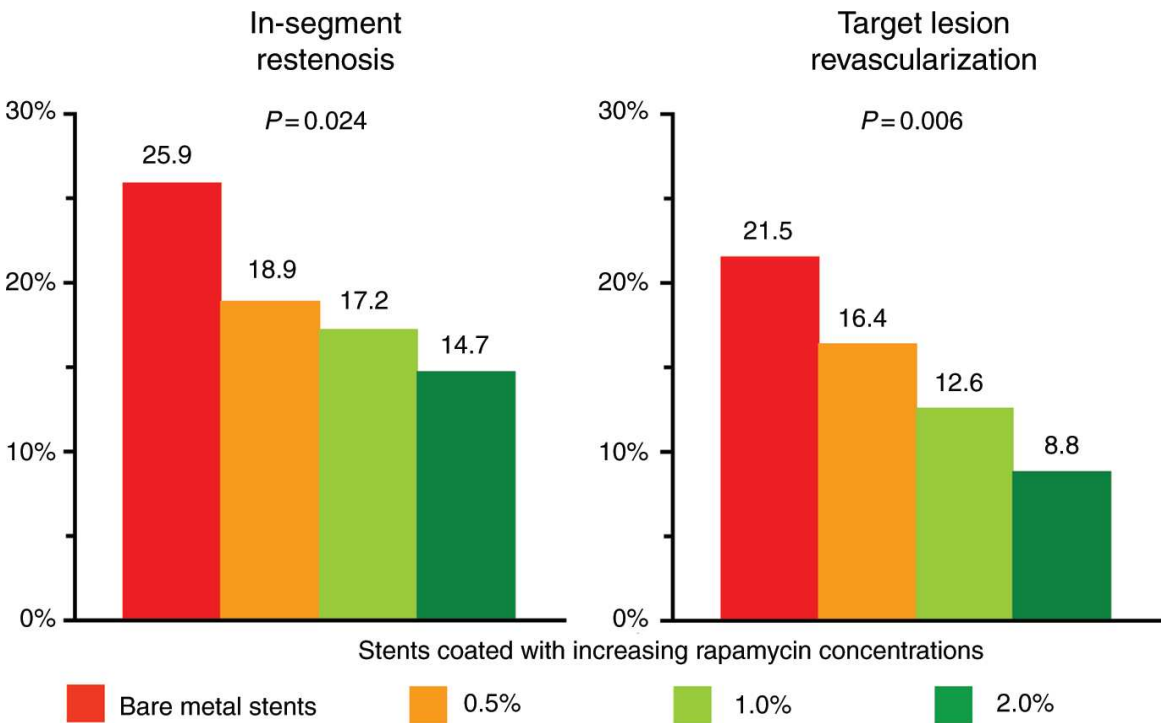

Fig.7.23: *Bar graph demonstrating the angiographic restenosis rates and the need for post-operative target lesion revascularization (repeat coronary intervention or bypass surgery) for sandblasted stents coated with increasing rapamycin concentrations (0.5–2.0%) compared with bare metal stents[from 112].*

Although, to date there is no indication how long drug should be released and the accurate drug dosis is also not known a sufficient time period for rapamycin to effectively reduce restenosis is assumed to be in the range of weeks [137-139]. Income relevant clinical studies reported in [112, 116] demonstrated that the placement of a polymer-free rapamycin eluting stent with a sandblasted strut surface is feasible and safe. All indices of restenosis improve with increasing drug doses on the stent. When compared with the BMS group, the biologic potency of the polymer-free rapamycin eluting stent reduces the risk of angiographic in-segment restenosis by a maximum of 43% with a corresponding 59% reduction in the need for target lesion revascularization (TLR) [116].

7.3 Influence of the selected polymer properties on drug release

As mentioned previously (Chapter 4.2), the polymer properties play a decisive role in drug release from devices. Two PDLLA polymers with different molecular weights were investigated to check the influence of this parameter on rapamycin release.

Up to an incubation time of one month, the drug release from both polymer matrices was almost identical. After this time the matrix with lower molecular weight (202H, 16kDa) releases more drug than the matrix with the highest molecular weight (203S, 30kDa; Fig. 7.24). These phenomena correlate with molecular weight (MW) changes in the polymer matrix during incubation in the Ringer solution.

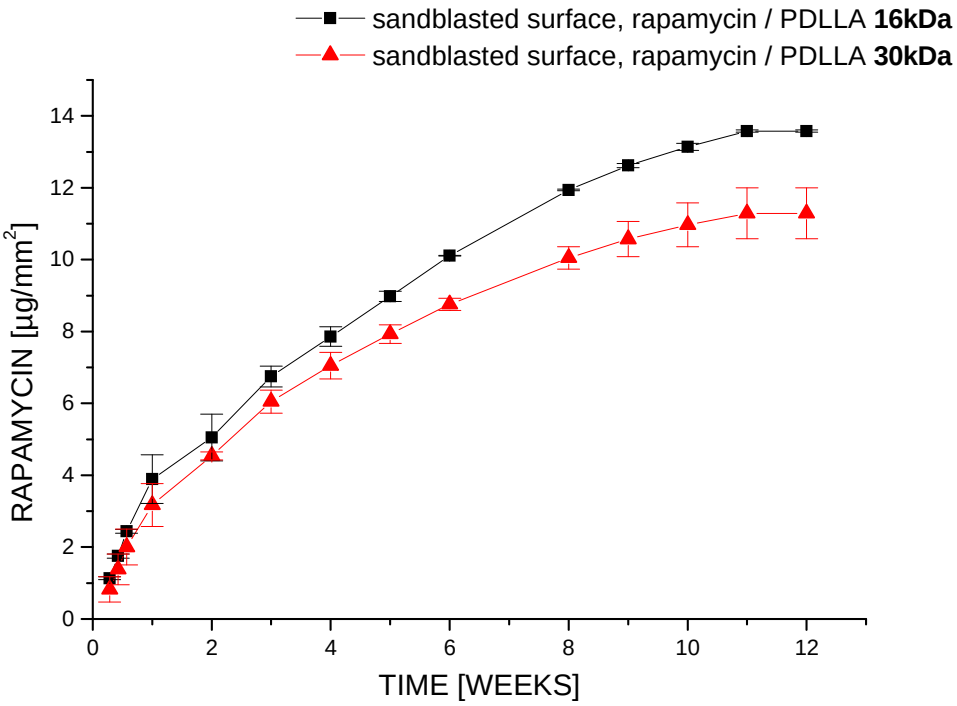

Fig. 7.24: *Influence of the polymer molecular weight on the cumulative release concentration of rapamycin. Independently of the initial molecular weight of PDLLA the drug release increased with degradation of polymer matrix.*

A correlation between molecular weight changes and drug release could be observed (Fig.: 7.25 – 7.26). For both matrices, independently of the initial molecular weight, the drug release was found to increase with decreasing molecular weight of the polymer.

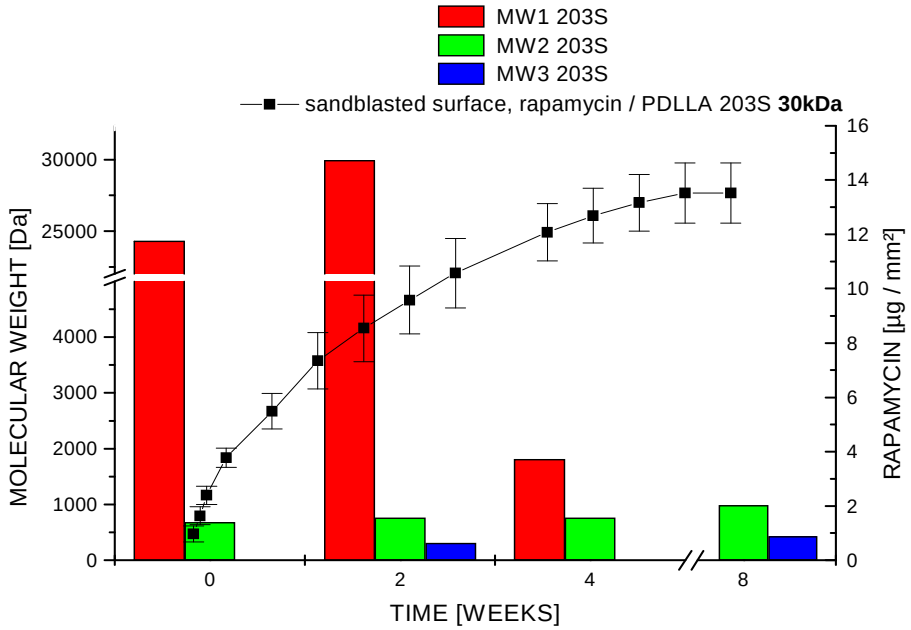

Fig. 7.25: *Comparison of polymer degradation (203S, MW= 30 kDa) with rapamycin release from the sandblasted surface. MW_i- molecular weight which indicates degradation. In the polymer bulk there are present polymer chains which did not degrade yet as well as oligomers which refer to polymer degradation. After four weeks in polymer bulk there are only oligomers with maximum MW of approx. 2000 Da. detectable. With increasing matrix degradation grade drug release is faster.*

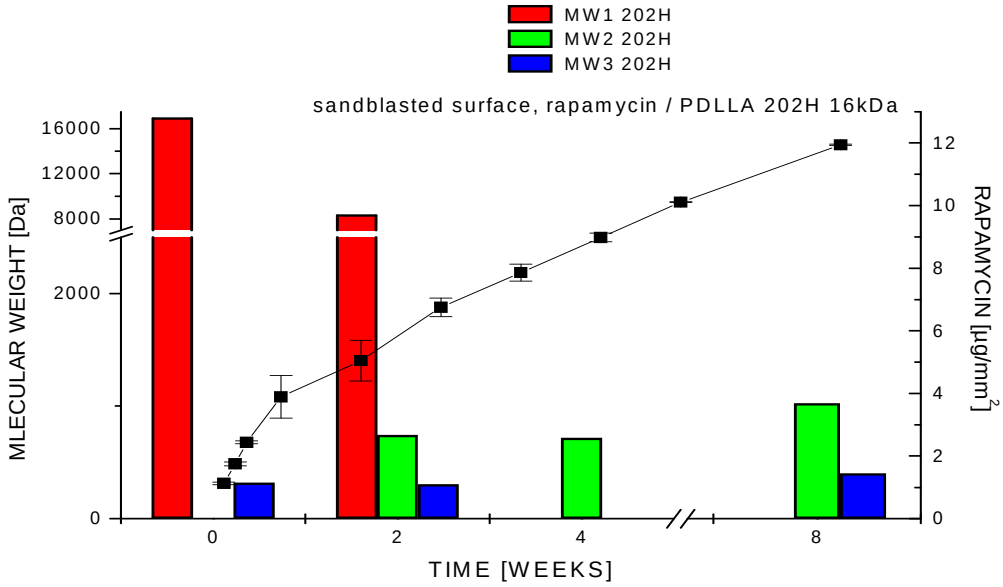

Fig. 7.26: *Comparison of polymer degradation (202H, MW= 16kDa) with rapamycin release from the sandblasted surface.*

The degradation of the polymer was investigated using gel permeation chromatography (GPC) calibrated with polystyrene standards. After a defined immersion time in Ringer solution the coated stents were washed using THF and the molecular weights were determined from the solution using GPC (see Chapter 6.3.3). There are three main peaks on the GPC chromatogram which represents three retention times.

The polymer with the lower molecular weight (16kDa) experienced significant degradation directly after start and during the following two months, while the polymer with the higher molecular weight (30kDa) did not show any detectable change during the first two weeks.

Polymer 202H degrades relatively quickly and continuously over two months (Fig. 7.26). After four weeks only one peak is detected which corresponds to a molecular weight of approx. 700 Daltons. For the 203S-rapamycin coating on the sandblasted stent surface the molecular weight is changes linearly (Fig. 7.25). The degradation of the polymer is significant after four weeks of immersion in the Ringer solution. Even after two weeks of immersion the first changes are observable and peaks corresponding to polymer molecular weights of 1000 and 300 Da appear. After eight weeks there are no peaks detectable greater than 1500 Da what indicates total polymer degradation.

Degradation of polylactides has been broadly discussed in literature [78,80,93]. Generally it is said that oligomers having a high molecular weight have a lower biodegradation rate. Additionally there is one more parameter which is characteristic in the degradation of polylactides, namely the crystallinity. In contrast to amorphous poly-*d,l*-lactide, pure poly-*l*-lactide exhibits a relatively high crystallinity degree. Wu and Wang et al [120] proved that during the release there is increase in crystallinity from 3 to 30% as samples degrade from high to low molecular weight. Another factor influencing strongly the degradation phenomena is that PLLA with low molecular weight but high crystallinity, degrades slower than PLLA with high molecular weight which exhibits the lowest crystallinity degree. Crystallinity governs the degradation time, and for PLLA due to the inversely proportional degree of crystallinity with the molecular weight, the lower the molecular weight the slower the degradation and drug release.

Since PDLLA is amorphous the degradation process depends only on the molecular weight and the drug release slows down progressively as the molecular weight increases.

Furthermore, the coating thickness changes in time and becomes thinner with increasing immersion time. Lateral sections of stents embedded in epoxy resin were observed and the coating thickness was measured using SEM integrated software (Fig. 7.27).

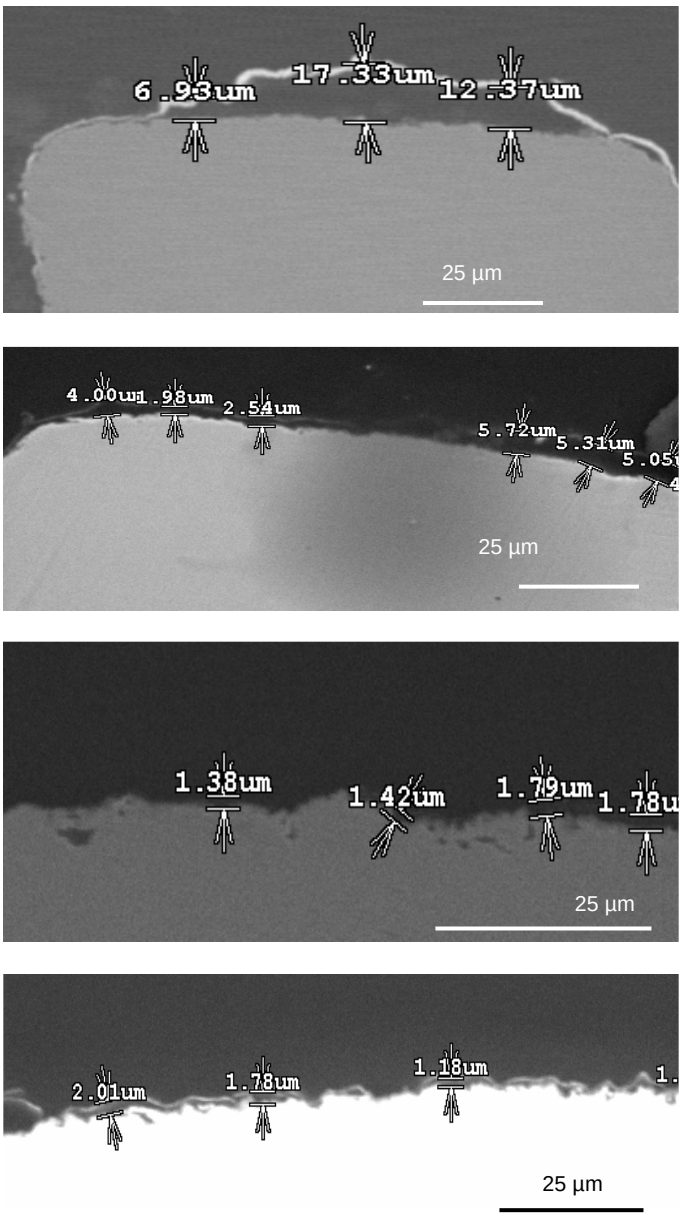

Immersion time = 0h
Coating thickness = approx. 12 µm

Immersion time = 2 weeks
Coating thickness = approx. 4 µm

Immersion time = 4 weeks
Coating thickness = approx. 2 µm

Immersion time = 8 weeks
Coating thickness = approx.1.5 µm

Fig. 7.27: *SEM pictures: Measurement of thickness changes of polymer 203S / rapamycin coating during release. Example photos of the investigated specimens – for each parameter at least 10 photos were made to give an average coating thickness. The coating thickness decrease continuously with the degradation of polymer and drug release in time.*

The correlation between changes in coating thickness and drug release is clearly visible, but the behaviour at the beginning of the immersion does not strictly correspond with the results obtained from the molecular weight measurements (Fig. 7.28 – 7.29). For PDLLA with a molecular weight of 30kDa, changes in molecular weight are not detectable after two weeks immersion in Ringer solution but the coating thickness decreases significantly (Fig. 7.29). A similarly phenomenon could be observed at the beginning of the release measurements for the polymer with the lower molecular weight (16kDa). In addition, in another period of release (between two and four weeks) a very fast degradation of the polymer does not correlate to small changes in the coating thickness (Fig. 7.28). This phenomenon could be explained due to the relatively fast release of rapamycin at the beginning followed by a deceleration of rapamycin release from the polymer matrix.

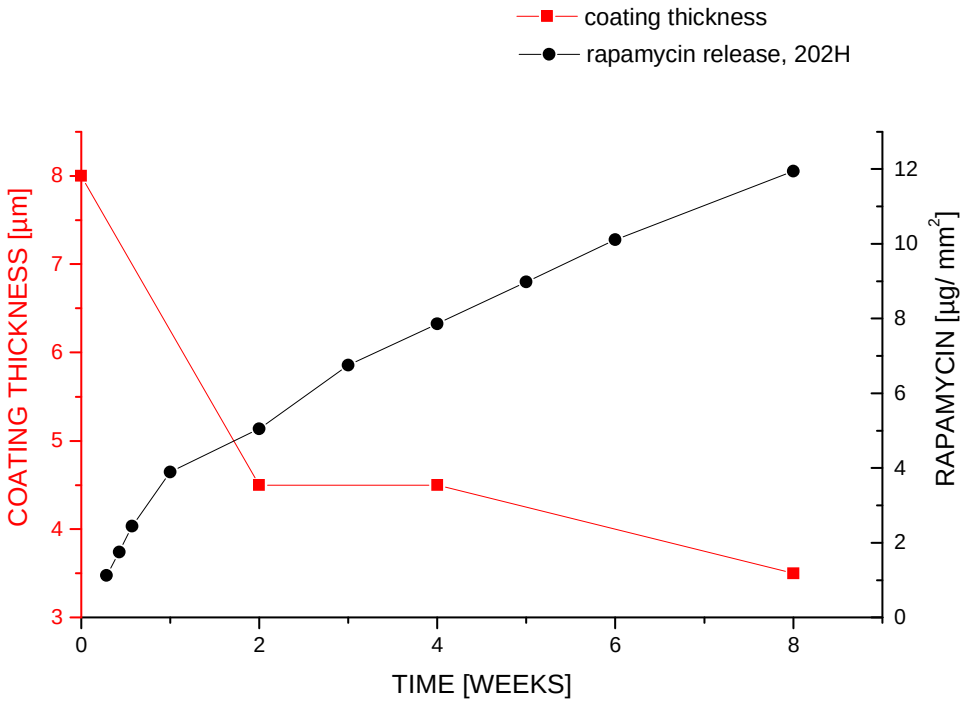

Fig. 7.28: *Comparison of coating thickness and rapamycin release for PDLLA with 16kDa molecular weight. The coating thickness decreases during stent immersion time in Ringer solution what corresponds to the fast rapamycin release in the first two weeks. Then coating thickness reduces slowly and drug release also decelerates.*

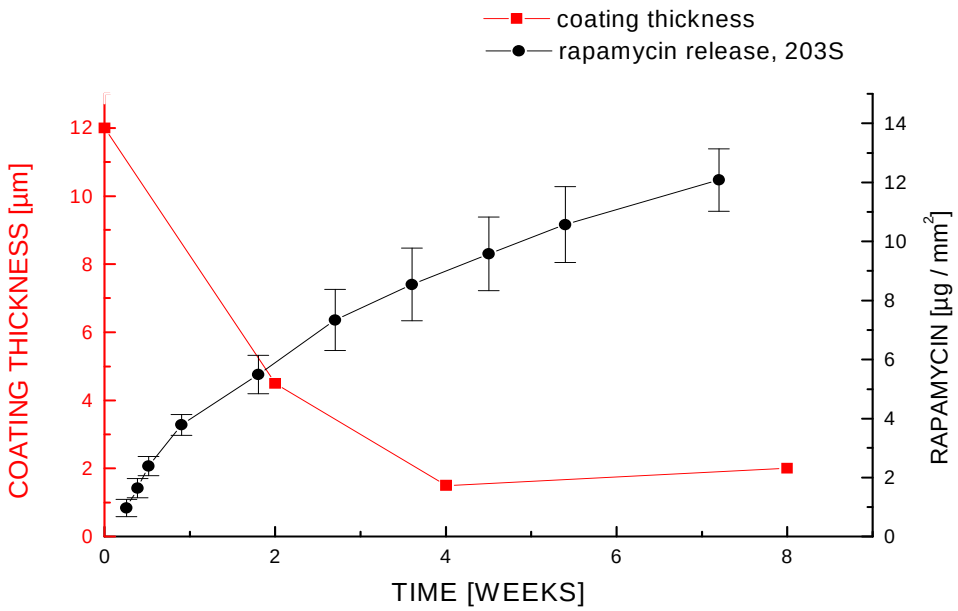

Fig. 7.29: *Comparison of coating thickness and rapamycin release for PDLLA with 30kDa molecular weight.*

7.3.1 Influence of rapamycin on the polymer degradation

The influence of rapamycin on the polymer degradation was investigated using the 203S polymer. Three stents were coated only with the 203S polymer in the same way as the rapamycin/polymer coatings and all parameters used for the release measurements were identical to those used for the drug/polymer coatings. By comparing GPC chromatograms of 203 S with and without the addition of rapamycin it could be observed that rapamycin accelerates the degradation process (Fig. 7.30 – 7.31). Authors reporting drug influence on polymer degradation [121] affirm that the drug amount in the matrix and the effect of the chemistry of the drug on the matrix degradation dominates the release patterns by influencing the rate of degradation.

Rapamycin diffusion (dissolution) process started within the first 24 hours after stent immersion in Ringer solution (Fig.: 7.28) and simultaneously PDLLA undergoes the bulk erosion. The reason for faster degradation of polymer when drug is incorporated in coating, in comparison to degradation of “pure” PDLLA could be due to the better penetration of release medium in the bulk of polymer caused by free spaces of released rapamycin.

Furthermore it can be concluded that the formation of local radicals causes a local decrease of the pH, which can cause an inherent acceleration of the degradation process [121].

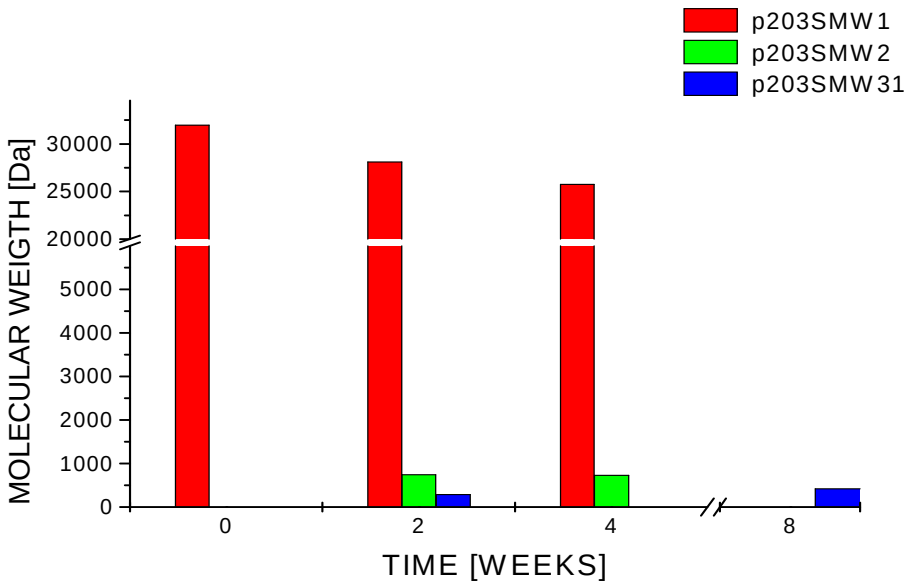

Fig. 7.30: *Changes in the molecular weight of 203S PDLLA coating during immersion in Ringer solution. After four weeks the peak corresponds to the molecular weight of approx. 30kDa is still present. Degradation progress is slowly in comparison to the coating incorporating rapamycin. Firstly after eight weeks polymer degradation is considerable.*

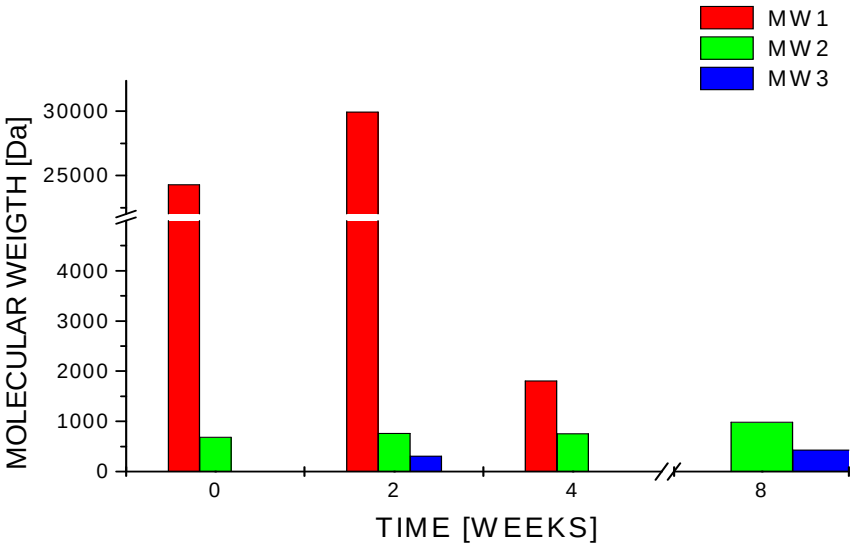

Fig. 7.31: *Changes in the molecular weight of 203S PDLLA / rapamycin coating during immersion in Ringer solution. Drug incorporation in the polymer bulk noticeable accelerated PDLLA degradation. After one month of degradation tests the biggest detected peak corresponds to the molecular weight of approx. 2kDa.*

8 Conclusion and outlook

Motivation for this work was the development and investigation of safe stent coatings which allow the customized treatment of stenosis to effectively prevent or minimize the restenosis rate. This could be achieved by improving the stent coating method and optimizing the physical properties of the coating solutions.

The focus of this work was to prove that the on-site coating of stents with drug and drug/polymer coatings is possible, reasonable and safe.The aim was to investigate if there is a possibility to control the drug release from stents coated directly before implantation.

Coating stents only with the drug without any additional protective layer is possible and reasonable only if made directly before implantation. Due to the chemical and mechanical properties of the rapamycin layer, coated stents cannot be stored in the catheter laboratory.

Drug-coated stents available on the market have a shorter date of expiration than uncoated ones and have only one drug dosage which is used for all patients independent of their disease pattern.

On-site coating can solve simultaneously two problems: first, the therapy can be individualized for each patient depending on their disease pattern and second, it is economically advantageous for hospitals not to have to store a large number of stents with different properties. Required are only stent platforms with the appropriate geometry and size which can subsequently be coated with the required drug amount.

In summary the control of drug release from coronary stents is possible and can be done in two ways:

- surface modification
- addition of biodegradable polymers

A combination of the following parameters, surface modifications and different drug amounts in the coating solution without any barrier layer, results in fast drug release. For stents coated only with rapamycin, the release behavior depends on these parameters and varies from seven days for an electropolished surface coated with 1% rapamycin solution to 40 days for an oxalic-acid etched surface coated with 2% drug solution.

Sandblasted stents coated with rapamycin directly before implantations were investigated in first short-term human trials and showed reduction of restenosis incidence in comparison with non-coated bare metal stents [112]. Polymer addition to stent coatings with rapamycin resulted in slow release kinetics of the drug. In literature there has been some concern over the suitability of using polymers in stent coatings due to the inherent risks of inflammatory responses [1]. In fact the use of a stable and theoretically inert polymer as a stent coating has been shown not to assure long-term biocompatibility [2].

The release pattern of rapamycin depends on the degradation time of amorphous PDLLA and drug uptake into the polymer matrix. Polylactides serve as a decelerator of drug release compared with drug-coated stents (DC-stents). Polymer-rapamycin coatings release less drug in the same time intervals than non-polymeric ones and exhibit elongation of total drug release time.

Based on the results of this work, the stent coating device should be improved to ensure more reproducible coatings especially for polymer-drug mixtures. In general, the new concept of customizing the stent drug coating to inhibit restenosis was successfully developed and investigated. Moreover the coating method could be used not only for rapamycin, but also for other agents, in combination with other surface modifications.

To reduce the restenosis rate after stent implantation not only properly coating should be taken under consideration, also stent design and mechanical properties of stent material should be better investigated and improved.

9 References

1. World Health Organization, Preventing chronic diseases: a vital investment: WHO global report. WHO press Geneva, Switzerland, 2005
2. Ross R. The pathogenesis of Atherosclerosis. In: Heart disease – textbook of cardiovascular disease. Braunwald E., ed. Philadelphia-London- Toronto-Montreal-Sidney-Tokyo: W. B. Saunders 1997;1105 - 1125
3. Hombach V. Klinik der koronaren Herzkrankheit. In: Interventionelle Kardiologie, Angiologie und Kardiovaskularchirurgie. Schattauer, Stuttgart, New York 2001; 323-331
4. Mitchell ME, Sidawy AN. The pathophysiology of atherosclerosis. Semin. Vasc. Surg. 1998; 11(3): 134 -141
5. Schwartz RS, Henry TD. Pathophysiology of coronary artery restenosis. Reviews in cardiovascular medicine, 2002; 3(5): 4-9
6. Adams M.R, Kinlay S, Blake G.J, Orford JL, Ganz P, Selwyn A.P. Pathophysiology of atherosclerosis: development, regression, restenosis. Curr Atheroscler Rep. 2000, 2(3): 251-258
7. Gawaz M, Blood Platelets. Georg Thieme Verlag, Stuttgart, New York, 2001; 118-149
8. Hombach V. Koronare Herzkrankheit. In: Interventionelle Kardiologie, Angiologie und Kardiovaskularchirurgie, Schattauer, Stuttgart , New York, 2001; 331-333
9. Carter A.J, Tsao P. Histopathology of restenosis. In: Handbook of drug eluting stents, Ed. Serruys P., Gehrshlick A. H., Taylor & Francis 2005; 15-47
10. Hoffmann R, Dussaillant M.G, et al. Patterns and Mechanisms of In-Stent Restenosis. Circulation. 1996; 94: 1247-1254
11. Spertus J A, Nerella R, Kettlekamp R, House J, Marso S, Borkon A.M, Rumsfeld J.S. Risk of Restenosis and Health Status Outcomes for Patients Undergoing Percutaneous Coronary Intervention Versus Coronary Artery Bypass Graft Surgery. Circulation, 2005 (111); 768-773
12. Schwartz R.S. Animal models of human coronary restenosis. In: Textbook of International Cardiology, 2nd ed. Topol. W. B. Saunders, Philadelphia 1994; 96 – 98
13. Virmani R. Pathology of in-stent restenosis. Current Opinion Lipidology, 1999; 10(6): 499-506
14. Colombo A, et.al. Restenosis: Multiple Strategies for Sent Drug Delivery. In: PC Technology Biocompatibles, Editorial MT. Rothman, London, 2001; Vol.1:12-31
15. Sigwart, U. Intravascular stents to prevent occlusion and restenosis after transluminal angioplasty. New England Journal of Medicine. 1987; 316(12): 701-706.
16. Fischman DL, Baim L, Schatz DS, Savage M.P, Penn I, et. al. A Randomized Comparison of Coronary-Stent Placement and Ballon Angioplasty in the Treatment of Coronary Artery Disease. The New England Journal of Medicine. 1994; 331(8): 496-501.

17. Herrman J P, Hermans WR, Vos J, Serruys PW. Pharmacological approaches to the prevention of restenosis following angioplasty: the search for the Holly Grail? (Parts I and II) Drugs 1993; 46: 18-52, 249-262

18. Moreno R. Drug-eluting stents and other anti-restenosis devices. Rev Esp Cardiol 2005; 58 (7) 842-862

19. Serruys PW, Foley DP, Pieper M, Kleijne JA, de Feyter J. The TRAPIST study. A multicenter randomized placebo controlled clinical trial of trapidil for prevention of restenosis after coronary stenting, measured by 3-D intravascular ultrasound. Eur. Heart J 2001;22: 1938 - 1947

20. Westedt U. Barbu-Tudoran,. Schaper AK, Kalinowski M., Alfke H, Kissel T.. Effects of different application parameters on penetration characteristics and arterial vessel wall integrity after local nanoparticle delivery using a porous balloon catheter. European Journal of Pharmaceutics and Biopharmaceutics 2004;58(1):161-168

21. Serruys PW, Rensing BJ. Handbook of coronary stents. 4th edition Martin Dunitz 2002

22. Brieger D. Local drug delivery systems and prevention of restenosis. Cardiovascular Research, 1997; 35(3): 405-413

23. Garas SM, Huber P, Scott NA. Overview of therapies for prevention of restenosis after coronary interventions. Pharmacology & Therapeutics 2001; 92 (2-3) 165-178

24. Gibson CM, Karmpaliotis D, Kosmidou I, Murphy SA, Kirtane AJ, Budiu D, Ray KK. et al. Comparison of Effects of Bare Metal Versus Drug-Eluting Stent Implantation on Biomarker Levels Following Percutaneous Coronary Intervention for Non–ST-Elevation Acute Coronary Syndrome. The American Journal of Cardiology. 2006; 97(10):1473-1477

25. Agostoni P, Valgimigli M, Biondi-Zoccai GL, Abbate A, Garcia HM, Anselmi M, Colombo A, et al. Clinical effectiveness of bare-metal stenting compared with balloon angioplasty in total coronary occlusions: Insights from a systematic overview of randomized trials in light of the drug-eluting stent era. American Heart Journal. 2006;151(3) 682-689

26. Carter A, et al. Long-Term effects of polymer-based, sirolimus-eluting stents in a porcine model. Cardiovascular Research, 2004;63:617-624.

27. Guagliumi G, et al. Drug-eluting versus bare metal coronary stents: long-term human pathology. Finding from different coronary arteries in the same patient. Italian Heart Journal, 2003; 4(10):713-720.

28. McFadden E. Late thrombosis in drug-eluting coronary stents after discontinuation of antiplatelet therapy. Lancet, 2004;364:1519-1521.

29. Serruys PW, de Jagegere P, Kiemeneij F, et al. For the BENESTENT study group. A comparison of balloon-expandable –stent implantation with balloon angioplasty in patients with coronary artery disease. N Engl J Med 1994;331:489 – 495

30. Kiemeneij F, Serruys PW, Macaya C, et al. Continued benefit of coronary stenting versus balloon angioplasty: five-year clinical follow-up of Benestent – I trial. J Am Coll Cardiol 2001;37:1598 – 1603

31. Faxon DP, Williams DO, Yeh W, et al. Involved in-hospital outcome with expanded use of coronary stents: results from the NHLBI dynamic registry. J Am Coll Cardiol 1999;33:91A

32. Al Suwaidi J, Berger PB, Holmes DR Jr. Coronary artery stents. JAMA 2000;284:1828 – 1836

33. Van Belle E, Bauters C, Hubert E, et al. Restenosis rates in diabetic patients: a comparison of coronary stenting and balloon angioplasty in native coronary vessels. Circulation 1997; 2(96): 1454 – 1460

34. Carrozza JP, Kuntz RE, Levine MJ et al. Angiographic and clinical outcome of intracoronary stenting: immediate and long-term results from a large single-center experience. J Am Coll Cardiol 1992;20:328 – 337

35. Moussa I, Leon MB, Baim DS, O'Neill WW, Pompa JJ, et al. Impact of sirolimus-eluting stents on outcome in diabetic patients: a SIRIUS substudy. Circulation 2004;109:2273 – 2278

36. Colombo A, Moses JW, Morice MC, Ludwig J, Holmes DR, Jr. et al. Randomized study to evaluate sirolimus-eluting stents implanted at coronary bifurcation lesions. Circulation 2004; 109:1244 – 1249

37. Bauters C., Hubert E. Bougrmi K., et al. Predictors of restenosis after coronary stent implantation. J Am Coll Cardiol. 1998; 29:13 – 20

38. vom Dahl J, Dietz U, Haager PK, Silber S, Niccoli L, Buettner HJ, Schiele F, Thomas M, Commeau P, Ramsdale DR, Garcia E, Hamm CW, Hoffmann R, Reineke T, Klues HG. Rotational atherectomy does not reduce recurrent in-stent restenosis: results of the angioplasty versus rotational atherectomy for treatment of diffuse in-stent restenosis trial (ARTIST). Circulation. 2002;105(5):583-588.

39. Sharma SK, Reich D, Kini A. Instent restenosis: balloon angioplasty, rotablation or laser therapy. Indian Heart J. 1998;50 Suppl 1:109-119.

40. Al-Sergani HS, Ho PC, Nesto RW, Lewis SM, Leeman D, Fitzpatrick P, Mittleman M, Waxman S, Shubrooks SJ Jr. Stenting for in-stent restenosis: A long-term clinical follow-up. Catheter Cardiovasc Interv. 1999 ;48(2):143-148.

41. Waksman R, Bhargava B, Mintz GS, Mehran R, Lansky AJ, Satler LF, Pichard AD, Kent KM, Leon MB. Late total occlusion after intracoronary brachytherapy for patients with in-stent restenosis. J Am Coll Cardiol. 2000; 36(1):65-68

42. Serruys PW, Foley DP, Jackson G, Bonnier H, et al. A randomized placebo-controlled trial of fluvastatin for prevention of restenosis after succesful coronary balloon angioplasty; final results f FLARE trial. Eur Heart J. 1999;20:58-69

43. Holmes DR Jr, Savage M, la Blanche JM, Grip L. Serruys PW, et al. Results of prevention of Restenosis with Tranilast and its outcomes (PRESTO) trial. Circulation 2002; 106: 1243 - 50

44. Kastrati A, Schuhlen H, Hausleiter J, et al. Restenosis after coronary stent placement and randomization to a 4-week combined antiplatatelet or anticoagulant therapy: six month angiographic follow-up of the intracoronary stenting and antithrombotic regimen (ISAR) Trial. Circulation 1997; 96: 462-67

45. Ellis SG, Effron MB, Gold HK, et al. Acute platelet inhibition with abciximab does not reduce in-stent restenosis (ERASER study) Circulation 1999; 100:799-806

46. Meurice T, Bauters C, Hermant X, et al. Effect of ACE inhibitors on angiographic restenosis after coronary stenting (PARIS): a randomized, double-blind, placebo controlled trial. Lancet. 2001;375:1321-1324

47. Serruys PW, Foley DP, Jackson G, et al. A placebo-controlled trial of fluvastatin for prevention of restenosis after successful coronary balloon angioplasty: final results of the fluvastatin angiographic restenosis (FLARE) trial. Eur Heart J 1999;20:58-69

48. Brara PS, Moussavia M, Grise MA, et al. Pilot trial of oral rapamycin for recalcitrant restenosis. Circulation 2003;107:1722-1724

49. Rodriguez AE, Alemparte MR, Vigo CF, et al. Pilot study of oral rapamycin to prevent restenosis in patients undergoing coronary stent therapy. Argentina Single-Center Study (ORAR Trial). J Invasive Cardiol 2003;15:581-584

50. Virmani R, Farb A, Guagliumi G, Kolodgie FD. Drug eluting stents: caution and concerns for long-term outcome. Coron Artery Dis 2004;15: 313 – 318

51. Tsui T, Tamai H, Igaki K, et al. Biodegradable stents as a platform to drug loading. Int J Cardiovasc Intervent 2003;5: 13 – 16

52. Tsui T, Tamai H, Igaki K, et al. Biodegradable polymeric stents. Curr Interv Cardiol Rep 2001;3: 10 – 17

53. Waksman R. Adjunctive therapy: Biodegradable stents: they do their job and disappear. J Invasive Card 2006;18(2):70 – 74

54. Erne P, Schier M, Resink TJ. The road to bioabsorbable stents: reaching clinical reality? Cardiovasc Intervent Radiol 2006;29: 11 – 16

55. Heublein B, Rohde R, Kaese V, Niemeyer M, Hartung W, Haverich A. Biocorrosion of magnesium alloys: a new principle in cardiovascular implant technology? Heart 2003 ;89(6):651-6

56. Antoniucci D, Bartorelli A, Vaenti R et al. Clinical and angiographic outcomes after coronary artery stenting with the Carbostent. Am J Cardiol. 2000;85:821 – 825

57. Antoniucci D, Vaenti R, Migliorini A. et al. Clinical and angiographic outcomes following elective implantation of the Carbostent in patients at high risk of restenosis and target vessel failure. Cathet Cardiovasc Interv. 2001;54 :141 – 145

58. Zheng H. Barragan P. Corcos T. et al. Clinical experience with a new biocompatible phosphorylchoilne – coated coronary stent. J Invas Cardiol 1999; 11: 608 – 614

59. Galli M, Bartorelli A, Bedgoni F et al. Italian BiodivYsio open registry (BiodivYsio PC-coated stent): study of clinical outcomes of the implant of a PC-coated coronary stent J Invas Cardiol 2000;12 :452 – 458

60. Whorle J, Al-Khayer E, Grotzinger U, et al. Comparison of the heparin coated vs. the uncoated Jostent: no influence on restenosis or clinical outcome. Eur Heart J. 2001;22:1808 – 1816

61. Kastrati A, Schömig A, Dirschinger J, et al. Increased risk of restenosis after replacement of gold-coated stents. Circulation 2000;101 : 2478 – 2483

62. Babapulle MN, Eisenberg MJ. Coated stents for the prevention of restenosis. Part I. Circulation 2002; 106:2734-40

63. Lee CW, Chae JK, Lim HY, et al. Prospective randomized trial of corticosteroids for the prevention of restenosis after intra coronary stent implantation. Am Heart J 1999;138:60 – 63

64. Ong AT, Serruys PW. Drug-eluting stents: current issues. Tex Heart Inst J. 2005;32(3):372-377

65. Babapulle MN, Eisenberg MJ. Coated stents for the prevention of restenosis. Part II. Circulation 2002; 106:2859 – 2866

66. Perin CE. Choosing a drug-eluting stent: a comparison between Cypher and Taxus. Rev. Cardiovasc. Med. 2005;6: 13 – 21

67. McLean DR, Eiger NL. Stent design: implications for restenosis. Rev. Cardiovasc. Med 2002;3:16 – 22

68. Virmani R, Guagliumi G, Farb A, et al. Localized hypersensitivity and late coronary thrombosis secondary to a sirolimus-eluting stent: should we be cautious? Circulation. 2004;109: 701–705

69. Kastrati A, Mehilli J, von Beckerath N, Dibra A, Hausleiter J, Pache J, Schuhlen H, Schmitt C, Dirschinger J, Schomig A; ISAR-DESIRE Study Investigators Sirolimus-eluting stent or paclitaxel-eluting stent vs balloon angioplasty for prevention of recurrences in patients with coronary in-stent restenosis: a randomized controlled trial. JAMA. 2005;293(2):165-171

70. Finn AV, Kolodgie FD, Harnek J, et al. Differential response of delayed healing and persistent inflammation at sites of overlapping sirolimus and paclitaxel eluting stents. Circulation 2005; 112: 270 – 278

71. Guagliumi G, Farb A, Musumeci G, et al. Sirolimus-eluting stent implanted in human coronary artery for 16 months: pathological findings. Circulation 2003; 107: 1340 – 1341

72. Goodwin SC, Yoon H-C, Chen G, et al. Intense inflammatory reaction to heparin polymer coated intravascular Palmaz stents in porcine arteries compared to uncoated Palmaz stents. Cardiovasc Intervent Radiol 2003;26: 158–167

73. Virmani R, Liistro F, Stankovic G, et al. Mechanism of late in-stent restenosis after implantation of a paclitaxel derivate-eluting polymer stent system in humans. Circulation 2002;106: 2649 –2651

74. Wessely R, Kastrati A, Schömig A. Late Restenosis in Patients Receiving a Polymer-Coated Sirolimus-Eluting Stent. Annals of Internal Medicine 2005;143 (5): 392- 393

75. Farb A, Heller PF, Shroff S, et al. Pathological analysis of local delivery of paclitaxel via polymer-coated stent. Circulation 2001;104: 473 -479

76. Wessely R, Hausleiter J, Schömig A, et al. Inhibition of Neointima Formation by a Novel Drug-Eluting Stent System That Allows for Dose- Adjustable, Multiple and On-Site Stent Coating. Arterioscler Thromb Vasc Biol 2005;25:748-753

77. Mathiowitz E. Encyclopedia of controlled rug delivery. John Wiley 1999 Vol.1

78. Linhardt RJ. Biodegradable Polymers for Controlled Release of Drugs in Controlled release of Drug: Polymers and aggregate systems, Ed. Rosoff M. VCH Publishers 1989, 53 – 94

79. Robinson JR, Lee VHL, Controlled drug delivery fundamentals and applications. Second edition 1990, 6 – 11

80. Langer R, Chasin Mark. Biodegradable Polymers as Drug Delivery Systems. 1990

81. Kuehler M, de Schreerder I, Drug delivery coatings in Handbook of drug-eluting stents. Ed. Serruys PW, Gershlick AH. Taylor and Francis Group 2000, 65 – 74

82. Langer R, Peppas NA. Present and future applications of biomaterials in controlled rug delivery systems. Biomaterials 1981;2 : 201 – 214

83. Narasimhan, B. In: Handbook of Pharmaceutical Controlled Release Technology Wise, D. L., Ed. Marcel Dekker, New York, 2000:155-181

84. U.S. Patent Number 5,288,711, Robert D. Mitchell et al. April 28, 1992

85. Lee PI, Controlled release technology. Pharmaceutical applications. William R. Good New York, 1987: 2 – 13

86. Siepmann J, Peppas, NA. Modeling of drug release from delivery systems based on hydroxypropyl methylcellulose (HPMC). Advanced Drug Delivery Reviews 2001;48: 139 – 157

87. Siepmann, J Göpferich, A Mathematical modeling of bioerodible, polymeric drug delivery systems. Advanced Drug Delivery Reviews 2001;48: 229-247

88. Peppas NA., Mathematical modeling of diffusion processes in drug delivery polymeric systems. In :Smolen VF, Ball L. Controlled drug bioavailability. Willey. 1984;Vol. 1: 203 – 237

89. Crank J. Mathematics of diffusion. Clarendon press, Oxford 1975

90. Baker R.W, Lonsdale H.K. Controlled release: mechanisms and rates in Tanquary A.C., Lacey R.E.. Controlled release of biologically active agents, 1974: 15-72

91. Peppas NA,. Analysis of Fickian and non-Fickian drug release from polymers. Pharm. Acta Helvet. 1985;60 110 – 111

92. Peppas NA, Korsmeyer RW. Dynamically swelling hydrogels in controlled release applications in: Peppas NA Hydrogels in medicine and pharmacy 1986; 3: 109 – 136

93. Heller J, Baker RW. Theory and practice of controlled drug delivery from erodible polymers, in: Baker, Controlled release of bioactive materials. Academic Press, 1980 1- 18

94. M. Stöver, Surface microstructuring for controlled drug release in coronary stents, Dissertation, Technische Universität München, 2006

95. Wood M. Rapamycin: biological and therapeutic effects, binding by immunophilins and molecular targets of action. Persp Drug Discovery Des, 1994; 2: 57-84

96. Sehgal SN, Rapamune (RAPA, rapamycin, sirolimus): mechanism of action immunosuppressive effect results from blockade of signal transduction and inhibition of cell cycle progression. Clin Biochem, 1998;31: 335-340.

97. Vezina C, K.A., Sehgal S N, Rapamycin, a new antifugal antibiotic. I Taxonomy of the producing stretomycete and isolation of the active principle. Journal of Antibiotics. 1975; 28:721-726.

98. Sehgal SN, B.H., Vezina C, Rapamycin, a new antifugal antibiotic. II Fermantation, isolation and characterization. Journal of Antibiotics, 1975;28:727

99. Raught B, G.A.C., Sonenberg N, The target of rapamycin (TOR) proteins. Proc Natl Acad Sci, 2001. 98: 7037 - 7044

100. Groth CG, B.L., Morales JM, et al. SIROLIMUS (RAPAMYCIN)-BASED THERAPY IN HUMAN RENAL TRANSPLANTATION: Similar Efficacy and Different Toxicity Compared with Cyclosporine1,2. Transplantation, 1999;67: 1036-1042

101. Skiens WE, Burton FG, Duncan GW. In: Biodegradables and delivery systems for contraception. Editor Hafez ESE, van Os WAA; Vol.1, Hall Medical Publishers, Boston 1980

102. Schindler A, Coat JF, et al in Contemporary topics in polymer science. Editor Pearce EM, Schaefgen JR; Vol.2 Plenum Press New York 1977: 264

103. Park A, Cima AG. In vitro cell response to differences in poly-L-lactide crystallinity. Journal of Biomedical Materials Research; 1996; Vol. 31, (1): 17-30

104. Benagiano G, Schmitt E., Wise D., Goodman M.: Sustained release hormonal preparations for the delivery of fertility-regulating agents. J. Polymer Scie. 1977; 66:129-48

105. P.G. de Gennes. Wetting: statics and dynamics Rev. Mod. Phys. 1985; 57 (3): 827-863

106. S. Ringer. Concerning the influence exerted by each of the constituents of the blood on the contraction of the ventricle. Journal of Physiology, Cambridge, 1880-1882, 3: 380-393. Journal of Physiology, Cambridge, 1883-1884, 4: 29-42, 222-225.

107. V. Gupta, J. Yuan, A. Pronin. Recent developments in the laser spallation technique to measure the interface strength and its relationship to interface toughness with applications to metal/ceramic, ceramic/ceramic and ceramic/polymer interfaces. J. Adhesion Sci. technol. 1994; 8: 713-747

108. J. Yuan, V. Gupta. Measurement of interface strength by modified laser spallation technique. I. Experiment and simulation of the spallation process. J. Appl. Phys. 1993;74 (4): 2388 – 2396

109. H.A Krebs., K. Hanseleit. Untersuchungen über die Harnstoffbildung im Tierkörper. Hoppe-Seyler´s Zeitschrift für Physiol. Chemie. 1932, 210: 33-66

110. F. J. Sutherlandu, D. J. Hearse. The isolated blood and perfusion fluid perfused heart. Cardiovascular Research, Pharmacological Research, 2000;41(6)

111. Sina Ebnesajjad Surface treatment of materials for adhesion bonding. 2006 William Andrew Inc.

112. Wessely R, Hausleiter J. et al. Inhibition of neointima formation by a novel drug-eluting stent system that allows for dose-adjustable, multiple, and on-site stent coating. Arterioscler. Thromb. Vasc. Biol. 2005;25:1-6

113. Kinloch A.J.. The science of adhesion. Surface and interfacial aspects. J. Mat. Sci., 1980;15: 2141-2166

114. Riedel W. Zur Galvanisierung von ABS-Propfpolymerisaten. Die Schälfestigkeit nach der Druckknopftheorie. Galvanotechnik. 1966; 57:579-583

115. Hausleiter J., et al. Prevention of restenosis by a novel drug eluting stent system with a dose-adjustable, polymer free, on-site stent coating. European Heart Journal 2005; 26, 1475–1481

116. Sousa JE, Costa MA, Abizaid AC, et al. Sustained suppression of neointimal proliferation by sirolimus-eluting stents: one-year angiographic and intravascular ultrasound follow-up. Circulation. 2001;104:2007-2011

117. Lincoff et al. Sustained Local Delivery of Dexamethasone by a Novel Intravascular Eluting Stent to Prevent Restenosis in the Porcine Coronary Injury Model. J Am Coll Cardiol 1997;29:808–16

118. Tamai H. et al Initial and 6-Month Results of Biodegradable Poly-l-Lactic Acid coronary Stents in Humans, Circulation 2000;102;399-404

119. Wang N and Wu XS, in Tailored Polymeric Materials for Controlled Delivery Systems, CS Symposium Series 709, ed by Mc Culloch I and Shalaby SW. Washington DC, 1998 :255–265

120. F. Aleksis, Review: Factors affecting the degradation and drug-release mechanism of poly(lactic acid) and poly[(lactic acid)-co-(glycolic acid)] Polym Int. 2005; 54:36–46

121. R. Virmani; G. Guagliumi, et al. Localized Hypersensitivity and Late Coronary Thrombosis Secondary to a Sirolimus-Eluting Stent Should We Be Cautious? Circulation. 2004;109:701-705

122. Y. V. Il'ichev, L. Alquier, C. A. Maryanoff Degradation of rapamycin and its ring-opened isomer: Rrole of base catalysis. Cordis Corporation, a Johnson & Johnson Company, ARKIVOC 2007:110-131

123. F.C. Tanner, Z.Y Yang, et al. Expression of cyclin-dependent kinase inhibitors in vascular disease, Circ. Res. 1998;82: 396-403

124. M.N. Babapulle, M.J. Eisenberg, Coated stents for the prevention of restenosis: Part II Circulation 106 (2002) 2859-2866; E.J. Topol, P.W. Serruys, Frontiers in interventional cardiology, Circulation 1998;98: 1802- 182

125. M. Stöver, Surface microstructuring for controlled drug release in coronary stents, Dissertation, Technische Universität München, 2006

126. Wintermantel E., Schratzenstaller T., Coating system. Patent DE 102 00 388 A1

127. Wintermantel E., Schratzenstaller T., Coating system. Patent EP 1325 758 A2

128. Wintermantel E., Schratzenstaller T., Coating system. Patent EP 1325 758 A3

129. GT Burstein, IM Hutchings, and K Sasaki, "Electrochemically Induced Annealing of Stainless-Steel Surfaces," Nature 2000; 407, 6806: 885–887

130. Sader M. S., A. Balduino et al. Effect of three distinct treatments of titanium surface on osteoblast attachment, proliferation, and differentiation. Clinical Oral Implants Research. 2005;16(6):667–675

131. Mustafa K, Wroblewski J et al. Effects of titanium surfaces blasted with tio2 particles on the initial attachment of cells derived from human mandibular bone. a scanning electron microscopic and histomorphometric analysis. Clinical Oral Implants Research, 2000;11(2):116–28

132. Buser D, Schenk RK. et al. Influence of surface characteristics on bone integration of titanium implants. a histomorphometric study in miniature pigs. Journal of Biomedical Material Research. 1991;25:889–902

133. Baley SJ, Kamil N, et al. Potassium vasoactivity – a biphasic effect. Surgery. 1970;67 (2): 350-354

134. Vysnianskiene J, Allemann R, Flammer J, Haelfinger IO. Vasoactive responses of U46619, PGF2 alpha, latanoprest and travoprost isolated porcine ciliary arteries. Invest. Ophthamol Vis Sci, 2006;47 (1): 295 – 298

135. Forstermann U, Mugge A, Frolich JC. Endothelium-dependent relaxation of human epicardial coronary arteries: frequent lack of effect of acetylcholine. Eur. J. Pharmac. 1986;128:277 – 281

136. Thews G. Anatomie, Physiologie, Pathophysiologie des Menschen : 135 Tabellen. 5., völlig neu bearb. und erw. Aufl. ed, ed. G. Thews, Mutschler, E., Vaupel, P. 1999, Stuttgart: Wiss. Verl.-Ges.

137. Sousa JE, Costa MA, et al. Lack of neointimal proliferation after implantation of sirolimus-coated stents in human coronary arteries. a quantitative coronary angiography and three-dimensional intravascular ultrasound study. Circulation, 2001;103:192

138. Serruys PW, Sianos G, et al. The effect of variable dose and release kinetics on neointimal hyperplasia using a novel paclitaxel-eluting stent platform: The paclitaxel in-stent controlled elution study. Journal of the American College of Cardiology, 2005;46(2):253–260

139. Duda SH, Poerner TC, et al. Drug-eluting stents: Potential applications for peripheral arterial occlusive disease. Journal of Vascular and Interventional Radiology, 2003;14:293

140. Pistner H. Gutwald R. et al. Poly(L-lactide): a long-term degradation study in vivo. Part I: Biological results. Biomaterials. 1993; 14 (9):671-676

Abbreviations

A	area of the controlled release device exposed to the release medium
ABC	**A**rtificial **B**lood **C**ircuit
ACA	**A**nthracene **C**arboxylic **A**cid
ACE inhibitors	**A**ngiotensin **C**onverting **E**nzyme
Ach	**A**cetylcholinchloride
AFM	**A**tomic **F**orce **M**icroscopy
BMS	**B**are **M**etal **S**tent
CAD	**C**oronary **A**rtery **D**isease
CCD chip	**C**harge **C**oupled **D**evice, image sensors
c_0	initial drug concentration
c_s	solubility of the drug in the polymer
d,l - lactic acid	racemic mixture of d and l enantiomers of lactic acid
D_0	initial drug permeability
D_{12}	drug diffusion coefficient
DAPI	microscopy fluorescence excitation filter
DCC	N,N'-dicyclohexylcarbodiimide
DES	**D**rug-**E**luting **S**tents
DMAP	4-(dimethylamino)pyridine
D_t	drug permeability at time *t*
EtOH	ethanol
FKBP12	binding protein
FTIC	microscopy green excitation filter
FTIR	**F**ourier **T**ransform **I**nfra**r**ed spectroscopy
GPC	**G**el **P**ermeation **C**hromatography
HPLC	**H**igh **P**ressure **L**iquid **C**hromatography
HUVEC	**H**uman **U**mbilical **V**ein **E**ndothelial **C**ells
ISR	**I**n-**S**tent **R**estenosis
ISAR	**I**ndividualized **S**tent system to **A**brogate **R**estenosis
k	constant reflecting the design variables of the drug eluting system
KCl	potassium chloride
kDa	kilo Daltons

KHS	**K**rebs-**H**anseleit **S**olution
LASAT	**L**aser **S**hock **A**dhesion **T**ests
LDL	**L**ow-**D**ensity **L**ipoprotein
M_∞	absolute cumulative amount of drug released at infinite time
m_G	drug amount in tissue related to artery weight
$m_{R,SB}$	drug amount on the expanded stent
m_{RG}	drug amount in tissue
M_t	cumulative absolute amount of drug released at the time t
mTOR	**m**ammalian **T**arget **O**f **R**apamycin
MWD	**M**olecular **W**eight **D**istribution
N	number of initial bonds in polymer
Nd:YAG	neodymium-doped yttrium aluminium garnet laser
NE	norepinephrinhydrochloride
PDE	**P**ermitted **D**aily **E**xposure
PDLLA	poly (d,l-lactic acid)
phase G1	cell cycle phase
PLA	polylactide
PTCA	**P**ercutaneous **T**ransluminal **C**oronary **A**ngioplasty
PVC	polyvinyl chloride
RCX	**R**amus **C**ircumfle**x**us
RIVA	**R**amus **I**nter**v**entricularis **A**nterior
RMS	**R**oute **M**ean **S**quare
SBF	**S**imulated **B**ody **F**luid
SCM	**S**tent **C**oating **M**achine
SEM	**S**canning **E**lectron **M**icroscopy
SIMS	**S**econdary **I**on **M**ass **S**pectroscopy
T_g	glass transition temperature
THF	tetrahydrofuran
TLR	**T**arget **L**esion **R**evascularization
$v_{r.}$	factor of surface area enlargement
VSMC	**V**ascular **S**mooth **M**uscle **C**ells
Z	of polymer bond cleavages during the time interval [0 ; *t*]
θ	contact angle
δ	thickness of film released drug
202H	poly (d,l-lactic acid) with molecular weight of 16 kDa
203S	poly (d,l-lactic acid) with molecular weight of 30 kDa
2PLSM	two **P**hotons **L**aser **S**canning **M**icroscopy
316 L	stainless steel

Appendix

Appendix A1: Calibration curves of rapamycin for UV-Vis measurements

The concentration measurements of released rapamycin were carried out with the help of an UV - Vis – Spectrometry. First a calibration curve was established. Moreover 14 different concentrations were produced by rapamycin in Tetrahydrofuran (THF). With the measurement 14 data points resulted (Fig. A1.1).

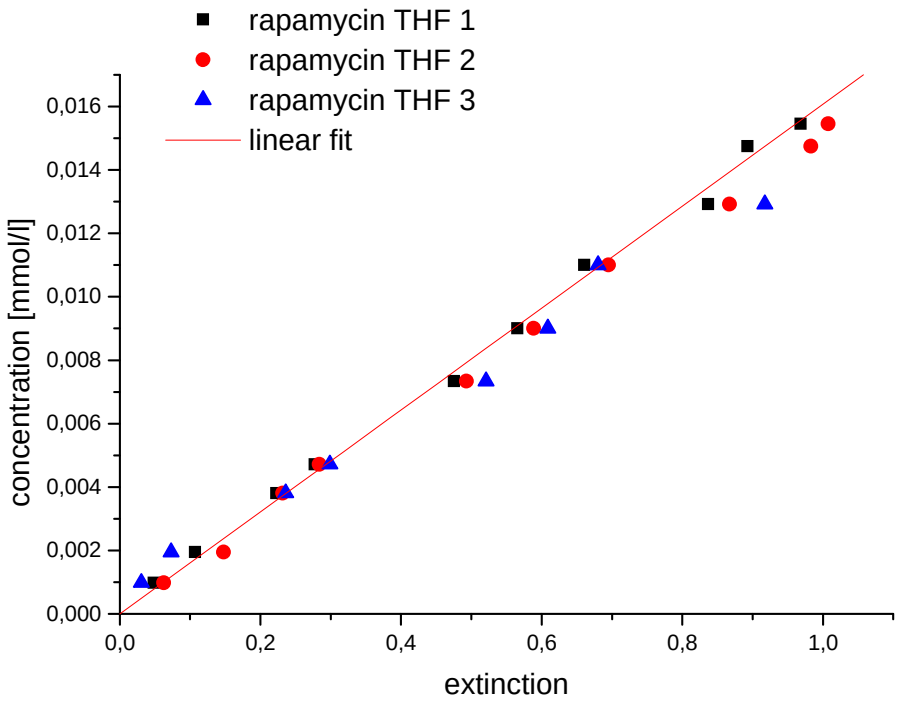

Fig. A1.1: *Calibration curve of rapamycin in THF. UV-Vis spectroscopy*

The corelation between absorption and concentration can be desribed by the Lambert - Beer'sche law (equation A1.1)

$$I = I_0 * e^{-\varepsilon * d * c} \qquad \text{(Eq. A1.1)}$$

where:

I: intensity of the incident light

I_0: intensity after the material

ε: extinction coefficient

d: thickness of specimen

c: concentration

Due to the correlation between extinction ((I_0 / I)) and concentration (c) is a linear function in the Lambert - Beer law, it is possible to trace a line of best fit by the measured data points.

From the given equation the concentration of the rapamycin solutions can be calculated directly.

Other calibration curve for rapamycin solved in Ringer solution was identically provided. (Fig A1.2).

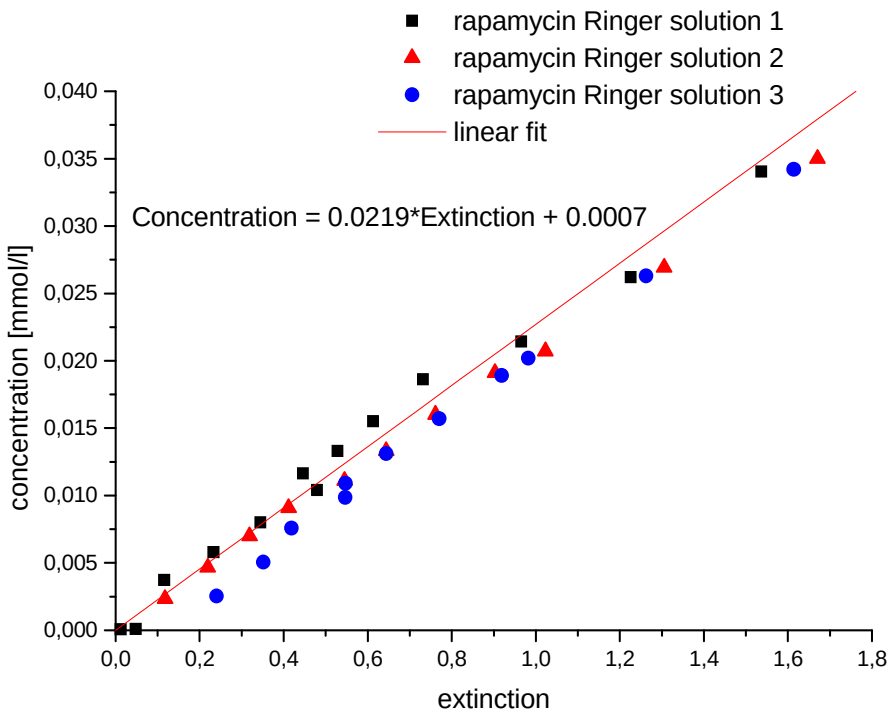

Fig. A1.2: *Calibration curve of rapamycin in Ringer solution. UV-Vis spectroscopy*

Appendix A2: Example of counting of rapamycin lost from coating process to expansion int the air on in the artificial blood circuit

Stent surface: sandblasted
Stent length: 12mm
Stent surface: 19.4 mm^2
Coating solution: Rapamycin 1% = 10mg rapamycin in 1 ml ethanol

Rapamycin amount needed to coat 12mm length stent:
0.25ml of 1% solution = 2.5 mg rapamycin

$Rapa_{100\%}$ = 2.5mg

Rapamycin amount needed to coat 12mm length stent in [mg/mm^2]

$$Rapa_{100\%}\left[mg/mm^2\right] = \frac{Rapa_{100\%}}{stent\ surface} = \frac{0.25}{19.4} = 0.129\left[mg/mm^2\right] \quad \text{(Eq. A 2.1)}$$

$Rapa_{100\%}$ = 0.129 mg/mm^2 = 100%

Rapamycin amount after coating on unexpanded stent crimped on the balloon:

$Rapa_{s+b}$=0.0258 mg/mm^2 = 20%

$$Rapa_{s+b} = \frac{Rapa_{s+b} \cdot 100\%}{Rapa_{100\%}} = \frac{0.0258 \cdot 100\%}{0.129} = 20\% \quad \text{(Eq. A 2.2)}$$

Rapamycin amount on stent after expansion in the air:

$Rapa_{air}$= 0.01806 mg/mm^2

$$Rapa_{air} = \frac{Rapa_{air} \cdot 100\%}{Rapa_{100\%}} = \frac{0.01806 \cdot 100\%}{0.129} = 14\% \quad \text{(Eq. A 2.3)}$$

$Rapa_{air}$=0.01806 mg/mm^2 = 14%

Rapamycin amount on stent after expansion in the artificial blood circuit:

$Rapa_{ABC}$= 0.0162 mg/mm^2

$$Rapa_{ABC} = \frac{Rapa_{ABC} \cdot 100\%}{Rapa_{100\%}} = \frac{0.0162 \cdot 100\%}{0.129} = 12.6\% \qquad \text{(Eq. A 2.4)}$$

$Rapa_{ABC}$=0.0162 mg/mm^2 = 12.6%